



UNIVERSIDAD AUTÓNOMA DE SAN LUÍS POTOSÍ

Doctorado Institucional en Ingeniería y Ciencia de Materiales

**Study on sylvite flotation through controlled crystallization
methodology**

PARA OBTENER EL GRADO DE

DOCTORA EN INGENIERÍA Y CIENCIA DE MATERIALES

QUE PRESENTA

Yuan Yuan

ASESORES

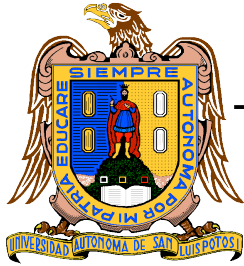
Dr. Alejandro López Valdivieso

Dr. Shaoxian Song

PATROCINADO POR CONAHCyT Beca número 812586

San Luis Potosí, S.L.P. Mayo de 2025





UNIVERSIDAD AUTÓNOMA DE SAN LUÍS POTOSÍ

Doctorado Institucional en Ingeniería y Ciencia de Materiales

**Study on sylvite flotation through controlled crystallization
methodology**

QUE PARA OBTENER EL GRADO DE

DOCTORA EN INGENIERÍA Y CIENCIA DE MATERIALES

PRESENTA

Yuan Yuan

ASESORES

Dr. Alejandro López Valdivieso

Dr. Shaoxian Song

Sinodales

Dr. Shaoxian Song _____

Dr. Yuri Nahmad Molinari _____

Dra. Mildred Quintana Ruiz _____

Dr. Bernardo José Luis Arauz Lara _____

Dra. Yanmei Li _____



San Luis Potosí, S.L.P., Mayo de 2025



Study on Sylvite Flotation through controlled crystallization methodology by Yuan Yuan is licensed under [Attribution-NonCommercial-NoDerivatives 4.0 International](https://creativecommons.org/licenses/by-nc-nd/4.0/)

Acknowledgement

This work was financially supported by the Consejo Nacional de Humanidades Ciencias y Tecnologías (CONAHCYT) for the scholarship of Yuan Yuan with No. 812586. Thanks are given to the National Key Research and Development Program of China (2022YFC2904004). This work was partially done by Luis A. Cisternas into visit at the Wuhan University of Technology, supported by MINEDUC-UA project, code ANT 22991.

As I encounter the end of my PhD study period, I would like to look back to the past three and a half years of my researching life with a mixed feeling of happiness and sadness, where the previous exceeds the latter due to the gratitude full within my heart. Firstly, I would like to express my sincere gratitude for the invaluable advices in my work from Dr. Alejandro Lopez Valdivieso, who had been always busy focusing on scientific research with his whole heart. Whenever I met difficulties in my research, he could see through the fundamental problem and provided me essential suggestions. He has been the aim of my research imagine and I would like to keep working to be more alike to him. Likely, Dr. Shaoxian Song, as the co-advisor of my PhD study, has been leading me in my scientific road for 8 years since the very beginning and has taught me much knowledge not only about research attitude but also how to hold a broad and forward-looking plan in life. He is always clever, optimistic and lenient like a father to our group. It has been my great honor to meet such two great professors as my advisors.

What's more, I'd like to show my sincere gratitude to Dr. Bernardo Jose Luis Arauz Lara and his lab members like Dr. Rosario, Dr. Rodrigo, Dr. Noe and his family member Dr. Monica and Emiliano, and to my friend Juan Carlos and Dr. Beni in San Luis Potosí. I also want to express my gratitude to Dr. Viridiana, Dr. Aurora and Dr. Yuri. The above warm-hearted people have helped and accompanied me to experience local life in San Luis Potosí, it has been really great time to be here.

Besides, I also thank Dr. Maria de Jesus Martinez Lopez, a previous doctor student from Dr. Arauz's lab. Her friendship and love from the family "Martinez" have shown me the most traditional and great part of Oaxaca, where I met wonderful people like Karen, Melissa, Chayo, Aide, Conchis, Irving and especially our perfect parents. The "family" gave me endless happiness and love during my life in Mexico. The joint beautiful memories will be kept in my deep heart forever. Viva Oaxaca, Viva Mexico!

The last but not the least, I appreciate everyone in Institucional en Ingenieria y

de Ciencia de Materiales de la Universidad Autonoma de San Luis Potosí, I thank Dra. Mildred Quintana Ruiz very much who was responsible for this doctorate program and provided suggestion for my study and life. I also appreciate the great help of Eva and Maricela during my study process. I want to thank my family members and my two cats Panda and Miumi. Thank your help and support in my work and life.

Abstract

With vast reserves on earth and high value, various types of minerals have been extracted, well purified and applied in multiple fields including architecture, transportation, technology, etc. The key of flotation process is to realize a hydrophobic state of mineral surfaces which always relies on the proper chemical reagent-collector. Numerous researchers devoted much into the designing of collector or back-end processing of mineral particles shape, ignoring the fact that most minerals belong to different types of crystals. In this work, the main idea is to understand minerals as crystals so as to put up with a novel strategy through crystallization controlled flotation with great application prospect for soluble and semi-soluble minerals. Here, the modulation of crystallization as well as following flotation behaviors were detailed researched by taking potassium chloride as an example which is the main resource for extraction of potassium element. The various crystallization paths were also unveiled through surficial studies and related flotation mechanisms were elaborately researched, paving a path to the strategy of crystallization modulated flotation for other soluble and semi-soluble minerals.

Chapter I and II briefly introduced the justification, objectives and previous researches of antecedents about this research. In Chapter III, the materials, researching methods and characterization in this thesis were shortly introduced. Chapter IV focused on a development of green supersaturation method for preparing KCl crystals with various shapes. Chapter V was about the preparation of KCl samples with two different exposing facets as (200) and (222), where their corresponding flotation behavior with ODA as collector and the related mechanism were studied in detail. Chapter VI presented the successful growth of KCl samples with needle-, hopper- and cubic-like structure, and their growing mechanism, flotation behaviour as well as mechanism were elaborately unveiled. In the Chapter VII, we further demonstrated the influence of ethanol on crystallization and flotation process of KCl, where the mechanism of promoted KCl flotation behavior induced by ethanol addition was well researched. At last, Chapter VIII summarized the conclusions of this thesis and provided a few perspectives on soluble salt flotation research.

Keywords: Crystallization; AFM; KCl; Surficial properties; Supersaturation; Soluble salt flotation.

Extended Abstract

Chapter I: A concise description of justification in this work was firstly given. Besides, the objectives and related goals of this thesis were listed, to help draw an outline of significant purposes in upcoming chapters.

Chapter II: A thorough out introduction of researching background of sylvite flotation was provided in this chapter, including the information of its resource, common minerals type. Afterwards, the good water solubility of sylvite was emphasized where basic physical and chemical properties of other similar soluble minerals were introduced. Notably, the recovery methods, in most cases, flotation processes of the soluble minerals were discussed. At last, the flotation mechanisms of NaCl (as the most common associate mineral of KCl) and KCl researched in last a few decades were described, followed by some promising researching aspects for understanding their flotation mechanisms.

Chapter III: The materials, main methods as well as characterizations applied in experiments of Chapter IV, V, VI and VII.

Chapter IV: Controllable and green construction of morphology and structure in potassium chloride (KCl) crystals is necessary in the fields of pharmaceuticals, catalysis, minerals, and jewels design. Here, the work presented a lucid way for preparing KCl crystal with various morphology including hopper-, sphere- and hollow cube-like structure through green supersaturation modulation. Parameters including stirring speed, cooling range, cooling rate, and excess inorganic composing ions influenced the growth kinetics of hopper KCl crystal as well as the surficial morphology and structure: (1) Metastable region and stable conditions were beneficial for uniform growth of crystal; (2) Small size of crystal particles were obtained with high shear force; (3) Corner angle of crystal would be abraded in slow cooling rate; (4) Non-uniform crystal appeared in improper cooling range condition; (5) Additional composing ions might introduce deformed structure according to the basic crystal repeating unit with corresponding elements. Based on the above study of growth kinetics, hopper-, sphere- and hollow cube-like crystal were obtained. The morphology and structure properties of various crystal were researched by three-dimensional visualization, X-ray diffraction (XRD), and scanning electron microscope (SEM) for optimized application such as higher exposing surface area of hopper-like crystal than original cubic crystal. The main exposed faces for smooth cubic, hollow cubic, and hopper structure exhibited were (200), (220), and (400) facet, respectively, which could be a consequence of the inner beveling. Surface of spherical structure was a circular arc with relative high roughness, being ascribed to the formation mechanism of spherical structure from cubic structure. Therefore, the work presented a strategy to controllably design KCl crystal with different structure and morphology in a green way.

Chapter V: Sylvite (KCl) is a classical soluble mineral with high solubility, endowing the possibility to precisely adjust its surficial structure for flotation recovery. In this work, efforts have been originally made to study flotation behaviors of KCl with (200) and (222) exposing facets. KCl (200) crystals had a higher recovery than that of KCl (222) with octadecylamine hydrochloride (ODA). FTIR and XPS results indicated that interaction force between KCl and ODA was not chemical absorption. Zeta potential results further implied the mechanism that the ODA reacted with KCl by static force and KCl (200) possessed a lower potential than KCl (222) and thus facilitated the flotation process. 2D as well as 3D AFM results provided microscopic details of perfect cubic KCl (200) and octahedron KCl (222) samples where layered growing method of former samples exhibited more edges with hanging Cl bonds, leading to its more negative surficial potential and less hydrophilic property, enhancing flotation recovery. Moreover, adhesion & adsorption force further illustrated that KCl (200) obtained a stronger interaction with bubbles, in coincidence with its better flotation recovery. KCl crystals with (200) exposing faces promoted flotation in comparison with crystal with (222) faces, offering strategy to reserve (200) faces for designing KCl crystals with high recovery.

Chapter VI: By understanding minerals as crystals, a crystallization-controlled methodology was performed to enhance the floatability of soluble minerals. Here, aimed strategies were applied to modulate the crystallization of KCl salt to grow crystals with various shapes as cubic-, hopper- and needle-like structure. Stereoscope and scanning electronic microscopy (SEM) helped to unveil the morphologies where X ray diffraction (XRD) characterized their high crystallinities. Afterwards, Atomic Force Microscope (AFM) was performed to research the crystallizing behaviors that cubic-like structure was obtained by turbid fast growth, while hopper-like structure formation was due to the constant high supersaturation and needle-like crystal occurred under still fast crystallization. Flotation tests with octadecylamine hydrochloride (ODA) as collector demonstrated the floatability of samples obeyed the order as needle-like (96.19 %) > hopper-like (81.59 %) > cubic-like (80.08 %) KCl samples. The mechanism was studied by surface area and related interaction tests. BET result demonstrated the highest surface area of needle-like structure than that of hopper-like and cubic-like structure. Besides, induction time combined with adhesion & desorption force tests further explained the better interaction of needle-like sample with bubble than cubic-like sample. While the special structure of hopper-like structure with lower weight but inner filled solution resulted in its near equivalent floatability with cubic-like sample. In conclusion, a new strategy for promoting flotation behavior by designing the crystallization of soluble KCl was proposed, shedding some light on further application on other soluble or semi-soluble minerals.

Chapter VII: As one kind of Face centered cubic crystal, sylvite has stressed great importance since it is main resource of potassium element. For decades, flotation is the most used method to yield an ideal recovery. The fact that ethanol could be mixed with water with any proportion gave the chance to modulate mother liquor of KCl flotation. In this work, the impact of ethanol on flotation behavior of sylvite was firstly researched, also the inner mechanisms were unveiled in detail. It was concluded that the addition of ethanol from 0.05% to its maximum limit 0.4% could promote the flotation, where 0.2% dosage was the best recovery as 94.79%. Ethanol would not only change the morphology of KCl with more exposing (111) faces area but also decrease the surface tension of solution. The (111) faces with worse interaction with collector ODA would inhibit the flotation while lower surface tension would help with the flotation. That was the reason for the best flotation behavior of KCl in co-saturated solution of ethanol and KCl. This research provided a new method to elevate the flotation recovery of sylvite.

Keywords: Sylvite, crystallization, supersaturation, cooling method, evaporation, Pb^{2+} , zeta potential, flotation, stereoscope, AFM, FTIR, XPS, BET, adsorption/desorption force, conducting time, ethanol, surface tension, surfaces;

Contents

Abstract.....	I
Extended Abstract.....	II
Index of Tables	XI
Chapter I. Introduction.....	1
1.1. Justification.....	1
1.2. Objectives	2
1.2.1. <i>General objective</i>	2
1.2.2. <i>Goals</i>	2
Chapter II. Literature Review	3
2.1. Introduction.....	3
2.2. Research state of typical soluble salts.....	5
2.2.1. <i>Carnallite</i>	6
2.2.2. <i>Picromerite</i>	7
2.2.3. <i>Sylvite</i>	8
2.2.4. <i>Hailite</i>	10
2.3. Flotation mechanism of sylvite and hailite.....	10
2.3.1. <i>Ions exchange theory</i>	10
2.3.2. <i>Dissolution heat theory</i>	11
2.3.3. <i>Surface charge/collector adsorption theory</i>	13
2.3.4. <i>Interfacial water structure theory</i>	14
2.4. Summary	16
References.....	17
Chapter III. Materials and Methods.....	22
3.1. Materials	22
3.2. Methods.....	22
3.2.1. <i>Methods for Chapter IV-Controllable reparation of KCl with various shapes through green supersaturation modulation</i>	22
3.2.2. <i>Methods for Chapter V-Preparation of KCl samples with various exposing facets</i>	23
3.2.3. <i>Methods for Chapter VI-Preparation of KCl samples with various shapes</i>	25
3.2.4. <i>Methods for Chapter VII-Preparation of KCl samples with various shapes</i>	28
3.3. Characterizations.....	30

3.4. Summary	30
References.....	30
Chapter IV. Controllably constructing morphology and structure of potassium chloride crystal by green supersaturation modulation	32
4.1. Introduction.....	32
4.2. Results and discussion	33
4.2.1. <i>Supersaturation controlled crystallization</i>	33
4.2.2. <i>Crystal Products</i>	39
4.2.3. <i>Structural and surficial properties</i>	47
4.3. Conclusions.....	49
References.....	50
Chapter V. Novel insights into sylvite flotation modulated by exposing facets.....	55
5.1. Introduction.....	55
5.2. Results and discussion	56
5.2.1. <i>Morphology characterization</i>	56
5.2.2. <i>Crystal Structure</i>	57
5.2.3. <i>Flotation affected by crystal facets</i>	58
5.2.4. <i>Interaction between KCl crystal and collector</i>	59
5.2.5. <i>Illustration for flotation process</i>	64
5.3. Conclusions.....	65
References.....	66
Chapter VI. Novel strategy for improved sylvite flotation through controlled crystallization.....	71
6.1. Introduction.....	71
6.2. Results and discussion	72
6.2.1. <i>Crystal structure and morphology</i>	72
6.2.2. <i>Crystal growth mechanism</i>	74
6.2.3. <i>Flotation test</i>	77
6.2.4. <i>Flotation Mechanism</i>	78
6.3. Conclusions.....	85
References.....	85
Chapter VII. Impact of Ethanol on flotation of sylvite flotation	90
7.1. Introduction.....	90
7.2. Results and Discussion	91
7.2.1. <i>Morphology and structure</i>	91

7.2.2. <i>Flotation experiments</i>	94
7.2.3. <i>Mechanism</i>	94
7.3. <i>Conclusions</i>	97
References	98
Conclusions	100
Personal achievement	102

Index of Figures

Fig. I. 1. World map of significant potash-bearing marine evaporite basins[3].	4
Fig. I. 2. Mineralogical subdivision of brine substrate[5].	4
Fig. I. 3. Ternary phase diagram of $MgCl_2$ -KCl- H_2O under $35^\circ C$ [11].	7
Fig. I. 4. The configuration of system containing (a) KCl saturated solution with KCl crystal, (b) only KCl saturated solution[33].	9
Fig. I. 5. Radial distribution function of electrolyte ions systems[42].	12
Fig. I. 6. Optical microscopy photographs of the KCl salt surface with 1×10^{-4} M ODA in a saturated KCl solution[46].	14
Fig. I. 7. Interfacial water structure at KI, KCl, and NaCl surfaces[48].	16
Fig. IV. 1. Effect of conditional parameters for KCl crystal grown through batch cooling experiments: Effect of stirring speed on crystal grown, (a) 100, (b) 200, (c) 400, and (d) 600 rpm from $30^\circ C$ to $27^\circ C$ in 60 min; Effect of cooling range on crystal grown, (e) $24-2^\circ C$, (f) $27-24^\circ C$, (g) $30-27^\circ C$, and (h) $33-30^\circ C$ (with cooling period of 60 min); Effect of cooling rate on crystal grown, (i) $12^\circ C/h$, (j) $3^\circ C/h$, (k) $1.2^\circ C/h$ and (l) $0.75^\circ C/h$ from $30^\circ C$ to $27^\circ C$ with 400 rpm; Effect of additive seeds amount on crystal grown, (m) 0.1 g, (n) 0.2 g, (o) 0.3 g, and (p) 0.4 g. Scale bar= $500\ \mu m$.	34
Fig. IV. 2. Stereoscopic results of hopper-like KCl crystals grown by batch cooling experiments from $30^\circ C$ to $27^\circ C$ in 60min, with 300 and 500 rpm, respectively.	34
Fig. IV. 3. Illustration of atoms on face, edge, and corner position of cubic crystal.	36
Fig. IV. 4. Stereoscopic results of hopper-like KCl crystals grown by batch cooling experiments from 30 to $27^\circ C$ in with stirring speed at 500 rpm and cooling rate as 6, 4, 2.4, 2, 1.5, 1, 0.86 and $0.6^\circ C/h$. Scale bar= $500\ \mu m$.	38
Fig. IV. 5. Stereoscopic results of KCl reagent.	38
Fig. IV. 6. X-ray diffraction and Stereoscopic results of cubic and hopper like structure KCl crystals	40
Fig. IV. 7. Stereoscopic results of KCl crystals grown by batch cooling experiments from $30^\circ C$ for increasing period with cooling rate at $3^\circ C/h$, scale bar= $500\ \mu m$.	41
Fig. IV. 8. Stereoscopic results of KCl crystals grown by batch cooling experiments with stirring rate of 400 rpm and cooling rate at $1^\circ C/h$ from $40^\circ C$ for 1, 2, 3, 4, 6 and 9 h, respectively (3.2.2)	41
Fig. IV. 9. Stereoscopic results of KCl crystals grown by batch cooling experiments from $40^\circ C$ to $30^\circ C$ with decreasing cooling rate at 20, 13.33, 10, 6.67, 5, 2.5, 1.67, 1.25 and $1^\circ C/h$. Scale bar= $500\ \mu m$.	43
Fig. IV. 10. Stereoscopic results of KCl crystals grown by batch cooling experiments with stirring rate of 400 rpm and cooling rate at $3^\circ C/h$ from $30^\circ C$ for 30, 45, 75, 90, 120, 180, 210 and 300 min, respectively. (3.2.3).	44
Fig. IV. 11. Stereoscopic results of KCl crystals grown by batch cooling experiments from 30 to $27^\circ C$ with existence of 0.1mL of KOH (a) and HCl (d), and 1mL of KOH (b) and HCl (e) from 30 to $23^\circ C$ for 700 min, especially. Scale bar= $500\ \mu m$. Atomic illustration of KCl with Cl (c) or K (f) as center atom.	45

Fig. IV. 12. SEM morphology result of KCl crystals grown by batch cooling experiments with 0.1 mL additive as NH ₄ Cl, KNO ₃ , HNO ₃ , and NH ₃ ·H ₂ O stirring rate of 400 rpm and cooling rate at 3 °C/h from 30 °C for 60 min, respectively.....	46
Fig. IV. 13. SEM morphology result of KCl crystals grown by bath cooling experiments with 2.0 mL additive as NH ₄ Cl, KNO ₃ , HNO ₃ , and NH ₃ ·H ₂ O stirring rate of 400 rpm and cooling rate at 3 °C/h from 30 °C for 120 min, respectively.....	47
Fig. IV. 14. XRD results of smooth cubic with KOH, spherical, hollow cube with HCl, hopper and standard cubic KCl structure, and corresponding stereoscopic results.....	48
Fig. IV. 15. SEM results of smooth cubic with KOH, spherical, hollow cube with HCl, hopper and standard cubic KCl structure, and their surficial 3D plot results.....	49
Fig. V. 1. SEM results of cubic (a) and octahedron (b) crystals, and their corresponding stereoscope results.	57
Fig. V. 2. XRD results of cubic and octahedron crystals.	58
Fig. V. 3. Flotation kinetics results of KCl(200) and KCl(222) crystals using ODA.	58
Fig. V. 4. FTIR results of KCl(200) and KCl(222) crystals before and after flotation, respectively.	59
Fig. V. 5. XPS spectra of KCl(222) samples before: (a) survey, (c) Pb 4f, (e) K 2p, (g) Cl 2p and after flotation: (b) survey, (d) Pb 4f, (f) K 2p, (h) Cl 2p.	60
Fig. V. 6. Zeta potential results of KCl (200), KCl (222) crystals before and after reacting with ODA, and of ODA in saturate KCl solution.	61
Fig. V. 7. (a, b) Micrographs, (c, d) two dimensional & (e, f) three-dimensional AFM and (g, h) contact angle results of KCl (200), KCl (222) crystals, respectively.....	63
Fig. V. 8. Adhesion & adsorption force results of (a) KCl (200) and (b) KCl (222) crystals with saturated KCl drop, inserted in (a) were the photograph of (a ₁) approaching, (a ₂) contacting, (a ₃) adhesion and (a ₄) adsorption process, and (c) corresponding force information.....	64
Fig. V. 9. Illustration of flotation behavior of KCl crystals with various exposing faces.....	65
Fig. VI. 1. XRD patterns of cubic-, hopper- and needle-like KCl crystals.....	73
Fig. VI. 2. Stereoscopic (left) and SEM (right) images of (a, b) cubic-, (c, d) hopper- and (e, f) needle-like KCl crystals.....	74
Fig. VI. 3. Two-dimensional (left) and three-dimensional (right) AFM images of (a, b) cubic-, (c, d) hopper- and (e, f) needle-like KCl crystals.....	75
Fig. VI. 4. Stereoscopic images of cubic- and hopper-like KCl crystals.....	75
Fig. VI. 5. AFM image of KCl seeds with low concentration.	76
Fig. VI. 6. Flotation kinetics results of cubic-, hopper- and needle-like KCl crystals using ODA as collector.....	77
Fig. VI. 7. FTIR results of cubic-, hopper- and needle-like KCl crystals before and after flotation with ODA as collector, respectively.....	79
Fig. VI. 8. Potassium XPS survey of (a, d) cubic-, (b, e) needle- and (c, f) hopper-like KCl crystals before and after flotation.....	80
Fig. VI. 9. Chloride XPS survey of (a, d) cubic-, (b, e) needle- and (c, f) hopper-like KCl crystals before and after flotation.....	80
Fig. VI. 10. BET results of cubic-, hopper- and needle-like KCl crystals with size of 178-250 μm.	

.....	82
Fig. VI. 11. Induction time results of cubic-, hopper- and needle-like KCl crystals using ODA as collector.....	83
Fig. VI. 12. Adhesion & adsorption force results of (a) cubic- (b) hopper- and (c) needle-like KCl crystals with saturated KCl drop, and (d) corresponding force information.	85
Fig. VII. 1. SEM result of cubic shaped KCl crystals through cooling method.	91
Fig. VII. 2. XRD result of cubic shaped KCl crystals through cooling method.	92
Fig. VII. 3. SEM results of cubic shaped KCl crystals immersed with co-saturated solution of ethanol and KCl with increasing ethanol content as 0%, 0.05%, 0.10%, 0.20%, 0.30%, 0.40% and 0.50%, respectively.	92
Fig. VII. 4. XRD results of cubic shaped KCl crystals immersed with co-saturated solution of ethanol and KCl with increasing ethanol content as 0.02%, 0.05% and 0.10%, respectively.	93
Fig. VII. 5. Flotation recovery of KCl samples with size range of 150-178 μm using ODA as collector and increasing amount of ethanol addition as 0%, 0.05%, 0.10%, 0.20%, 0.30%, 0.40% and 0.50%, respectively.	94
Fig. VII. 6. FTIR spectra of pure KCl before and after flotation using ODA as collector.	95
Fig. VII. 7. XPS spectra of KCl before and after flotation using ODA as collector: survey(a), (d); K 2p(b), (e) and Cl 2p(c), (f).....	96
Fig. VII. 8. Surface tension of KCl solution with increasing amount of ethanol addition as 0%, 0.05%, 0.10%, 0.20%, 0.30%, 0.40% and 0.50%, respectively.....	97

Index of Tables

Table V. 1. Kinetic parameters for flotation kinetics of classical first-order model.....	58
Table VI. 1. Peaks of potassium and chloride XPS survey of cubic-, needle-, and hopper-like KCl crystals before and after flotation.	78

Chapter I. Introduction

1.1. Justification

As one of the essential parts on our planet, plants have been playing a vital role not only for atmospheric balance but also as key part in the whole food chain. Respiration and photosynthesis reactions are the most two important functions for plants growth where potassium element is critical during these processes. Global potassium resources mostly exist in the form of potassium sulphate, potassium chloride and potassium nitrate, with relatively simple composition and high potassium content, accounting for more than 80% of the global total. Efficient development and comprehensive utilization of salt-lake resources has been an inevitable choice for mining companies to reduce costs, improve benefits, optimize structure, and enhance core competitiveness. In addition, salt-lake has been regarded as the main resource of potash where potassium element exists in form of carnallite, whose chemical component is $\text{KCl}\cdot\text{MgCl}_2\cdot 6\text{H}_2\text{O}$. For decades, the most applied method to recover potassium from salt-lake is by decomposition of carnallite, followed by flotation or anti-flotation process in order to yield high purity of KCl out of NaCl for later fertilization production preparation. Hitherto, most researches focused on the improvement of flotation reagents with higher recovery, where the industrial production has already reached a mature efficiency with limited room for further improvement but unclear flotation mechanism. The interaction between the most applied collectors and KCl or NaCl is a key parameter to understand the flotation behavior which remains unclear yet. Novel aspects with hope to realize a better flotation behavior are in urgent need to not only understand the flotation behavior but also shed innovative light on the potassium fertilizer industrial production.

In order to realize a new prospective of soluble salts, the fundamental properties normally provide some possibilities. One obvious and important feature of KCl or NaCl is their high solubility in water which allows the formation of salt-lake as potash to be resolved in water to reach a supersaturated saline. Unlike normal solid minerals, soluble as well as semi-soluble minerals share an adjustable formation process, *i.e.*, malleable crystallization. Conventional strategies to adjust the mineral particle properties mostly focus on grinding process via various types of grinding medium or controlled grinding period, to prepare mineral with aimed particle size distribution, shape or exposing facets. However, the grinding process always consumes much energy with limited modulation efficiency. The fact that most minerals belong to various types of crystals has been ignored for long, which should stress attention for a better understanding of minerals so as to modulate their properties.

Among the broad types of minerals, soluble or semi-soluble minerals hold a relatively special nature where the resolve/re-crystallization process provides the possibility to construct the surfaces with ideal properties. It is a promising aspect to understanding them as crystals to modulate the particle shape as well as surficial structure for aiming purposes. The relationship between crystallization process and mineral processing is in urgent need to be unveiled in order to yield a comprehensive understanding of possible new strategy to modulate flotation behaviors of soluble/semi-soluble minerals such as sylvite, hailite, carnallite and phosphogypsum, *etc.*

1.2. Objectives

1.2.1. General objective

To propose a novel idea of crystallization modulated flotation strategy for soluble and semi-soluble minerals. Taking a typical soluble mineral-potassium chloride as an example, the relationship between solution condition and grown crystals should be firstly unveiled to prepare KCl particles with various shapes, where their corresponding flotation behavior as well as mechanism should also be well studied to pave the path to the idea of crystallization modulated flotation for broader applications.

1.2.2. Goals

- 1) To investigate the properties of KCl on basis of its crystallization features. By modulating the solution condition, KCl crystal particles with various structures and surficial properties will be prepared.
- 2) To study the formation process of KCl samples with (200) or (222) exposing surfaces. To measure the effect of exposing facets on the flotation behavior of KCl particles where the corresponding mechanism will be well studied.
- 3) To investigate diverse KCl particles preparation including hopper-like, needle-like and cubic-like structures. The related formation mechanisms, flotation behaviors as well as mechanisms will be elaborately unveiled.
- 4) To research the impact of ethanol which has been applied as the dispenser during filtering process on KCl particle structure and flotation behavior. The inner mechanism will be investigated in detail.

Chapter II. Literature Review

2.1. Introduction

For centuries, ores with high values have been found widely distributed around the world, where most abound with impurities which greatly hinder the extraction process as well as applications. Multiple methods were applied to recover useful minerals out from gangue. Based on physical properties like density and magnet, several minerals could be well distinguished from others with dramatically different properties[1]. However, for most types of minerals with indistinguishable density or non-magnetic ore as well as lower grade minerals, conventional physical strategies were inapplicable. To solve the urgent challenge, flotation method based on chemical properties was proposed which brought mineral engineering field with fresh new hope followed by extremely high accuracy with aiming strategies. In the process of mineral separation, the technical method of extracting useful minerals from ores by using the difference in mineral hydrophobicity (mostly with help of collector adsorption based on surficial properties of minerals) is called flotation.

Among the multiple types of ores, there are several minerals playing an important role for plants growth where fertilizers are always in high demand with necessary elements include potassium, nitrogen, phosphorus, magnesium, and so on. Taking potassium element as an example, it not only helps with the main functions of plants' cells but also promotes the balanced adsorption and utilization of nitrogen and phosphorus[2]. The main original ore of potassium is potash constituted by potassium chloride. Due to the importance of fertilizers for agricultural crops, the annual demand for potash keeps steadily increasing with the continuous growth of the global population and the upgrading of the human diet habits. According to incomplete statistics, the global potassium resources are relatively rich, the total amount is about 250 billion tons with extremely uneven distribution worldwide. As can be seen from the global potassium resource distribution in Fig. 1[3], most of the global potassium resources are concentrated in a few countries such as Canada, Russia, Laos and a few northern European countries, resulting in obvious regional distribution characteristics of potassium resource distribution and high demand of importing potassium resources for most countries especially agricultural ones like China, India, Brazil, etc[4].

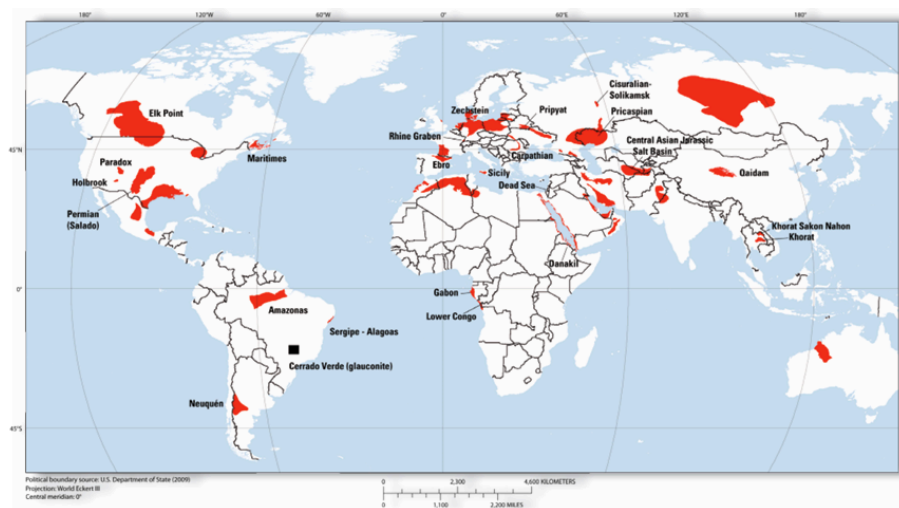


Fig. II. 1. World map of significant potash-bearing marine evaporate basins[3].

As resource of abundant types ions including potassium, sodium, chlorine, magnesium as well as other elements like lithium, boron, rubidium, cesium, iodine, bromine, etc, as shown in Fig. 2[5]. Due to the great importance of potassium element to fertilizers, salt-lake has been the main resource for production of potassic fertilizer. The largest salt industrial is Sakatchewan company in Canada[3,5]. In nowadays industrial production, the most applied recovery methods of potash salts to valued productions include decomposition of carnallite, transformation of picromerite followed by flotation or indirect flotation[6]. In order to realize a high efficiency and benefits, abundant researches have been focused on the improvement of flotation process.

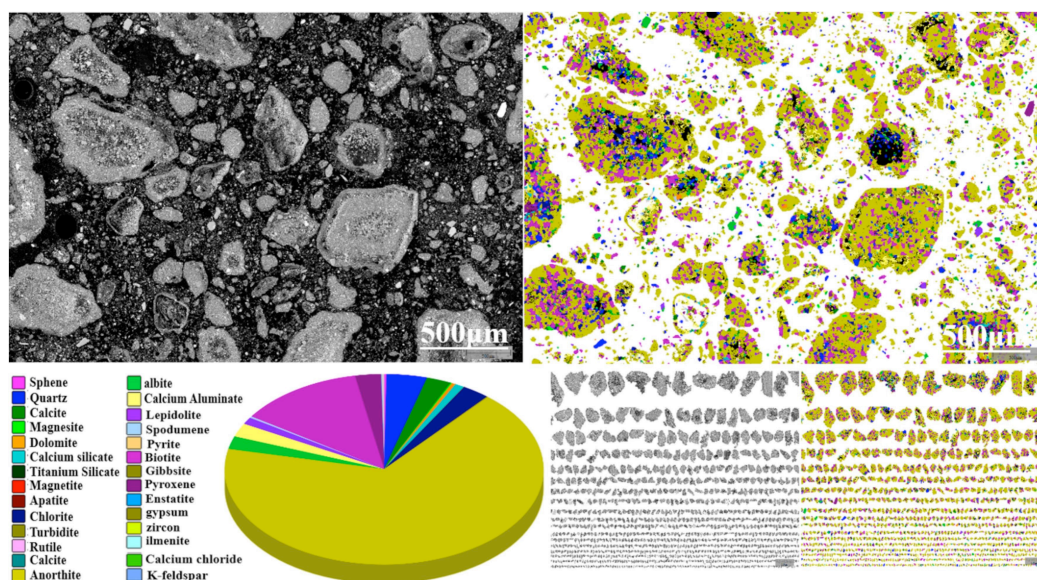


Fig. II. 2. Mineralogical subdivision of brine substrate[5].

Compared to classic flotation process of non-soluble minerals, the high solubility property of salts brings several notable features during the flotation process. Firstly,

unlike most flotation process with water as slurry, all the solution included should be replaced by the saturated brine consisting of the same salt being floated[7]. Besides, the reagents with higher concentration than CMCs in brine will form flocs and then be attached to surfaces of salt particles and bubbles[8]. Furthermore, it is worth mentioning that specific details should be addressed with different salts according to their properties. For instance, the temperature of solution might bring drastic influence to the formation of some salts like potassium chloride, magnesium sulfate and potassium nitrate but slight effect on sodium chloride. One other notable detail is that the brine slurry usually contains various types of ions with high concentration, resulting in large ion strength property, viscosity and surface tension of the solution which might magnify the influence of foreign ions. At last, the long-existing dissolution/recrystallization on surfaces of KCl leads to the unstable property of mineral surfaces which further hinders the related research of surficial status. As a consequence, the experiments of soluble salts as well as semi-soluble minerals should be carefully designed according based on the crystal properties, especially those soluble salts whose formation process will be greatly affected by the solution conditions like temperature, ions type and concentration, disorder degree, etc. In the following section, research status of several typical soluble salts will be firstly introduced to provide a basic understanding especially the crystal structure as well as flotation methods.

2.2. Research state of typical soluble salts

For the past decades, the industrial extraction of salt-lake mainly focused on the purification and application of potassium, magnesium and sulfate compounds. Among the multiple soluble salts in salt-lake, there are a few types of salts with attention due to their complicated reaction during industrial extraction like carnallite and picromerite. As one of the most important products, sylvite is one of the aiming valuable mineral while hailite is its common association mineral[9]. As described in previous paragraph that flotation happens when the mineral particles exhibit a hydrophobic surface (either by natural property or modified by chemical reagents, *i.e.*, collectors), one drawback of soluble salts is that they normally have a hydrophilic surfaces due to the high hydration energy of composing ions. As a result, collectors design is one of the most researched aspects for the flotation process. Here, these typical soluble salts will be divided into two types as double salt (carnallite, picromerite, kailite) and single salt (sylvite, hailite) where their basic property and research status will be introduced in detail.

2.2.1. Carnallite

As demonstrated by previous section that potassium holds a vital function in plants growing process, properties of its raw material-carnallite should be well understood to help modulate the later formation of KCl. The carnallite crystals belong to the orthorhombic (rhombohedral) halide minerals. The constitution of carnallite is $\text{KCl} \cdot \text{MgCl}_2 \cdot 6\text{H}_2\text{O}$, where by adding specific saline it will be resolved, decomposed, filtered, rinsed and filtered to obtain crude potassium chloride. During the decomposition process, the high concentrated K^+ and Cl^- ions will crystallize out in form of solid crystals under proper conditions with left saturated carnallite saline[10]. The key parameter of the decomposition process is to add saline which should be carefully determined through the $\text{MgCl}_2\text{-KCl-H}_2\text{O}$ ternary phase diagram as shown in Fig. 3[11]. The main method to apply carnallite is to decomposition for potassium chloride with relative high concentration followed by flotation. M. Hancer and J. Miller studied the flotation of mixed salt that in the process of flotation, it was difficult to directly float $\text{KCl} \cdot \text{MgSO}_4 \cdot 3\text{H}_2\text{O}$ and carnallite which must be firstly converted into other salts such as picromerite[12].

After decomposition of carnallite, there are mainly two methods to prepare potassium chloride productions with high purity: directly flotation where potassium salts like potassium chloride and potassium sulfate are the aiming flotation target and indirect flotation where tailing mineral sodium chloride is the aiming target with left potassium chloride with high purity[6]. For indirect flotation method which requires special conditions for the raw ore with high cost of flotation reagents, it is not available in many areas. At the meantime, due to the advantages of direct flotation such as strong adaptability to the grade of sun-dried raw ore in salt pan, low investment in plant construction and simple process, it is widely used in many salt lake area for potassium fertilizer production of the industry around the world[13].

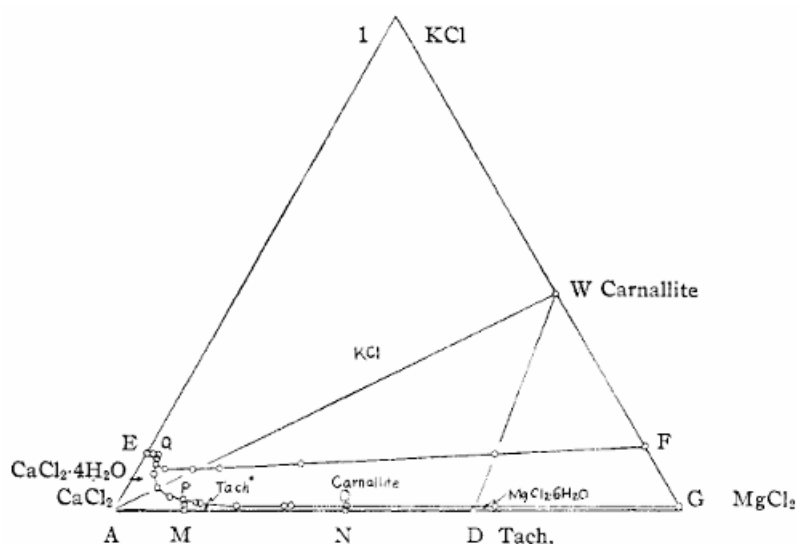


Fig. II. 3. Ternary phase diagram of $\text{MgCl}_2\text{-KCl-H}_2\text{O}$ under 35°C [11].

In real production process, carnallite always appears with other impurities where sodium chloride is the most common salt. Wang Shijun, et al. researched that according to the ratios of potassium chloride, sodium chloride and magnesium chloride, raw carnallite ores could be divided into normal type, high magnesium type, high sodium type and high sodium & magnesium types where the ratios would greatly influence the decomposition process[14]. Based on their decomposition calculation at different temperatures, it was demonstrated the higher recovery rate of decomposition occurred when using high sodium type carnallite with ratios of MgCl_2/KCl as 1.625 and KCl/NaCl as 2.795. Besides, Bao Jiqing et al. studied the dissolution & transformation process of carnallite in solutions with different concentrations of NaCl which was found to show little influence on the dissolution of carnallite[15]. Xia Shuping et al. focused on the decomposition & crystallization kinetics of carnallite and investigated the effects of solution temperature, stirring speed and magnesium ion content in the decomposition mother solution on the decomposition & crystallization process of carnallite[16,17]. They found that the concentration of magnesium ion in solution had a direct effect on the decomposition rate of carnallite where the solution viscosity would be dramatically influenced by the magnesium ions content[18]. Besides, Qian Lihua et al. further researched the effects of stirring condition, blade material on the decomposition behaviors of carnallite as well as the nucleation and growth of potassium chloride crystal in different mother solution in detail[19]. It was pointed out that due to the presence of a large number of magnesium ions in carnallite mother liquor, the nucleation rate of potassium chloride crystal increased greatly while the growth rate decreased, resulting in smaller potassium chloride crystals with carnallite mother solution than that in pure potassium chloride mother solutions[20].

2.2.2. Picromerite

Picromerite is also known as schoenite, which is composed by potassium, magnesium and water with chemical formula as $\text{K}_2\text{SO}_4\cdot\text{MgSO}_4\cdot 6\text{H}_2\text{O}$. As demonstrated above that potassium is important during plants growing, while other elements like sulfur and magnesium are also essential to plants. As a consequence, picromerite can be applied as fertilizer for various types of agriculture field. For instance, picromerite has been proved to help with the growth of cotton with a production increase up to 9.2%-19.6%[21]. Pan. et, al. found that by applying picromerite to pepper growth, the productivity as well as vitamin C content could be promoted to reach a better economic benefit[22]. Other plants like grapes and

tomatoes have also been demonstrated to show promoted growth with picromerite fertilizer[23,24]. What's more, due to the alkalescence property, picromerite is also applied with saline-alkali soil remediation amendments to repair and regulate the soil for crops planting[25–27].

High grade picromerite can be obtained by adding a certain proportion water to dissolve and evaporate the mixed salt from natural evaporation of salt-lake brine as raw material[28]. Cheng, et al. applied a multiple-temperature dynamic evaporation experiments to obtain mixed salts containing picromerite by adding water to the raw ore from salt-lake where picromerite concentrate could be collected by indirect flotation of the mixed salts[29]. Jannet D.B. et al. studied the precipitation process of potassium sulfate from K^+ , Mg^{2+} // Cl^- , SO_4^{2-}/H_2O five-phase diagram system solutions at 25°C[30]. It was found that picromerite was an intermediate product during the precipitation of potassium sulfate, indicating that the metastable zone of picromerite extended to and covered the crystalline zone of K_2SO_4 . Cao, et al. prepared picromerite from mixed salt of potassium-sulfate brine through natural evaporation by two-step decomposition and conversion method where the product quality could meet the market requirement with high production effect[31]. Besides, Zhang, et al. learnt the crystallization properties of picromerite to design a hot melt cold crystallization method to prepare picromerite with large size[32].

2.2.3. Sylvite

The chemical composition element of sylvite is potassium chloride. It belongs to the Face Center Cubic (FCC) type crystals. In case of KCl, by understanding this typical soluble mineral as a type of crystal with the balance between resolve and crystallization process, the solution condition might be carefully modulated in order to realize a controllable formation process of KCl particles. Apart from the high solubility of KCl in water, one other important property is that the temperature of solution greatly affects the solubility which should be carefully maintained as consistent to avoid undesired crystallization or dissolution.

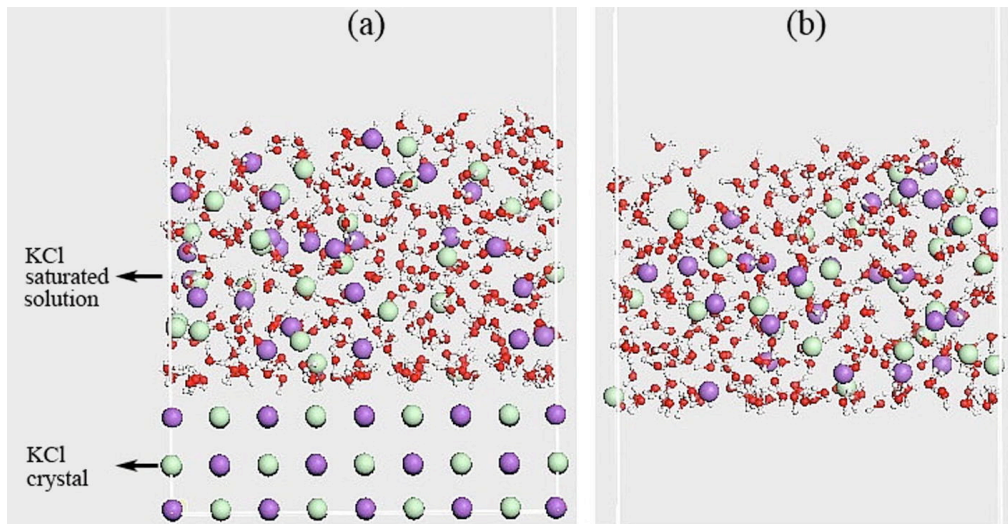


Fig. II. 4. The configuration of system containing (a) KCl saturated solution with KCl crystal, (b) only KCl saturated solution[33].

As mentioned above that to recover sylvite, flotation methods are mainly divided into two types including direct flotation where KCl is the target mineral through the addition of collectors to directly obtain potassium chloride products. The other method is indirect flotation referring to obtain non-target minerals, leaving potassium chloride products in the tailings to reach a high purity. In most cases, hailite is the typical indirect flotation target which will be introduced in the next section. The research status of potassium chloride and sodium chloride should be introduced for a better understanding.

For the direct flotation of KCl, collectors play a vital role to modify the surficial property. Till now, both alkyl aliphatic amines and anionic alkyl sodium sulfonate are the most applied collectors which firstly forms as flocs to be selectively adsorbed on the surface of the potassium chloride crystal to change the hydrophobicity[34,35]. The modified potassium chloride crystal exhibits hydrophobic property which could be combined with bubbles to complete the flotation. For these amine collectors, the length of molecules (*i.e.*, the number of carbon atoms) is the key to affect the dosage as well as flotation behaviors. At present, collector with carbon chain length above 12 has been the main choice around the world. For instance, cationic collector dodecylamine hydrochloride (DDA: $\text{CH}_3(\text{CH}_2)_{11}\text{NH}_3\text{Cl}$) and anionic collector sodium dodecyl sulfonate (SDS: $\text{CH}_3(\text{CH}_2)_{11}\text{SO}_3\text{Na}$) are mainly used for potassium chloride flotation in the United States[36], while in Canada the mainly used collector for potassium chloride is cationic octadecylamine hydrochloride (ODA: $\text{CH}_3(\text{CH}_2)_{17}\text{NH}_3\text{Cl}$)[37].

2.2.4. Hailite

Hailite is composed by sodium chloride (NaCl), which shares similar crystallinity with sylvite as FCC type, resulting in their similar crystallization habit as cubic structure according to their nature. However, they exhibit diametrically different surficial charge that sylvite has a negatively charged surface while hailite shows positive surface charges. Besides, with different hydration energy values, K and Na ions have various ionic hydration behaviors in solution. Their above different properties result in specific flotation strategies for sylvite and hailite, which will be discussed in following section.

2.3. Flotation mechanism of sylvite and hailite

As mentioned above that sylvite and hailite share the same crystal structure as face center cubic. However, they were found to exhibit opposite surface charges and other differences during flotation. Here, the main flotation mechanism of these two types of salts will be introduced, and some prospective speculations will be given to provide some new perspectives for the mechanism.

Although the direct flotation method to obtain potassium chloride concentrate has been widely applied around the world, the interfacial reaction process and flotation mechanism are still not well understood. The lack of theoretical guidance for the production of direct flotation and recognition of the flotation reaction process and the mechanism of adsorption of collector directly lead to the fact that there is no definite collector preparation in the factory where the dosage of is determined by experience. The type and grade of raw ore have been greatly changed compared to previous progress under different whether and region, resulting in the flotation system is not always in constituent but the factory fails to adjust the collector regime according to the changes. It can be seen that the flotation mechanism of soluble salt is an urgent key issue to the production process stabilization, collector development as well as the high utilization rate of limited resources. Tons of previous researches have been focused on the flotation mechanism of potassium chloride which could be divided into the following types.

2.3.1. Ions exchange theory

As described as the title, ions exchange theory is based on the composing ions of mineral and collector molecule. For potassium chloride, its composing ions are K^+ and Cl^- ions which should be compared with ions of functional groups in collectors. In 1935, this theory was provided by Gaudin for the first time that the most applied amine salts with generated RNH_3^+ during flotation for potassium chloride was due to the similar ion size of RNH_3^+ with K^+ [38]. In 1956, D. W. Fuerstenau et al. studied

the single salt flotation paired by alkali and halide elements and provided an extension for ions exchange theory[39]. The authors further demonstrated that those soluble salts with similar anion ion size with NH_3^+ would be exchanged so as to be attached on crystal surfaces through the ions exchange process. In other word, the RNH_3^+ ions could be substituted by the K^+ ions on surfaces of KCl minerals to reach a well adsorption state for further flotation behavior. The fact that K ions with radius as 1.35 Å could be well matched with RNH_3^+ whose similar radius is 1.43 Å concluded their relative high exchange possibility. Meanwhile, the mismatch of RNH_3^+ ions with other types of ions might render its difficulty to be attached, resulting its inability to float other minerals like sodium chloride where the ion radius of Na^+ is 0.95 Å which is far smaller than that of RNH_3^+ . As a consequence, only when the size of anion ion is in coincidence with that of functional group, the soluble salt could be floated by the collector by the ions exchange effect.

However, this theory was later found to be unacceptable to many other soluble salts flotation process. For example, alkyl sodium sulfonate with chemical component as RSO_3Na was also found to have good floatability for potassium chloride while the radius of RSO_4^{2-} is 2.4 Å which oversized that of Cl^- ions as 1.8 Å[40]. This theory was therefore obsolete as a result and new theories were put up to explain the related mechanism.

2.3.2. Dissolution heat theory

In the 1950s, Rogers and Schulman carefully studied the soluble salt flotation via Langmuir single molecule membrane, surface tension tests along with flotation experiments and proposed that the flotation of soluble salts mainly depends on the competitive adsorption of water molecules and collector molecules on the surface of soluble crystals[41]. They found that the hydration state of the crystal and the collector was the main factor contributing to the flotation process. According to the relevant theories, soluble salts could be classified into those with weak, moderate, and strong hydration capacities. Salts with weak hydratability could be floated simultaneously by both alkylamine collectors and alkyl sulfonate collectors. Those with stronger hydratability could be floated by fatty acid-based collectors, while those with very strong hydratability could not be floated. The strength of a salt's hydration capacity can be determined by its enthalpy of dissolution which refers to the difference between the lattice energy of the soluble salt crystal and the hydration energy of the lattice ions themselves. This theory was named as the dissolution heat theory.

According to this theory, ions with strong hydration capacities (such as magnesium, lithium, and sodium ions) could influence the thermal motion and also reduce the migration frequency of the water molecules in their vicinity. Ions with weaker hydration abilities, such as potassium, chloride, and iodine ions, would correspondingly increase the migration frequency of water molecules around the ions. Based on the varying hydration abilities of cations and anions, soluble salt crystals with weaker hydration capabilities like potassium chloride could be floated by fatty amine collectors and alkyl sulfonate collectors. Salts with stronger hydration abilities, however, could not be floated by these two types of collectors. Nevertheless, due to the lack of researching apparatus, the theory of dissolution heat was not further investigated by elaborate experiments. Indeed, it still provided a basic speculation for understanding the saline condition from an ionic aspect, promoting the later researches for hydratability of various ions (Fig. II. 5)[42].

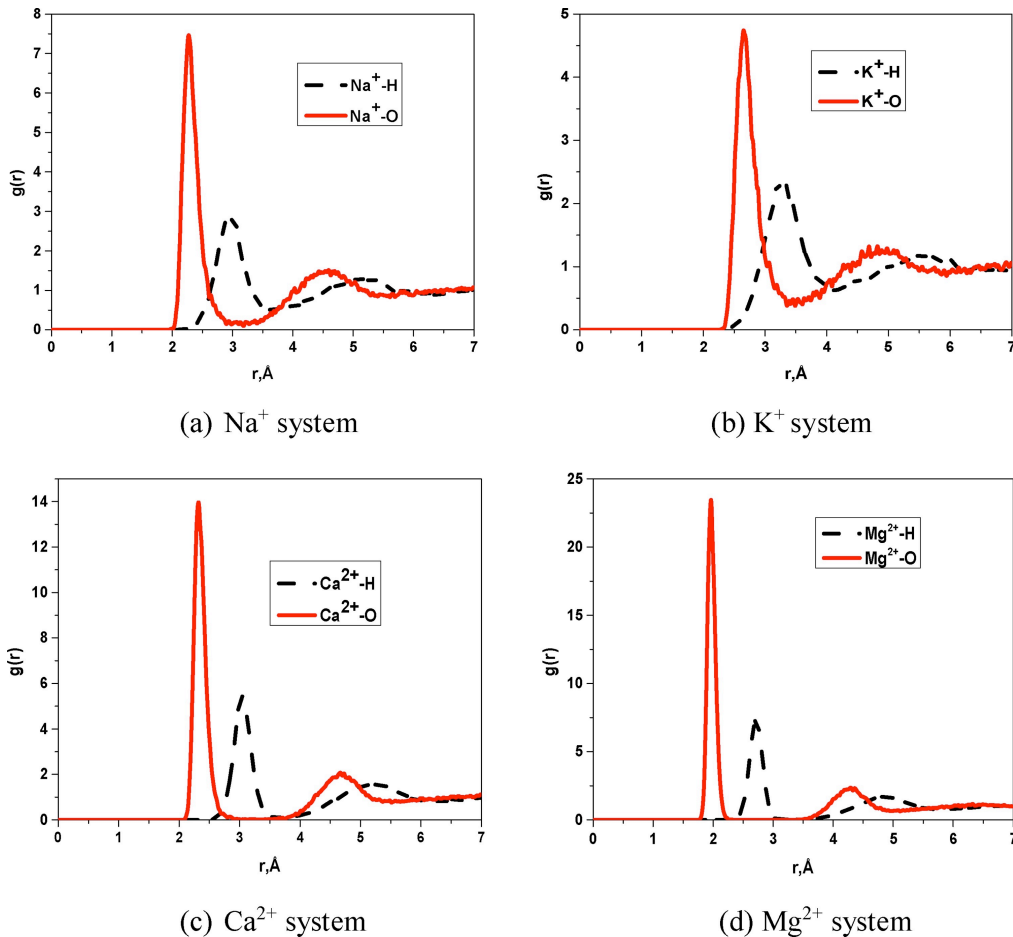


Fig. II. 5. Radial distribution function of electrolyte ions systems[42].

2.3.3. Surface charge/collector adsorption theory

One other classic theory about the soluble salt flotation is the surface charge/collector adsorption theory, which was proposed at almost the same period as the heat of solution theory. In 1968, Roman et al. proposed that the flotation process of soluble salts was mainly completed by electrostatic adsorption between dissolved collectors and crystal surfaces[43]. It was supposed that the surface charges of soluble salt crystal particles in their corresponding saturated solution were different-the surface of potassium chloride crystals was negatively charged, while the surface of sodium chloride crystals was positively charged. When applying positively charged amine collectors, it could be adsorbed on the surface of negatively charged potassium chloride crystals to complete flotation but not for sodium chloride with positive surface charges. This theory was a controversial theory since the flotation of soluble salts was carried out in a saturated solution of the corresponding salt with relatively high ionic strength. As a consequence, the double layer on the crystal particles surface was almost completely compressed which made it difficult to determine the charge on the surface of the soluble salt crystal particles.

In 1992, a research group of professor Miller from University of Utah measured the surface charge of potassium chloride and sodium chloride particles in their corresponding saturated solutions by experimental methods for the first time[44]. By measuring the unbalanced electrophoretic mobility, it was determined that the surface of potassium chloride was negatively charged while the surface of sodium chloride was positively charged. This groundbreaking progress successfully ended the years of controversy over the surface charge of soluble salts crystals. Furthermore, this group also measured the surface charge of various alkali halide single salts and theoretically calculated the surface charge of the crystals using the ionic lattice hydration theory with relatively consistent and reliable results. At the same time, the study found that the flotation of soluble salts could only occur with a large amount of collector in form of precipitation. In 2010, Cao Qinbo et al. also found that the ODA collectors were adsorbed on breaking KCl surfaces with lattice imperfection property[45]. It was demonstrated via experimental and theoretical methods that the positively charged hydrophilic group of cation collectors would interact with the negatively charged Cl⁻ of the lattice defect on the KCl crystal surface and thus being adsorbed to realize the flotation process as shown in Fig. II. 6.

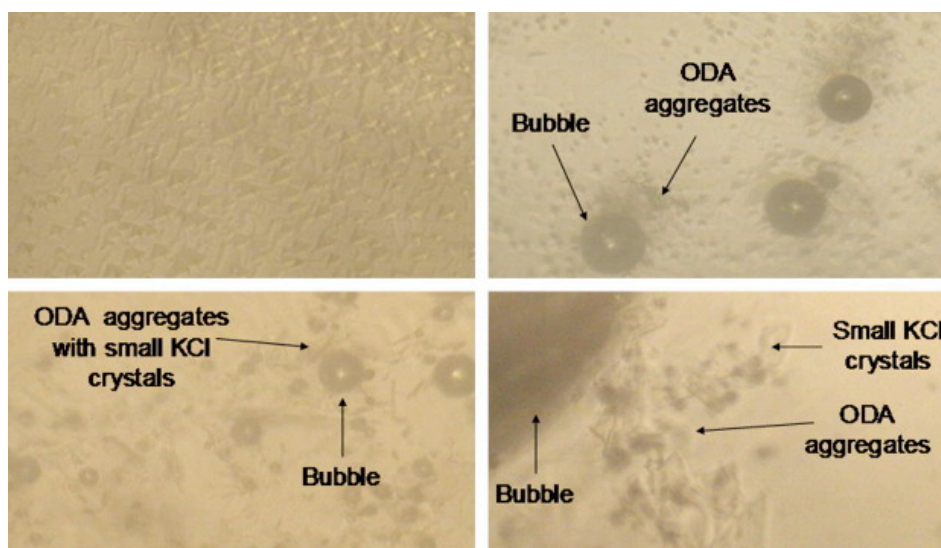


Fig. II. 6. Optical microscopy photographs of the KCl salt surface with 1×10^{-4} M ODA in a saturated KCl solution[46].

The surface charge collector adsorption theory has been well demonstrated by the direct evidence through quantities experiments for the first time with further support through theoretical calculations. This theory also unveiled the mechanism that potassium chloride was floated by amine cationic collectors while sodium chloride could not be floated by cationic collectors. However, further flotation experiments also showed some results that were completely different from this theory. In particular, it could not explain the phenomenon that potassium chloride could be floated by both cationic (like alkylamines) and anionic collectors (like sodium alkyl sulfonates). As a result, the surface charge collector adsorption theory indeed provided some possible suggestion for help understanding the mechanism but also was proved to be a dilemma. Although some later studies gave an explanation from the perspective of surface lattice oxidation defects which still remained controversial[47].

2.3.4. Interfacial water structure theory

Since the previous surface charge theory could not well explain the controversial fact that potassium chloride can be floated by both cationic and anionic collector, the research group of Dr. Miller proposed the interfacial water structure theory based on abundant experimental studies in 2000[48], The interfacial water structure theory is the latest theory on the flotation theory of soluble salts and has been recognized by other researches.

The interfacial water structure theory inherited and developed the heat of solution theory that it was also believed that the hydration degree of crystal ions was

an important parameter to flotation. One feature of aqueous saline is that water molecules can form hydrogen bonds in three forms: one is the “ice-like structure water” formed by hydrogen bonds, the other is the “liquid structure water” in the form of hydrogen bonds between non-idealized simple water molecules, and the free water molecules without formation of hydrogen bonds[49]. The interfacial water structure theory believed that for soluble salt crystals, both the anions and cations had a certain influence on the bulk water structure of the solution main influence on the "ice-like structure water" in the solution[50].

According to the theory of interfacial water structure, if a certain salt can enhance the “ice-like structure water” in the aqueous solution, then this salt is a “water-structured dense salt”. On the other hand, if a certain salt can weaken the “ice-like structure water”, then this salt is a “water-structured loose salt”[48]. For “dense water-structured salt” like sodium chloride, due to the enhancement of the hydrogen bond network of water molecules in the solution, a dense water molecule film can be formed on its crystal interface which prevents the collector molecules from being adsorbed on the crystal surface. As a result, this type of soluble salts cannot be floated by dodecylamine and sodium dodecyl sulfate collectors. As for “water structure loose salt” with a destructive effect on the water structure of the solution itself, the weakened hydrogen bond network between the water molecules in the solution hinders the interaction between the water molecules on the crystal surface. Therefore, when dodecylamine and sodium dodecyl sulfate are used for flotation, the collector molecules can easily penetrate through this loose layer of water molecule film to reach and be adsorbed on the crystal surface crystals of soluble salt to complete flotation process.

For the first time, the water structure theory completely explained the flotation process of soluble salts from the perspective of interfacial water structure. However, the impact of soluble salts on the water structure of the solution remained unclear. In 2000, Hancer et al. researched the alkali halide single salts based on their influence on the viscosity of the solution and flotation recovery[48]. It was concluded that since the “dense water structure salt” could significantly increase the “ice-like structure water” content in the bulk solution and lead to the increased viscosity of the solution in Fig. 7. On the contrary, the corresponding “loose water structure salt” would reduce the proportion of “ice-like structure water” in the solution and increase the ratio of “liquid water” and free water molecules, thereby reducing the viscosity of the solution. On the basis of the related viscosity measurement and further demonstration through flotation experiments, the influence of alkali halides on the water structure of the solution was preliminarily determined. Based on this theory, Ai Zhong et al. further

applied molecular simulation calculations to explain the amines collector adsorption behaviors on surfaces of potassium chloride and sodium chloride crystal[51]. It was found that for potassium chloride with relative lower hydration energy, its surface belonged to “loose water structure salt” with loose water film, benefiting the penetration of amine collector so as to complete the flotation process. However, for sodium chloride which was “dense water structure”, its dense water film on surface prevented the adsorption of amine collector and resulted a disability for flotation. To conclude, the interfacial water structure theory has been the newest and most acceptable rule for understanding the soluble salt flotation mechanism.

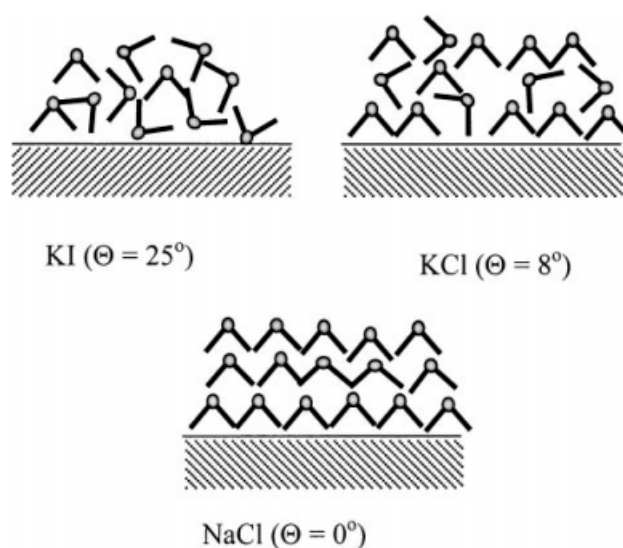


Fig. II. 7. Interfacial water structure at KI, KCl, and NaCl surfaces[48].

2.4. Summary

As a consequence, the mechanism of KCl flotation has remained unclear due to lack of direct observation during flotation process. However, there are still several paths which could be further researched to get steps closer to the reaction. Here, possible researching aspects or mechanism would be put up with to shed some light on the understanding of this complex soluble minerals flotation:

- 1) The surfaces of KCl and NaCl are meant to be flat due to their FCC crystal nature, which could provide possibility of directly observing in atomic level with help of professional apparatus like Atomic Force Microscope. One can observe the surface before and after the flotation process to understand the differences so as to understand how the crystals would resolve and recrystallize during the process. Besides, the adsorption of collectors on mineral surfaces could also be observed to study the interaction in between;

- 2) Mostly, the collectors applied for recovering KCl belong to organic substances, where the carbon chain and functional groups would mainly affect the floatability. Till now, the previous studies focused on the length of carbon chain, the size and charge feature of functional groups, and other physical-chemistry properties like dissolve heat, interfacial water structure. However, the key reaction could be the interaction between functional groups and mineral surfaces. To some extent, their molecular structure might have some match or mismatch effect, according to the crystallization prospect. For example, as FCC structure, the three-dimensional structure of the K and Cl ion could be octahedron where for various exposing faces they would show different repeating unit shape. From (100) facet, the main shape between atoms is square while for (111) facet is triangle or hexagon, which may conclude in a preferred interacting facet with a specific collector molecule;
- 3) As a typical soluble mineral, dissolve and re-crystallization may occur to the surface of KCl which means the final flotation behavior could be sum effect of both original particle property and also interaction between KCl and solution. The mediate status of KCl particles' surface should be stressed to help reproduce the details during flotation process and avert the difficulty for direct observation.
- 4) One special feature of KCl is its high solubility in water which endows the idea to control the crystallization process in order to modify its particle properties, such as shape, exposing faces, size, *etc.*, during crystallization process, to reach an ideal state for elevated flotation recovery compared to its original cubic shaped particles, which was the researching theme in this thesis.

References

- [1] Y.Z. Bao, Potash resources and supply and demand situation in the world, *Chinese Agricultural Resources* 8 (2010) 40–45.
- [2] J.P. Zhao, Geological characteristics and resource potential of soluble potash in China, *Mineral Deposits* 4 (2010) 649–656.
- [3] M.P. Ma Kai, Current situation of potash production and trade in the world, *Modern Chemical Industry* 12 (2009) 82–86.
- [4] L.S. Bao, The distribution situation of potash resources in the world and our countermeasures, *Land and Resources Information* 8 (2010) 44–47.
- [5] X. Tang, J. Chen, Y. Zhang, J. Yu, S. Lin, Echelon extraction of valuable components from salt lake brine substrate, *Desalination* 594 (2025) 118307. <https://doi.org/10.1016/J.DESAL.2024.118307>.
- [6] W.Q. Fang Qinsheng, The optimization of process for the production of KCl by counter-flotation-cool crystallization, *Inorganic Chemical Industry* 5 (2001) 32–33.

- [7] S. Titkov, Flotation of water-soluble mineral resources, *Int J Miner Process* 74 (2004) 107–113. <https://doi.org/10.1016/J.MINPRO.2003.09.008>.
- [8] X.L. C. H. Kitkoff, The cationic collector flotation of potassium ore and potassium-magnesium ore activated by a novel reagent, *Foreign Metal Ore Mineral Processing* 4 (2006) 26–29.
- [9] W.Q. Fang Qinsheng, The optimization of process for the production of KCl by counter-flotation-cool crystallization, *Inorganic Chemical Industry* 5 (2001) 32–33.
- [10] G. Zhu Hongwei, Comparison of the Production Technology of Potassium chloride from Chaerhan Salt Lake, *Sea Salt and Chemical Industry* 1 (2002) 1–3.
- [11] W.J. Lightfoot, C.F. Prutton, Equilibria in Saturated Solutions. III. The Quaternary System CaCl₂–MgCl₂–KCl–H₂O at 35°, *J Am Chem Soc* 70 (1948) 4112–4115.
https://doi.org/10.1021/JA01192A040/ASSET/JA01192A040.FP.PNG_V03.
- [12] M. Hancer, J.D. Miller, The flotation chemistry of potassium double salts: Schoenite, kainite, and carnallite, *Miner Eng* 13 (2000) 1483–1493.
[https://doi.org/10.1016/S0892-6875\(00\)00132-1](https://doi.org/10.1016/S0892-6875(00)00132-1).
- [13] Minerals yearbook 1989 Year 1989, Volume 1 1989 - UWDC - UW-Madison Libraries, (n.d.). <https://search.library.wisc.edu/digital/ADJ3TNNJ5XIGI38K> (accessed March 25, 2025).
- [14] S.J. Wang, Effect of raw ore type on the production of potassium chloride by cold decomposition flotation, *Journal of Lianyungang College of Chemical Technology* 2 (2000) 21–21.
- [15] X.S. Bao, Effect of sodium chloride on dissolution process of potassium halogen, *Journal of Salt Lake Research* 2 (1995) 51–58.
- [16] H.X. Xia, Kinetics and mechanism of dissolution of potassium carnallite and crystallization of potassium chloride, *Journal of Salt Lake Research* 4 (1993) 52–60.
- [17] X.S. Hong, Dissolution kinetics of carnallite, *Chinese Journal of Applied Chemistry* 3 (1994) 26–31.
- [18] H.X. Xia, Study on mechanism of carnallite decomposition to produce potassium chloride, *Journal of Salt Science and Chemical Industry* 2 (1994) 10–15.
- [19] L.B. Qian, Study on the Effect of Mixing Speed on KCl Crystallization, *Journal of Salt Science and Chemical Industry* 5 (2006) 17–19.
- [20] L.H. Qian, Research on the production process of potassium chloride from carnallite by controlled speed crystallization, *Journal of Salt Science and Chemical Industry* 5 (2011) 22–23.

- [21] Y.S. Wang Wenjun, Influence of the Application of Sulphate-potassium and Magnesium on Cotton Growth, Yield and Benefit, *Journal of Anhui Agricultural Sciences* 35 (2007) 811–812.
- [22] Z.W. Pan, Study on the application effect of Qinghai potassium magnesium sulfate fertilizer on pepper, *Modern Agricultural Science and Technology* 20 (2009) 115–116.
- [23] L.D. Pan, Effect of reduced application of potassium magnesium sulfate fertilizer on plant tomato, *Journal of Zhejiang Agricultural Sciences* 4 (2011) 762–764.
- [24] M.J. Wang Jianmei, Effects of potassium and magnesium sulfate as a fertilizer applied on grape, *Journal of Zhejiang Agricultural Sciences* 2 (2007) 144–145.
- [25] N.N.F. Aydemir S, Application of two amendments (gypsum and langbeinite) to reclaim sodic soil using sodic irrigation water, *Australian Journal of Soil Research* 43 (2005) 547–553.
- [26] G.H.C.D.J. Artiola J F, Use of langbeinite to reclaim sodic and saline sodic soils, *Commun Soil Sci Plan Anal* 31 (200AD) 829–842.
- [27] Gebrekidan H., Evaluation of the potential use of langbeinite as a reclaiming material for sodic and saline sodic soils, *University of Arizona* 166 (1995).
- [28] W.J. Li Gang, Study on preparation of soft potassium magnesium vanadium from potassium magnesium mixed salt ore, *Journal of Salt Lake Research* 6 (1998) 49–52.
- [29] M.H. Cheng Huaide, Study of Preparing Schoenite from Sulfate-type Saline Resources, *Journal of Salt and Chemical Industry* 37 (2007) 24–26.
- [30] D.B. Jannet, A. M'nif, R. Rokbani, Natural brine valorisation: Application of the system K^+ , Mg^{2+}/Cl^- , SO_4^{2-}/H_2O at 25°C observations on kinetics formation of K_2SO_4 and $K_2SO_4 \cdot MgSO_4 \cdot 6H_2O$, *Desalination* 167 (2004) 319–326. <https://doi.org/10.1016/J.DESAL.2004.06.141>.
- [31] S.Y. Cao Haiying, Preparation of picromerite with sulfate brine, *Industrial Minerals & Processing* 8 (2006) 14–16.
- [32] S.C. Zhang Zhanliang, Experimental Study on Soft Potassium, Magnesium and Vanadium Crystals, *Inner Mongolia Petrochemical Industry* 22 (2009) 19–20.
- [33] E. Li, Z. Du, S. Yuan, F. Cheng, Low temperature molecular dynamic simulation of water structure at sylvite crystal surface in saturated solution, *Miner Eng* 83 (2015) 53–58. <https://doi.org/10.1016/J.MINENG.2015.08.012>.
- [34] E. Burdukova, J.S. Laskowski, G.R. Forbes, Precipitation of dodecyl amine in KCl–NaCl saturated brine and attachment of amine particles to KCl and NaCl surfaces, *Int J Miner Process* 93 (2009) 34–40. <https://doi.org/10.1016/J.MINPRO.2009.05.001>.

- [35] J.S. Laskowski, Q. Liu, C.T. O'Connor, Current understanding of the mechanism of polysaccharide adsorption at the mineral/aqueous solution interface, *Int J Miner Process* 84 (2007) 59–68. <https://doi.org/10.1016/J.MINPRO.2007.03.006>.
- [36] M. Hancer, J.D. Miller, The flotation chemistry of potassium double salts: Schoenite, kainite, and carnallite, *Miner Eng* 13 (2000) 1483–1493. [https://doi.org/10.1016/S0892-6875\(00\)00132-1](https://doi.org/10.1016/S0892-6875(00)00132-1).
- [37] J.S. Laskowski, M. Pawlik, A. Ansari, Effect of Brine Concentration on the Krafft Point of Long Chain Primary Amines, *Canadian Metallurgical Quarterly* 46 (2007) 295–300. <https://doi.org/10.1179/CMQ.2007.46.3.295>.
- [38] Gaudin A. M., *Flotation*, 2nd Ed (1957).
- [39] F.M.C. Fuerstenau D W, Ionic size in flotation collection of alkali halides, *Transactions of the American Institute of Mining, Metallurgical and Petroleum Engineers* 205 (1956) 302–306.
- [40] Colo. Golden, *Quarterly of the Colorado School of Mines*, University of Michigan (1906) 98.
- [41] S.J.H. Rogers J, A mechanism of the selective flotation of soluble salts in the saturated solutions[C]//Electrical phenomena and solid/liquid interface, *Proceedings of the Second International Congress of Surface Activity III* (1957).
- [42] Y. Yuan, W. Zhan, H. Yi, Y. Zhao, S. Song, Molecular dynamics simulations study for the effect of cations hydration on the surface tension of the electrolyte solutions, *Colloids Surf A Physicochem Eng Asp* 539 (2018) 80–84. <https://doi.org/10.1016/J.COLSURFA.2017.12.005>.
- [43] R.R.J.S.D.C. Fuerstenau D W, Mechanism of Soluble Salt Flotation, *Transactions AIME* 241 (1968) 56–64.
- [44] S. Veeramasuneni, Y. Hu, J.D. Miller, The surface charge of alkali halides: consideration of the partial hydration of surface lattice ions, *Surf Sci* 382 (1997) 127–136. [https://doi.org/10.1016/S0039-6028\(97\)00115-5](https://doi.org/10.1016/S0039-6028(97)00115-5).
- [45] Q. Cao, H. Du, J.D. Miller, X. Wang, F. Cheng, Surface chemistry features in the flotation of KCl, *Miner Eng* 23 (2010) 365–373. <https://doi.org/10.1016/J.MINENG.2009.11.010>.
- [46] Q. Cao, H. Du, J.D. Miller, X. Wang, F. Cheng, Surface chemistry features in the flotation of KCl, *Miner Eng* 23 (2010) 365–373. <https://doi.org/10.1016/J.MINENG.2009.11.010>.
- [47] S. Veeramasuneni, M.R. Yalamanchili, J.D. Miller, The Influence of Oxygen Defect States on the Surface Charge of Alkali Halides, *J Colloid Interface Sci* 182 (1996) 275–281. <https://doi.org/10.1006/JCIS.1996.0460>.

- [48] M. Hancer, M.S. Celik, J.D. Miller, The Significance of Interfacial Water Structure in Soluble Salt Flotation Systems, *J Colloid Interface Sci* 235 (2001) 150–161. <https://doi.org/10.1006/JCIS.2000.7350>.
- [49] J.D. Miller, M.R. Yalamanchili, Fundamental aspects of soluble salt flotation, *Miner Eng* 7 (1994) 305–317. [https://doi.org/10.1016/0892-6875\(94\)90072-8](https://doi.org/10.1016/0892-6875(94)90072-8).
- [50] Z.S. Nickolov, O. Ozcan, J.D. Miller, FTIR analysis of water structure and its significance in the flotation of sodium carbonate and sodium bicarbonate salts, *Colloids Surf A Physicochem Eng Asp* 224 (2003) 231–239. [https://doi.org/10.1016/S0927-7757\(03\)00317-0](https://doi.org/10.1016/S0927-7757(03)00317-0).
- [51] Z. Ai, S. Li, Y. Zhao, H. Yi, L. Chen, P. Chen, G. Nie, S. Song, Atomic insights into flotation separation of KCl and NaCl from a new viewpoint of hydration layer: A molecular dynamic study, *Colloids Surf A Physicochem Eng Asp* 602 (2020) 125071. <https://doi.org/10.1016/J.COLSURFA.2020.125071>.

Chapter III. Materials and Methods

In this chapter, a general description of the materials, researching methods, experimental design as well as characterization technologies in chapter IV, V, VII and VIII will be epitomized.

3.1. Materials

Chemical reagents including potassium chloride, hydrochloric acid, potassium hydroxide, nitric acid, potassium nitrate, ammonia and ammonium chloride and absolute ethanol were purchased from Sinopharm Chemical Reagent Co., Ltd., China with analytical high purity. Pure lead chloride (PbCl_2) and octadecylamine hydrochloride (ODA) reagents (collector applied in this research for floating potassium chloride) was purchased from Aladdin Pharmacy company, China., also of analytical purity to eliminate the impact of impurities. Deionized water with a resistivity of $18.2 \text{ M}\Omega\cdot\text{cm}$ was obtained from Milli-Q (Millipore Corp., USA). Experiments were conducted under ambient temperature as around $25 \text{ }^\circ\text{C}$ and no frothers were applied during flotation process due to the exceptional floatability with only ODA.

3.2. Methods

The methodology of proposed crystallization controlled flotation strategy throughout this work is to modulate the solution condition and environment so as to control the crystallization process. Methods applied in chapter IV, V, VI and VII will be introduced as below where some shared the similar main idea which will be stressed. Each experiment was performed with a fresh solution according to the solubility of KCl in water under different temperature conditions.

3.2.1. Methods for Chapter IV-Controllable reparation of KCl with various shapes through green supersaturation modulation

Sample preparation: The growing process of crystals highly depends on the solution condition according to the solubility curve. For salt crystallization, the main variations include the concentration of composing ions, temperature range and evaporation area (liquid-gas area), and also the additives. After crystallization, the grown KCl samples were immediately filtered by diameter of $0.22 \text{ }\mu\text{m}$ filter paper after each crystallization experiment in order to avoid the further growth. Afterwards crystals were kept in an oven at $45 \text{ }^\circ\text{C}$ overnight to dry up for other measurements.

Experimental design: A designed vertical cylindrical jacketed crystallizer with 250 mL capacity combined with mechanical stirring machine and a double blade parallel

stir bar with length of 2 cm was performed, where warm water bath was provided by a constant speed programmable thermostatic bath (XOYS-2010 N, ATPIO Ltd., Nanjing, China) to realize an accurate modulation with minimal configuration of 0.01 °C. By means of modulating cooling range, cooling rate and reaction period of water bath, the KCl crystals with different morphology were grown in the crystallizer.

Typical batch cooling crystallization process: 100 mL of saturated KCl solution at 30 °C was added into the chamber of crystallizer and proper stirring speed was performed to ensure an ideal mixture of the solid-liquid system. Subsequently, the warm bath with 35 °C was set in advance for 30 min to keep all water cycle path warm enough to ensure the later saline clear, i.e., no existence of solid salt. Typical cooling program was set to cool the saturated KCl solution of 30 °C down to 27 °C within certain period, where the filtration device was kept in an oven at 27 °C before the program ended to minimize the further growth of KCl crystals during the sample drying process.

Parameter impacts experiments: The cooling programming was well designed to realize the modulation of cooling range and rate by setting different temperature and reacting time, where the former was set to be same range as 3 °C but different starting temperature as 24, 27, 30 and 33 °C without any other changes from typical cooling process. For cooling rate impactor, the cooling range was set to be 30-27 °C to emit the influence of environmental temperature condition with various cooling period from 15 to 300 min (cooling rate from 12 °C/h to 0.6 °C/h), where the longer the cooling period meant a lower cooling rate. For stirring speed parameter, increasing speed as 100, 200, 300, 400, 500, and 600 rpm were applied for the system while all other condition was kept the same with typical cooling experiment. In additive impacts experiments, low dosage as 0.01 % and 2 % in column (in this case with 100 mL saturate solution, 0.01 mL and 2.0 mL of addition was added) was chosen to research about the extra ions' influence on crystallization.

3.2.2. Methods for Chapter V-Preparation of KCl samples with various exposing facets

The growing process of crystals highly depends on the solution condition according to the solubility curve. For salt crystallization, the main variations include the concentration of composing ions, temperature range and evaporation area (liquid-gas area), and also the additives. Here, based on properties of KCl salt, mild crystallization reaction and addition of Pb ions methods were chosen to grow KCl crystals with (200) exposing facets and (222) facets, respectively. For flotation

experiments, the samples were sieved to gather same size range between 178 and 250 μm to exclude the impact of particle size. The detailed preparation methods were described as below.

Preparation of KCl crystals with (200) exposing facets: It's known the fact that crystal habit of KCl is cubic with six square (200) faces. However, perfect cubic with sharp corners only appears under gentle growing environment due to its easily crystallization with slight decline of temperature as well as evaporation of water. Hence, a mild isothermal evaporation method was performed to prepare the perfect cubic KCl crystal. In a typical experiment, saturated KCl solution was poured into a petri dish with diameter of 15 cm for 48 h with stirring speed at 300 rpm to grow even cubic KCl crystals. For bigger cubic crystals, the evaporation period was extended to one week and perfectly formed KCl samples were carefully moved to a filter paper for quick drying to maintain the flat and immaculate surface for delicate tests like AFM.

Preparation of KCl crystals with (222) exposing facets: According to previous research by L. Pastero, R[1], ratio of exposing facets including (200) and (222) of KCl crystals highly depends on the additive of PbCl_2 . The increasing amount of lead ions would promote the proportion of (222) face of KCl crystal. Thus, for pure (222) exposing face KCl crystals with octahedron morphology, ratio at 1:500 in weight of pure PbCl_2 in grams and saturate KCl solution in volume was prepared and ultrasonic process with intensity at 200 W for 20 min was performed to ensure the well mixture of composing substances. Then the solution was poured into a petri-dish for slowly evaporation & crystallization reaction for a certain period, based on the requirement of crystal size. After that, the well grown crystals were selected by a dropper and dewatered by filter paper immediately in order to keep perfect crystals unblemished for surficial observations as well as avoiding the further growth. Finally, Pb-KCl samples were kept in an oven at 45 °C overnight to dry up for next measurements to minimize the moisture absorption due to the high hydrophilia of KCl salt.

Flotation experiments: To study how potassium chloride with (200) exposing face and (222) exposing face would affect the recovery process with ODA as collector reagent, flotation experiments of cubic- and octahedron-shaped KCl crystals with same size range of 178-250 μm were conducted in a flotation cell with capacity of 60 mL and the pulp concentration was set to be 25%, under ambient temperature around 25 °C. prior to the experiment, the collector ODA reagent was prepared by mixing 2 mL pure HCl into 99 mL octadecylamine solution. The mixture was heat up to 80 °C until clear to maintain its high activity each time before flotation. During a standard flotation process. 15 g of grown KCl crystal particles was added into 60 mL of

saturated KCl solution and conditioned for 3 min. Then, 45 μL of transparent ODA was added with mixing for another 2 min. Afterwards, bubbles were performed at flow rate of 0.1 L/h with air as source for 2 min. Flotation process was carried out then for two minutes to get the flotation kinetics date. All samples were immediately filtered and transferred to an oven at 45 $^{\circ}\text{C}$ to dry up to avoid further crystallization with remnant saturated KCl solution on surface of crystals. The flotation kinetics was described by classical flotation kinetics

$$\varepsilon = \varepsilon^{\infty} [1 - \exp(-kt)] \quad (1)$$

where ε and ε^{∞} were real and theoretical recovery, %; k was flotation rate, min^{-1} , t was the flotation time, min.

Adhesion & adsorption force test: During flotation process, another key parameter is the interaction force between minerals and bubbles. Here, the adhesion & adsorption force tests were conducted by a surface tension measurement apparatus (Powereach JK99M2, China). Notably, the unstable bubble under solution hindered the accuracy of interaction test but liquid drop helped to get a better understanding. The interaction law between particles & bubble could be easily obtained by reversing the rule of particles & flotation solution. During the test, a ring tip with a droplet with $\sim 50 \mu\text{L}$ of saturated potassium chloride solution was hanged where its weight was evaluated by the digital sensor of instrument. Then, the cubic or octahedron samples were firstly immersed in saturated KCl solution with 60 g/t addition of collector ODA for 10 min in order to realize the same situation during flotation process. Then the samples were dried at 45 $^{\circ}\text{C}$ for 4 h to dry up and placed on the surface of a glass slide with a relatively smooth surface, which was later put on the instrument platform to move forward the droplet with velocity at 0.01 mm/s to ensure the accuracy of this test. The distance between droplet and particles was well designed in order to make sure about the contact. Afterwards, the sensed real-time mass changes were recorded and adhesion & adsorption force data could be read by analysis of the curve.

3.2.3. Methods for Chapter VI-Preparation of KCl samples with various shapes

The key idea of modulating the KCl crystal structure is to adjust the oversaturation to control the growth preference. Solubility of KCl highly depends on the temperature. For KCl crystallization process, the inter- face area of gas-liquid, turbulence of solution system as well as cooling conditions greatly affect the supersaturation thus further influent the growth of KCl crystals. Hence, various strategies have been tried to prepare cubic-like, needle-like and hopper-like KCl

crystals and the detailed methods are described as below. Notably, all samples were totally dried and then divided into different size ranges by standard dry sieving technique. Samples with size between 178 and 250 μm were prepared for later flotation in order to exclude the influence of particle size factor.

Preparation of cubic-like KCl crystals: It's known the fact that crystal habit of KCl is cubic structure. Here, a relatively fast but uniform crystallization method was performed to collect cubic samples. First, 100 mL saturate solution of 55 $^{\circ}\text{C}$ was prepared and heated up to 60 $^{\circ}\text{C}$ with a foil covered tightly to avoid evaporation of water. The transparent solution was then transferred to cold water bath at 0 $^{\circ}\text{C}$ using ice-water mixture with stirring speed as 400 rpm for 2 h. Afterwards, the grown cubic crystals with wide size distribution were filtered and dried up in an oven at 45 $^{\circ}\text{C}$ for overnight.

Preparation of hopper-like KCl crystals: The formation of hopper-like KCl crystals appeared under constant high value of oversaturation during crystallization of FCC crystals, which had been reported in previous work[2]. Similarly, a cooling process assisted by a constant speed programmable thermostatic bath machine. A designed vertical cylindrical jacketed crystallizer with 250 mL capacity was connected to the warm bath to realize a constant cooling process from 30 $^{\circ}\text{C}$ to 27 $^{\circ}\text{C}$ with cooling rate as 3 $^{\circ}\text{C}/\text{h}$. During this period, the corners of one cubic structure got the chance to grow faster to form hopper-like structure with large exposing (200) face area and relatively hollow cubic shape. These hopper-like KCl crystals were obtained in order to compare the flotation behavior with needle-like and cubic-like KCl crystals.

Preparation of needle-like KCl crystals: The needle-like formation of KCl crystals was due to the faster growth of KCl under one-dimension shape with a high level of supersaturation which means two ways including high cooling rate and evaporating rate. In order to yield the needle-like crystals, a combined method of cooling and evaporating was performed here. Similar to method of cubic-like sample, saturate KCl solution at 70 $^{\circ}\text{C}$ was prepared by adding weighed reagent to a proper amount of DI water and heat to 75 $^{\circ}\text{C}$ with a foil cover. Afterwards, the clear solution was immediately transferred to ice bath to accelerate the crystallization process but kept still. Notably, the cover was removed to let evaporation occur at the same time with cooling process. At the primary step, several thin and small needle-like crystals appeared on the surface of solution, *i.e.*, the liquid-gas interface, where the higher concentration of K and Cl ions under fast water evaporation condition helped needles to grew longer and thicker. During this period, due to the gravity, most of them fell

down to the bottom of solution where they could further grow while maintaining the initial shape of needle structure.

AFM tests: The morphologies of various micro needle-like KCl crystal and surface of cubic-like KCl crystals were tested by AFM. For needle-like sample, to study the mechanism of needle structure formation, a spinner was used to get a high speed of KCl solution evaporation, along with the fast growth of KCl crystals in nanometer size. Low and high concentration with 10 and 50 mg/L of KCl solutions were prepared to study the initial stage during fast growth of KCl crystals, respectively. To prepare the AFM sample, a fresh cleaved mica with 10×10 mm size, as the base for observation due to its layered property, was fixed on center of the spinner. Then, 10 μ L of solution was dropped on surface of clean mica and spun for 300 s to ensure a good dispersion as well as fast evaporation. The mica with dispersed samples was then dried at room temperature for 12 h for morphology scanning tests by AFM. For surface of cubic KCl structure study, a mild evaporation method helped to obtain perfect cubic crystals. Here, 200 mL saturated KCl solution at 25 °C was poured into a glass made petri dish with diameter of 15 cm for more than 7 days. During the crystallization period, well-structured cubic samples were carefully picked out and dried by filter paper on the bottom to protect the flat surface. For AFM tests, the ScanAsyst Air mode in the presence of equipped with probe with silicon tip on nitride lever was used to get the surficial details and professional software NanoScope Analysis 1.4 was performed to analyze the results.

Micro flotation experiments: Batch flotation experiments were performed with a flotation machine equipped with 60 mL cell. Typically, 15g samples were added into 60 mL saturated KCl solution and conditioned for 5 minutes. Subsequently, the mixture was poured into the cell and ODA was added as collector. It's worth mentioning that the flotation of KCl occurs only when concentration of ODA exceeds its solubility to work in form of flocs[3]. A proper concentration as 5.56×10^{-5} mol/L of ODA[4,5] was chosen to value the floatability of KCl samples. Samples were floated for 2 min with air at a flow rate of 50 cm³/min. All flotation tests were conducted under room temperature as ~25 °C.

Induction time tests: The set up was a self-made system with a platform for controllable movement of the tip with bubble. By connecting an industrial camera, the reacting moment of bubble with sample particles could be recorded. For each condition, the approaching and retracting process as one movement were repeated for 20 times to calculate the adhesion probability. With increasing reacting period, tests

of various adhesion probability were obtained and the period with 50% adhesion probability was thought to be induction time.

Adhesion & desorption force tests: The interaction between aiming minerals with bubbles and collectors also relies on their adhesion as well as adsorption force. Here, the related force tests of needle-, hopper- and cubic- like KCl crystals and saturated KCl solution were determined by a surface tension meter (Powereach JK99M2, China). Firstly, KCl samples with various structure and 180-250 μm were immersed in saturated KCl solution involving 5.56×10^{-5} mol/L ODA collector for 6 minutes in order to show the interaction force during real flotation process. Afterwards, the filtered and dried samples were carefully settled on the bottom of a container to make a flat mineral bed for later tests. The droplet of 100 μL KCl was attached to a needle with a small ring with diameter around 1 mm as tip, where the other end was connected to a micro force sensor with high sensibility as $\sim 0.1 \mu\text{N}$. During a typical adhesion & adsorption force test, the saturated KCl with a flat mineral bed composed by KCl particles on the bottom was put on the lifting platform with 2 mm distance from the bottom of KCl droplet. Notably, the gravity of droplet was cleared to zero before each test to get a better curve with baseline recoupling with x axis which helped reading interacted forces. The real time changes of reacted force on the droplet were recorded by the micro force sensor and adhesion & adsorption force data could be obtained with the data analyze.

3.2.4. Methods for Chapter VII-Preparation of KCl samples with various shapes

Synthesis of KCl crystals: Based on former study, the feature of KCl's high dependence of solubility on solution temperature implied us the strategy to grow cubic shaped (as FCC type crystal) KCl crystals. During the synthesis process, 100 mL hot saturate KCl solution at 55 $^{\circ}\text{C}$ by adding weight KCl reagent into DI water. Afterwards, the mixture was transferred to warm water bath at 60 $^{\circ}\text{C}$ to realize the total clear solution. When the saturate KCl solution was ready, a film cover was applied to avoid evaporation and then stirred at 400 rpm for 2 h till it cooled down to room temperature as $\sim 25^{\circ}\text{C}$. Consequently, the cooled mixture was filtered to collect the crystallized KCl samples. At last, those KCl crystals were heat up at 45 $^{\circ}\text{C}$ in an oven for 12 h to dry up for later characterization and tests.

Experiments of ethanol impact on KCl flotation: The fact that ethanol could be miscible in any proportion with water entangled its impacts on KCl flotation behavior. Here, the experiments were designed to above three parts to realize an ideal understanding of the mechanisms.

Addition of ethanol during filtering process: It is known that KCl is hydrophilic in solution which brings the difficulty to absolutely dewater of KCl crystals. With remnant water on surface, samples tend to form caking big clusters instead of individual single crystals. To resolve this caking problem, one common method was adding a certain amount of ethanol during filtering process. In this work, various amounts including 1, 2, 5 and 10 mL of pure ethanol was evenly sprayed onto KCl samples during filtering process as described in above section.

Impact of Ethanol during crystallization process: Salting-out reaction always occurred when large amount of ethanol was added into saturated KCl solution. To avoid this phenomenon, low percentage addition of ethanol as 0.05%, 0.10%, 0.20%, 0.30%, 0.40% and 0.50% were chosen to prepare ethanol-KCl co-saturated solution at 25 °C. Then 5 g grown cubic KCl crystals with size range as 150-178 μm were added into the co-saturated solution and conditioned for 3 minutes, then stirred at 400 rpm for 6 minutes. It is worth noting that the periods were designed for aim of repeating the same solution condition with flotation which will be introduced as below section. Following was the basic filtering and drying process which was the same with preparation of pure cubic KCl crystals.

Flotation tests: In the flotation process, pure saturate KCl and ethanol-KCl co-saturated solution with increasing percentage of ethanol were prepared firstly as mother liquor of the system. 5g of cubic KCl crystals were weight for each test with a flotation cell of 60 mL capacity. Collector ODA was prepared by adding 2 mL pure HCl into 98 mL ocadecylamine where the mixture was heat up to 80 °C to make sure about the total transparent solution for an ideal function. In a flotation test, the KCl samples were added into 60mL of mother liquor and conditioned for 2 minutes with stirring speed set as 1200 rpm. Then 45 L of hot ODA as collector was applied for another 2 minutes and then bubbles were produced with air as resource and flow rate as 0.1 L/h for 2 minutes. Froths were collected during the bubbles applying process and concentrate was collected while leaving part as tailing. By weighting the concentrate and tailing (after filtering and drying process), recovery data was obtained.

Surface tension tests: Co-saturated solutions of ethanol and KCl with increasing ethanol as 0.05%, 0.10%, 0.20%, 0.30%, 0.40% and 0.50% were firstly prepared and immediately transferred to tightly covered tubes to avoid evaporation of ethanol. Surface tension of solution was tested via Force tensiometer (Kruss, Bruker) with a flat platinum slice which was washed by DI water and then fire to remove any impurities.

3.3. Characterizations

For observation of crystals, a stereoscopic was performed due to their large scale of size with nearly perfect morphology. With smaller size crystals, scanning electron microscope (SEM, Phenom ProX G6, Netherlands) was used for detailed observation of intact octahedron and cubic KCl crystal surfaces. Atomic force microscope (AFM, Bruker MM8, German) with ScanAsyst Air mode equipped with Air tip helped to reveal the surficial morphologies of grown perfect cubic and octahedron KCl crystals and the results were analyzed by Bruker Nanoscope Analysis 1.4 software. X-ray photoelectron spectroscopy (XPS, Thermo Scientific ESCALAB Xi+, America) and X-ray diffraction with Cu K α radiation (XRD, D8 Advance, Germany) tests with Cu-K α sealed tube were applied to study the crystalline structure of KCl crystals and the latter also helped to understand the exposing face differences between variously-shaped KCl samples. Besides, FTIR (Nicolet 6700, UK) along with Zeta potential test (Malvern Zeta-sizer Nano ZS90, UK) were conducted to study the interaction between the collector ODA and mineral sample KCl. Especially for the zeta potential test, KCl samples were ground to obtain powder with particle size less than 5 μm to suspend in saturated KCl solution. For zeta potential tests related with ODA, the concentration was set to be the same as flotation process as 60 g/t in saturate KCl solution. The mixture was conditioned for 20 min and then measured for 6 times to yield the average zeta potential information. The exposing surface area information was studied by the Brunauer-Emmett-Teller (BET, V-Sorb 4800P, China) in pure N₂ atmosphere.

3.4. Summary

This chapter first briefly introduces the materials used in this thesis, and then the methods of the following four chapters were introduced. Afterwards, the characterization applied in the main research was listed. The content of this chapter is the experimental basis for the following chapters.

References

- [1] L. Pastero, R. Cossio, D. Aquilano, $\{100\} \rightarrow \{111\}$ morphological change in KCl crystals grown from Pb²⁺-doped aqueous solutions, *CrystEngComm* 17 (2015) 7844–7855. <https://doi.org/10.1039/C5CE01425E>.
- [2] J. Desarnaud, H. Derluyn, J. Carmeliet, D. Bonn, N. Shahidzadeh, Hopper Growth of Salt Crystals, *Journal of Physical Chemistry Letters* 9 (2018) 2961–2966.

<https://doi.org/10.1021/ACS.JPCLETT.8B01082>.

[3] H. Du, O. Ozdemir, X. Wang, F. Cheng, M.S. Celik, J.D. Miller, Flotation chemistry of soluble salt minerals: From ion hydration to colloid adsorption, *Minerals and Metallurgical Processing* 31 (2014) 1–20. <https://doi.org/10.1007/BF03402344>.

[4] E. Li, P. Duan, Z. Du, D. Li, F. Cheng, Colloidal properties of octadecylamine hydrochloride and the wettability of KCl crystal surface in different saturated salt solutions, *J Mol Liq* 223 (2016) 107–111. <https://doi.org/10.1016/J.MOLLIQ.2016.08.039>.

[5] H. Zhou, Z. Yang, Y. Zhang, H. Han, K. He, X. Luo, Enhanced flotation of hemimorphite: Adjusting mineral surface potential with sodium thiocyanate as activator, *Miner Eng* 171 (2021) 107088. <https://doi.org/10.1016/J.MINENG.2021.107088>.

Chapter IV. Controllably constructing morphology and structure of potassium chloride crystal by green supersaturation modulation

4.1. Introduction

Crystals lie everywhere near us not only as natural ones like snowflakes, ice, diamonds, or other gemstones but also artificial crystals were also precisely designed to ignite their great potential as nutrients, necessities and even treatment for disasters^[1-3]. For centuries, they have been playing an essential role in amazing variety of forms such as salt^[4], pharmaceuticals^[5], micronutrient delivery^[6], minerals^[7] and many other fields^[8].

As main resource of element potassium, which is essential for plants growing^[9]. Potassium chloride (KCl) has been designed with certain physical and chemical properties for being widely applied in different fields, leather making, explosives, porcelain, fertilizer, phosphors, and medicines^[10-12]. For instance, hydroscopic properties of KCl are reported to be closely related with effect of climate^[13]. Besides, enhanced Optical-simulated luminescence response of KCl aerosol was beneficial for regeneration effect in the materials of detector^[14-16]. Improving mechanical properties of KCl was helpful for warehousing, transporting, and storage process to far-abroad countries^[17]. What's more, served as carrier, KCl could be used to strengthen UV emission lines for generation of photo electronic devices^[18,19]. The nature of crystals shows vital effects in their function^[20,21], therefore, it is of high necessity to controllably synthesize crystal with many morphology and surficial properties to ignite their promising applications^[22].

The design of growing crystals has been a challenge to all researchers^[23,24]. Different methods like specific solvent especially organic solvent method^[25-27], additives method^[28,29] and extreme heat & pressure method^[30-32] are thought to be well-known ways to yield new structures of crystals. Besides, tons of efforts were attempted to synthesize diverse property of crystals^[33,34]. However, chemistry reagents pollution has been posing great threat to human society in all sorts of aspects including drinking water, food industry and even clothing contact. Demanding of eliminating the undesirable chemistry additives is urgent in social activities.

To some extent, only aimed morphology and exposure faces could bring the desired effects. In general, the natural crystallographic habits are known to be rarely influenced by normal conditions due to the crystallization thermodynamic equilibrium, while the crystal structural, morphological as well as surficial properties may differ depending on crystallization kinetics^[35]. By repeating the basic structure along different paths, orientation and quantities, the crystals may end up with parallelism, misaligned spiral growth, or secondary nucleation. Let along that in nature, the crystals are rarely found to be in their equilibrium form which requires steep conditions. The basic repeating unit finally pile up to form varied macroscopically crystals which is also known as crystal clusters that may seem far dissimilar from the ideal perfect structure, but the latter appears in a more common way.

It's of significant scientific and technological importance to investigate the method to design crystals without additives thus to pave an environmentally friendly path to the applications of industrial crystals. Hence, the phenomenon that crystal always grow in form of clusters sheds some new light to the controllable crystal design by only modulating the general conditions like crystallization rate, supersaturation, and temperature. In this work, as one of the most significant crystals in nature an actual application, KCl was taking as an example to research the strategies of controllable construction of crystals. The solubility of KCl highly depends on temperature of solution, ensuring the possibility of precise regulation of the oversaturation of salt thus to modulate crystals during the cooling process. Batch experiments were performed to research how the cooling method would affect the morphology, surficial properties of KCl crystal. This work aims to help understand the controllable design of crystals by supersaturation modulation, not only salts but also medicine crystals, minerals, jewels and semi-soluble minerals.

4.2. Results and discussion

4.2.1. Supersaturation controlled crystallization

As a common method of mixing as well as energy input for reactions, stirring not only helps the system unbalanced but also provides a certain level of mixing effect, especially for multi-phase systems like solid-fluid mixture. The energy input increases with higher stirring speed. To figure out the relationship between stirring speed and the morphology of crystal, batch crystallization experiment of cooling process with different speed including 100, 200, 300, 400, 500 and 600 rpm was performed and the results were shown in Fig. IV.1a-d and Fig. IV. 2.

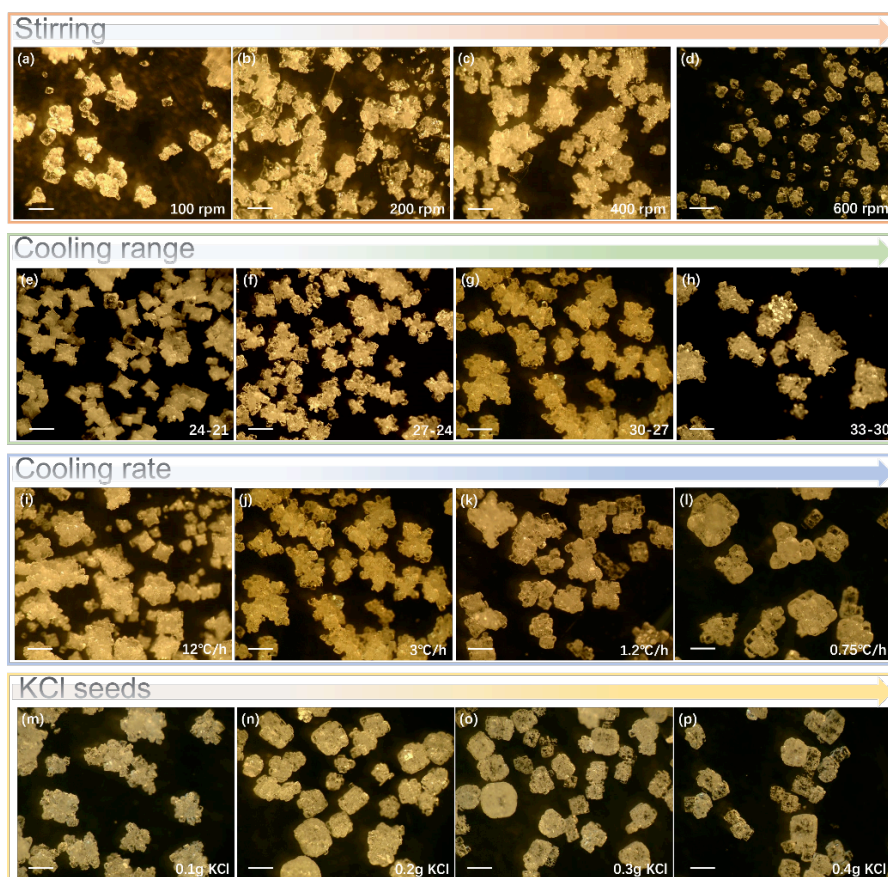


Fig. IV. 1. Effect of conditional parameters for KCl crystal grown through batch cooling experiments: Effect of stirring speed on crystal grown, (a) 100, (b) 200, (c) 400, and (d) 600 rpm from 30 °C to 27 °C in 60 min; Effect of cooling range on crystal grown, (e) 24-21 °C, (f) 27-24 °C, (g) 30-27 °C, and (h) 33-30 °C (with cooling period of 60 min); Effect of cooling rate on crystal grown, (i) 12 °C/h, (j) 3 °C/h, (k) 1.2 °C/h and (l) 0.75 °C/h from 30 °C to 27 °C with 400 rpm; Effect of additive seeds amount on crystal grown, (m) 0.1 g, (n) 0.2 g, (o) 0.3 g, and (p) 0.4 g.

Scale bar=500 μm .

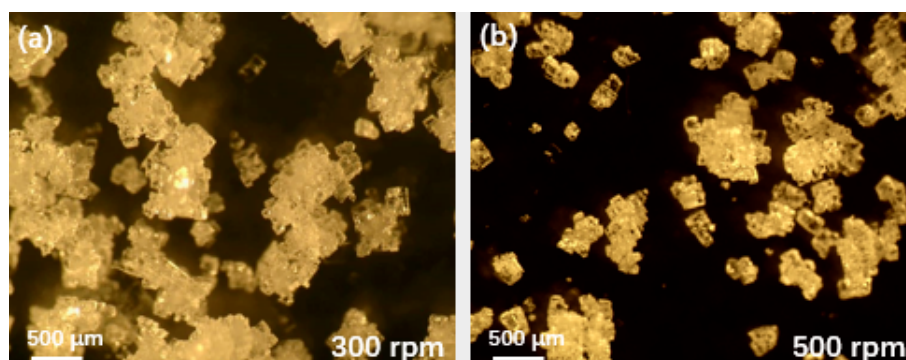


Fig. IV. 2. Stereoscopic results of hopper-like KCl crystals grown by batch cooling experiments from 30 °C to 27 °C in 60min, with 300 and 500 rpm, respectively.

Intuitively, the size of crystal reached a good distribution in hopper-like size under 400 rpm condition. With lower stirring speed (100, 200, and 300 rpm), the crystals showed hopper structure but in unevenly size and shape distribution, while small crystal pieces tended to be broken from the bigger hopper structure under high rotational speed (500 and 600 rpm). The crystallization process usually requires a gentle solution environment, *i.e.*, a proper mix ability of the crystal-saline system. The homogeneous morphology of crystal in Fig. IV. 1c demonstrated that this system well fitted the mixing purpose under 400 rpm. The mechanism could ascribe to the suspension critical speed Nt calculation according to Pavlushenko's formula:

$$Nt = 0.105 \frac{g^{0.6} \rho_D^{0.8} d_p^{0.4} D^{1.9}}{\mu^{0.2} \rho^{0.6} d^{2.5}} \quad (1)$$

With Nt the suspension critical speed of mixer (revolutions per second, rps); g the acceleration of gravity in m/s^2 ; ρ_D and ρ the density of solid-state particles and liquid-state solution in $kg \cdot s^2/m^4$, respectively; μ the viscosity of the fluid being mixed in $Kg \cdot s/m^2$; d , D and d_p the diameter of mixer, mixing vessel, and grown crystal in m, respectively. Based on the equation, the Nt would be 5.69 rps, *i.e.*, 391 rpm, close to the experimental result 400rpm. The satisfied distribution of hopper-like crystals came from the well mixed solid-liquid system, while the higher stirring speed offered redundant energy for crystallization, thus destroying the hopper structures to small pieces in Fig. IV. 2b.

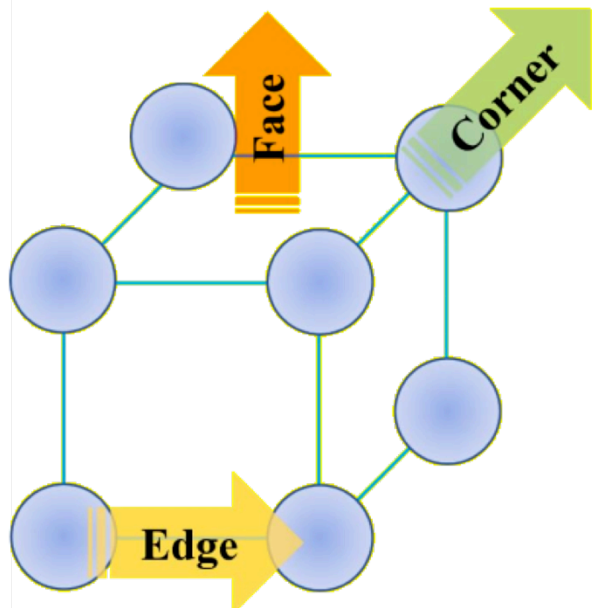


Fig. IV. 3. Illustration of atoms on face, edge, and corner position of cubic crystal.

The phenomenon that solubility of KCl is subject to changes in temperature, as mentioned above, gives an insight of the idea that the hopper structure may change under different cooling range. Batch cooling experiments of 3 °C within ranges of 24-21 °C, 27-24 °C and 33-30 °C were set to see the morphological differences of crystals from that of 30-27 °C crystals. As shown in Fig. 1e-h, the crystals in different conditions all exhibited hopper-like structure but diverse size distribution. In Fig. IV. 1e, the inner cubic owned a relatively large length attached with eight much smaller branches on corners. However, in Fig. IV. 1f and g, the size of branches on corners were better developed thus those crystals showed obvious hands with almost non-existent inner cubic structure. The different shapes could be well explained by various growing strategies that as shown in Fig. IV. 3, there will be three main growing directions on one cubic structure—from center to corner (green), along edge (yellow) and perpendicular to square face (pink) with a declined growing rate (vice versa during resolving process). During crystallization, it's obvious that corners are immersed in large area of saturation KCl with abundant K or Cl ions to help grow. On edges, there will be relatively less chances to contact with saturated solution while on faces, ions possessed the least saturated KCl solution. It could be inferred that the greater growing rate difference between corner and face direction occurred under increasing temperature conditions. In other words, when the temperature was set to be low, the (200) face of KCl crystals tended to grow which required a gentle environment, thus benefiting the formation of inner cubic structure. On the contrary, if the temperature was high, the difference of growing rate between corner and face direction was magnified that the growth along corner direction was better promoted than on face direction. The corners of primary small cubic became the secondary nucleation sites for later cubic. Consequently, the branches on eight corners got preferentially developed and the final crystals showed a hopper-like structure. Notably, according to the Oswald Ripening theory, dissolution and nucleation occurred during the crystal growing process. The temperature condition is a key parameter of the balance of these two reactions, improper condition might bring on non-uniform crystals. As demonstrated in Fig. IV. 1f, g and h, the best size distribution occurred under proper temperature condition (in Fig. IV. 1g, 30-27 °C), while IV. 1f and 1h displayed small pieces and oversized aggregations. Thus, the proper cooling range of hopper-like KCl crystals should be set as 30-27 °C.

Apart from cooling range, the cooling rate is another key factor of the grown hopper-like structure. Solubility of KCl highly depends the temperature, thus the cooling way offers oversaturation of crystallization. The cooling rate greatly affected the oversaturation thus induced the change in growing speed of crystals. To research the correlation between cooling rate and morphology of crystals, in this work, various cooling rate as 12.0, 3, 1.2 and 0.76 °C/h. Obviously, the lower cooling rate offered a steadier growing environment for KCl crystals. Representative results were shown in Fig. IV. 1i-l and others in Fig. IV. 4 with same evolution law.

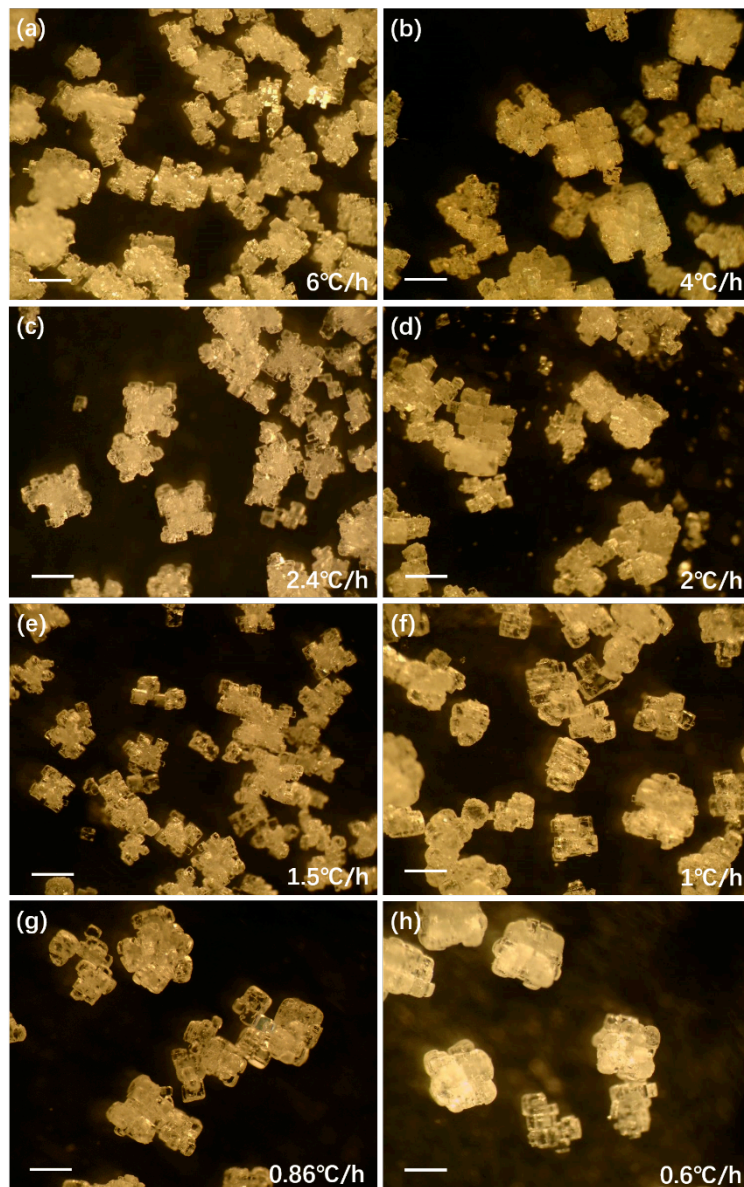


Fig. IV. 4. Stereoscopic results of hopper-like KCl crystals grown by batch cooling experiments from 30 to 27 °C in with stirring speed at 500 rpm and cooling rate as 6, 4, 2.4, 2, 1.5, 1, 0.86 and 0.6 °C/h. Scale bar=500 μm.

Crystals in figures showed the revolution trend from hopper-like structure with distinct cubic corners to spherical particles. In Fig. IV. 1i, the crystals were in different size but the same hopper-like morphology, which should be ascribed to the proper oversaturation as well as Oswald ripening theory as mentioned above. With the slower cooling rate, the crystals got a relative peaceful grow to display an even size distribution as in Fig. IV. 1j and k. However, the latter result exhibited a hopper-like structure with better developed branches compared to the former. This structure could be inferred that at the very beginning of cooling stage, the saline kept clear without crystal seeds formation due to the supersaturation of KCl under 25 °C. Burst of nucleation happened only when the real oversaturation exceeded that value. Immediately followed a fast growth, and dissolution of some KCl seeds, thus helped formation of the inner hopper structure. Later, however, with a steady cooling environment with 1.2/h in Fig. IV. 1k, the branches obtained chances to show an ideal development as big cubic. With a slower cooling rate in Fig. IV. 1l at 0.75 °C/h, the branches achieved a better grow as well as attrition on the surface of cubic corners where the latter phenomenon usually occurred with long enough crystallization process. As a result, the crystals showed an aggregation with several spherical small particles. Among which some remained a hopper-like structure with 8 spherical small particles as displayed on upper left corner in Fig. IV. 1l, illustrating the similar growing mechanism as above results.

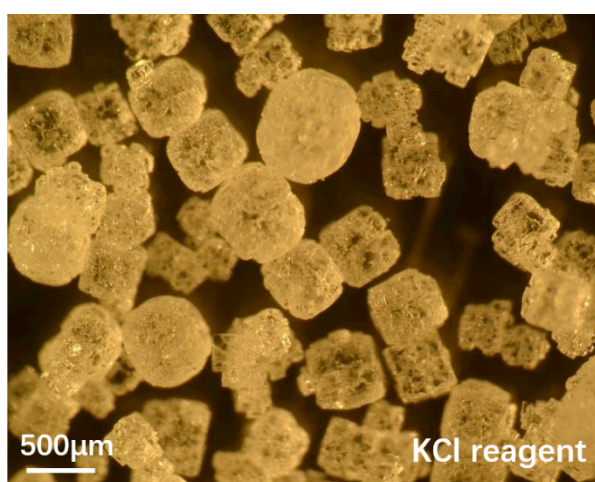


Fig. IV. 5. Stereoscopic results of KCl reagent

One other impactor involved was the additive seeds that always pertained great influence on the morphology of crystals. Analyzed grade of KCl was used as an

environment-friendly additive without non-necessary substance to study the influence on cooling experiments. The original reagent pertained a rough surface as shown in Fig. IV. 5. Limited amounts including 0.1, 0.2, 0.3 and 0.4g KCl was added into the saturated salinity at 30 °C and the results were displayed in Fig. IV. 1m, n, o and p. It's clear that crystals showed an even distribution and discrepancy from reagent morphology with only 0.1g additive seeds, while big size particle with a spherical shape remained with more seeds, indicating the possibility of adjusting crystal morphology and shape distribution with low amount of original reagent. Inferred was the mechanism that additive seeds helped breaking the balance of saturated solution, dissolve, and growth of KCl occurred on surface of seeds at the same time, thus to help average the morphology of grown crystals. However, excessive seeds aggravated the crystallization of KCl on surface of seeds but the dissolve was restrained thus reserved those big particles in reagent. As a consequence, proper amount of crystal seeds would help with modulating morphology of grown crystals with the dynamic adjustment between dissolve and crystallization of the additive seeds.

4.2.2. Crystal Products

4.2.2.1. Hopper-like structure

As a typical FCC (Face-centered cubic) type crystal, a standard basic KCl crystal would grow to be a cubic structure with sharp corners. In this work, the grown crystal by cooling method showed a hopper like structure, as shown in the inserted picture in Fig. IV. 6. The special anisotropic structure could be attributed to the faster growth on corners and edges than the centers of its faces. Before the core cubic grow as a bigger cubic, the eight corners turned to be the site of secondary nucleation, then the corners of secondary cubic became the sites of ternary nucleation, and so on, thus to form a hopper-like structure with higher exposure of crystal face area in comparison with basic cubic structure, as illustrated in the inserted pictures in Fig. IV. 6. Their corresponding X-ray diffraction (XRD) results demonstrated that they exhibited similar crystal faces but the hopper structure crystal pertained much stronger diffracted intensity, indicating the success of high exposing crystal faces area of the hopper-like structure. Notably, the connected part between two “steps” might be the extra crystal face (220) and (222), in consistent with XRD result. Aided by the multi-staged structure, the hopper-like crystal exhibited greater surface area than that of a cubic crystal.

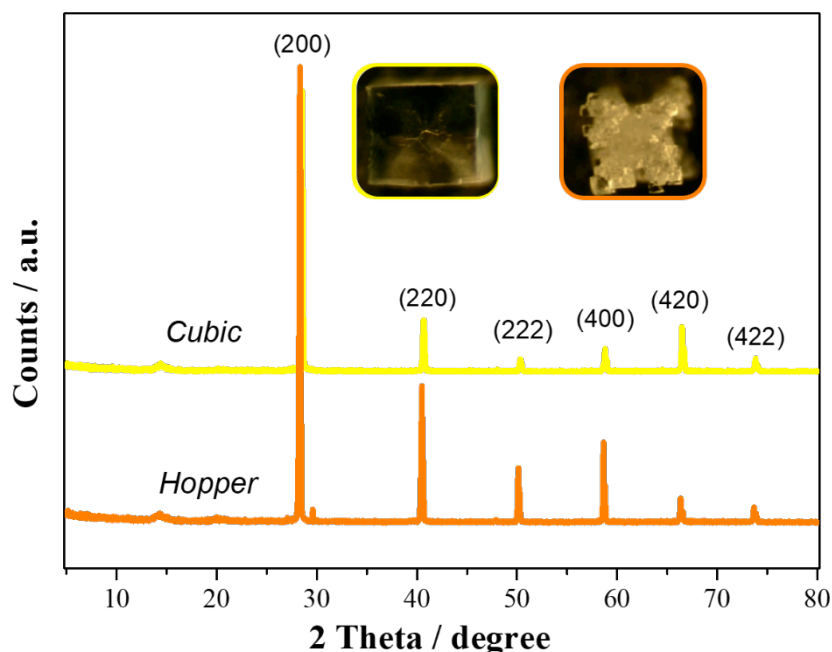


Fig. IV. 6. X-ray diffraction and Stereoscopic results of cubic and hopper like structure KCl crystals

Based on results above, the different growing rates of lattice plane contributed to the various appearances with the same hopper-like structure. To further unveil the influence of common cooling parameters, series of batch experiments were applied here to study the different shapes of KCl crystals by additive-free method.

Demonstrated above was the phenomenon that the KCl crystals tended to show a hopper-like structure during the cooling process in proper range and rate. Nevertheless, the evolution of this special structure remained unclear which should be an interesting part to help understanding the mechanism. In this part, the beginning temperature of solution and cooling rate were set to be 30 °C and 3 °C/h based on previous research to get the uniform hopper-like structure, thus the different crystallization period should be the only factor to influence the crystals. By collecting crystals of those batch experiments, evolution of hopper-like structure would be easily unveiled as shown in Fig. IV. 7.

It's clear that at the first stage of crystallization as in Fig. IV. 7a, hopper-structure appeared in a rough and frizzy way, indicating the fast nucleation with high supersaturation as mentioned before. Meanwhile, those crystals with thin and underdeveloped branches ended up in aggregations due to their high surficial energies. As time elapsed, the branches of crystals in Fig. IV. 7b acquired the chance to further

grow to exhibit less sharp structure, ensuring the hopper-like structure with a better distribution. By comparing Fig. IV. 7b, c and d, there was a tendency that the crystals kept in a form composing of 8 small units but increasing sphericity. Growth as well as attribution were thought to be the main mechanisms of this phenomenon. More detailed revolution results were displayed in Fig. IV. 8, with the similar conclusion illustrated by those typical morphologies.

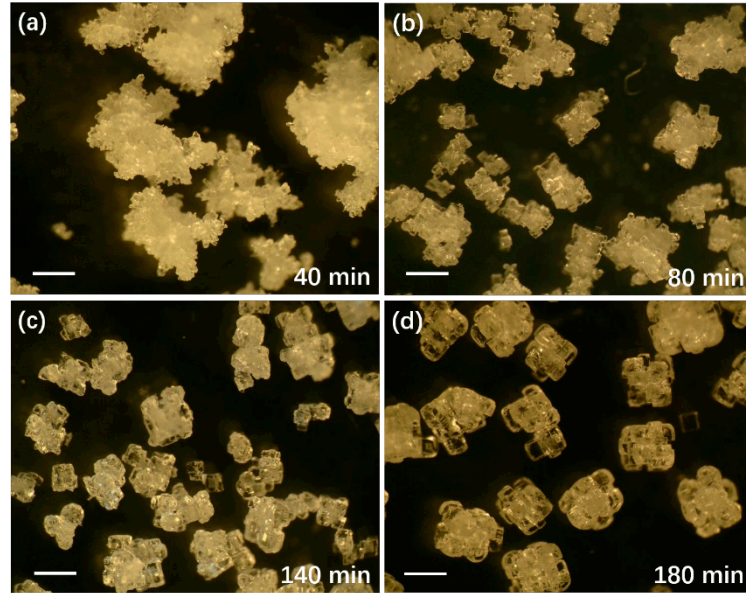


Fig. IV. 7. Stereoscopic results of KCl crystals grown by batch cooling experiments from 30 °C for increasing period with cooling rate at 3 °C/h, scale bar=500 μm.

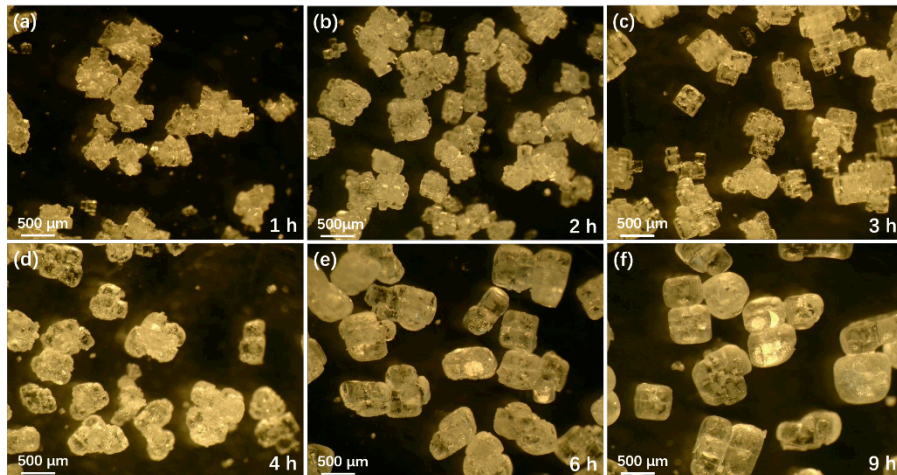


Fig. IV. 8. Stereoscopic results of KCl crystals grown by batch cooling experiments with stirring rate of 400 rpm and cooling rate at 1 °C/h from 40 °C for 1, 2, 3, 4, 6 and 9 h, respectively (3.2.2)

4.2.2.2. Sphere-like crystals

Normally, the perfect cubic structure exhibited six foursquare faces as the surface, coming with the high possibility of cohesion, thus hindered the separation of crystals during production transfer process and got medicine invalidated. Though by cooling method, superficial area of produced hopper-like crystal increased by the stackable growth of cubic units but remained the foursquare surface. Therefore, efforts have been made to grow crystals with special shapes to avoid clusters formation. It's known that the morphology of crystal production shows an important role in the transportation process as well as application. One of the most favored shape of crystals is spherical structure with low possibility of aggregation. Nevertheless, it's hard to change the intrinsic propriety of crystals at ambitious temperature and pressure without additives. Hence, in this part, only the spherical-like structure of KCl crystals by abrasion from cubic habit was studied to help understand the evolution of cubic-to-spherical crystal.

Shown in Fig. IV. 9 was the evolution of aspheric KCl crystals. During the cooling experiments, a greater value of cooling range between 40-30 °C was set to get a better morphology of crystals to help research the evolution process. Similar to the conclusions in Fig. IV. 1i, j, k, l and Fig. IV. 4, the former crystals displayed a hopper-like structure as in Fig. IV. 9a, b c and also d, demonstrating a common phenomenon during cooling process. However, in Fig. IV. 9e, the units of a hopper structure became smooth to form a bigger cluster. Notably, the eight units as the branches of a hopper structure got chance to grow completely as cubic formation to form a bigger cubic with obvious crossing lines in the center. Besides, due to the Oswald ripening, some crystals were dissolving and others growing, thus showing in various size distribution. With a slower growing rate in Fig. IV. 9f, the limited ions tend to form crystals only in relative greater size, single cubic-like crystals with crossing lines could also be found. Similar conclusion appeared in slower cooling rate as shown in Fig. IV. 9g and h. The final crystal in Fig. IV. 9i pertained a spherical morphology of size over 500 μm with smooth surfaces, indicating the tendency of increasing size and smoothness with smaller cooling rate. Apart from cooling rate, the evolution of the spherical crystal in Fig. IV. 9i (i.e., cooling rate at 1 °C / h) was also studied as shown in Fig. IV. 10. Cubic crystals with crossing lines pertain a great percentage in Fig. 10c, then they got abraded to show spherical surfaces instead of well-cubic forms. Finally, as time elapsed, the cubic crystal with eight smaller cubic units turned to show a whole structure with spherical structure in Fig. IV. 10f^[22]. The quantity of KCl crystals displayed a decreasing trend here which could be ascribed to

the Ostwald Ripening theory that small pieces of crystals would dissolve to form bigger crystal due to the difference of ions concentration near surface of crystals.

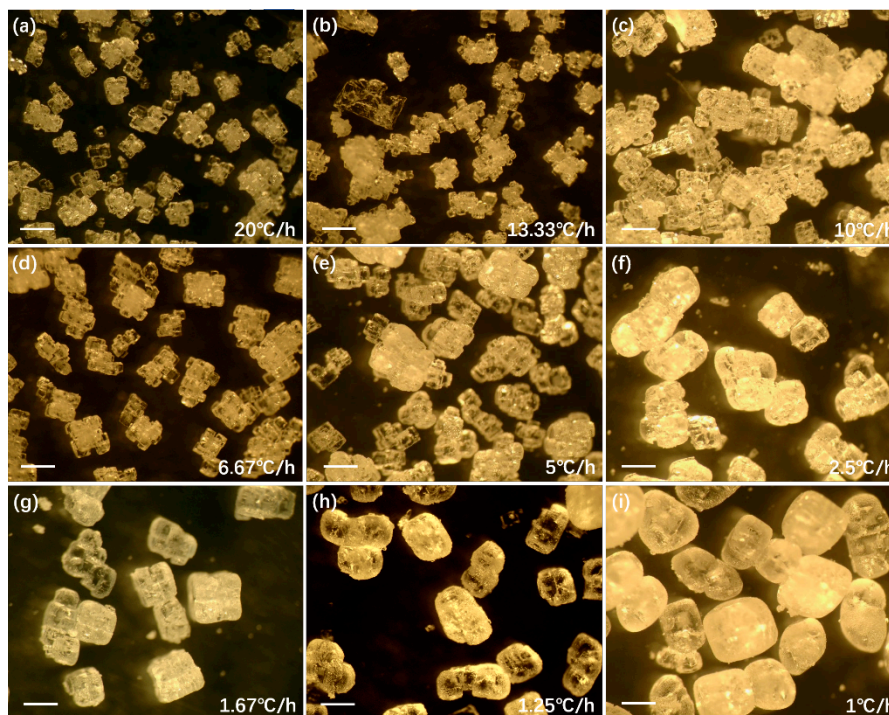


Fig. IV. 9. Stereoscopic results of KCl crystals grown by batch cooling experiments from 40 °C to 30 °C with decreasing cooling rate at 20, 13.33, 10, 6.67, 5, 2.5, 1.67, 1.25 and 1 °C/h. Scale bar=500 μm .

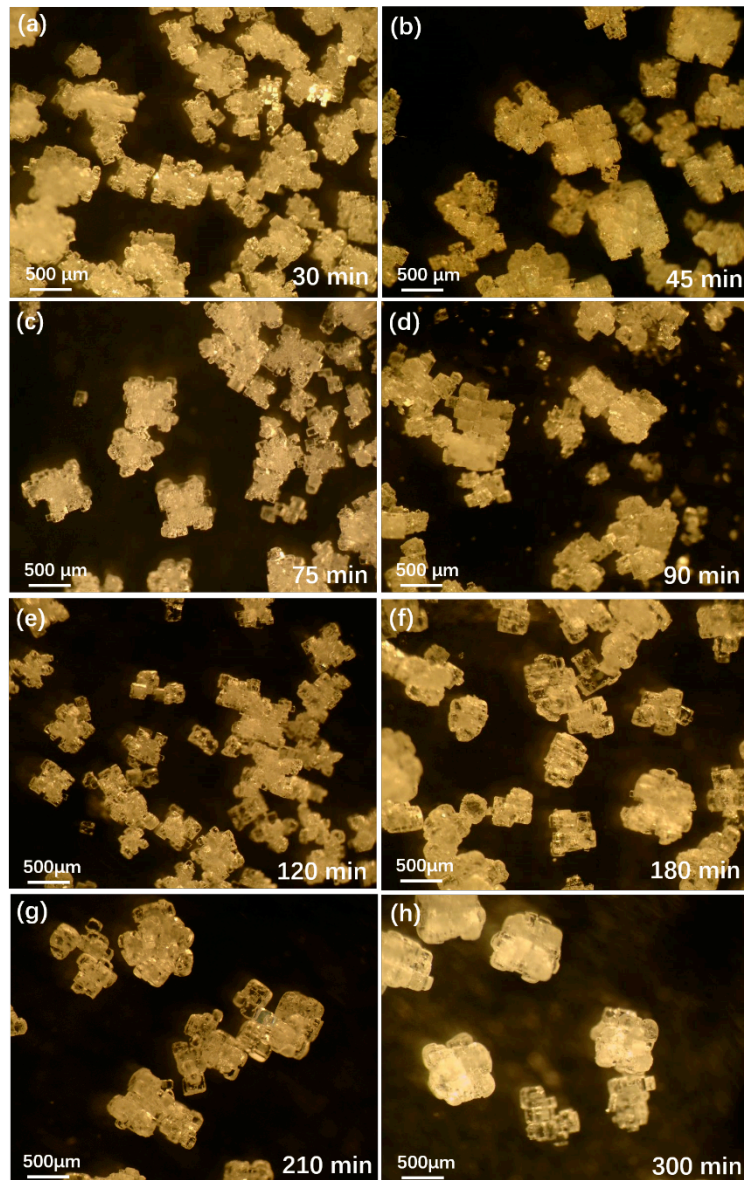


Fig. IV. 10. Stereoscopic results of KCl crystals grown by batch cooling experiments with stirring rate of 400 rpm and cooling rate at 3 °C/h from 30 °C for 30, 45, 75, 90, 120, 180, 210 and 300 min, respectively. (3.2.3)

4.2.2.3. *Hollow cube-like crystals*

Demonstrated was that the crystals shapes are affected by adding extra ions that might also introduce impurities thus lower the production qualities. Interestingly, the composing ions of crystals in solution may show influences on the final shape. Taking KCl for example, the structure of KCl is face-centered cubic, indicating the repeating unit consisted by K and Cl element with ratio of 1:1 as shown in Fig. IV. 11. Actually, there are many types of foreign chemical like NaCl, MgCl₂ and K₂SO₄ during industrial manufacture process of extracting KCl from salt-lake, and plentiful

attention has been stressed to research the impacts of Na^+ , Mg^{2+} and SO_4^{2-} which is not the main content in this discussion but only the two constituent ions of KCl. Moreover, the pH of solution is not always at 7 which means extra H^+ or OH^- ions, for example, flotation of KCl was always conducted under $\text{pH}\sim 6$ by using octadecylamine hydrochloride as collector^[36–38]. (Surface chemistry features in the flotation of KCl) In this section, to understand how excess K or Cl ions in solution will influence the KCl crystals shapes, certain quantities of KOH and HCl was added into the solution and cooling process was performed.

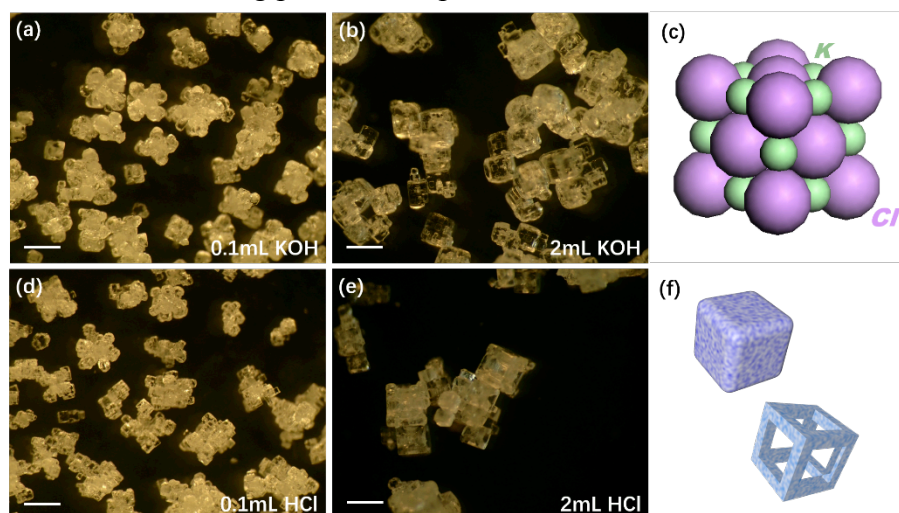


Fig. IV. 11. Stereoscopic results of KCl crystals grown by batch cooling experiments from 30 to 27 °C with existence of 0.1mL of KOH (a) and HCl (d), and 1mL of KOH (b) and HCl (e) from 30 to 23 °C for 700 min, especially. Scale bar=500 μm . Atomic illustration of KCl with Cl (c) or K (f) as center atom.

Shown in Fig. IV. 11 are the results of KCl crystals with 0.1%, 2% addition of KOH and 0.1% and 2% addition of HCl during crystallization procedure. Interestingly, the morphologies of Fig. IV. 11a and 11d shared the similar hopper-like structure but different details of branches. Here, the KOH and HCl were thought to be original of only K/Cl ions since OH/H ions with 0.1% and 2% dosage were later found to be not working as effective factors during crystallization. With limited extra K ions, the small units of hopper structure showed more spherical shape, indicating the importance of K ions as the face centered member of cubic structure. This phenomenon was further demonstrated in Fig. IV. 11b that when excessive K ions were added in solution for longer period and full reaction, the cubic structure of KCl maintained with smooth edges on prisms of cubic structure. According to the atomic structure diagram in Fig. IV. 11c, the K atoms occupied the center of each prism with Cl atom as corner atom, thus helping formation of structure by 12 K atoms as

structure of cubic without sharp corners (Cl atoms). In Fig. IV. 11d, when small amount addition of Cl ions was applied, crystals also exhibited hopper structure with thin arms on eight corners, while they grew to get connected by a framework structure with more Cl ions in Fig. IV. 11e. The phenomenon should be explained by the same mechanism above that connected Cl atoms on corners promised the structure of prisms. Notably, the deformation of crystallization habit requires restrict conditions which promises KCl crystals with cubic-like structure under constant temperature and pressure. For the cooling process with extra K or Cl ions, the abundant adding ions would work as frames of cubic-like structure, thus exhibiting crystals as smooth cubic with K element at center on prisms or hollow cubic with Cl ions at corners as illustration in Fig. IV. 11f.

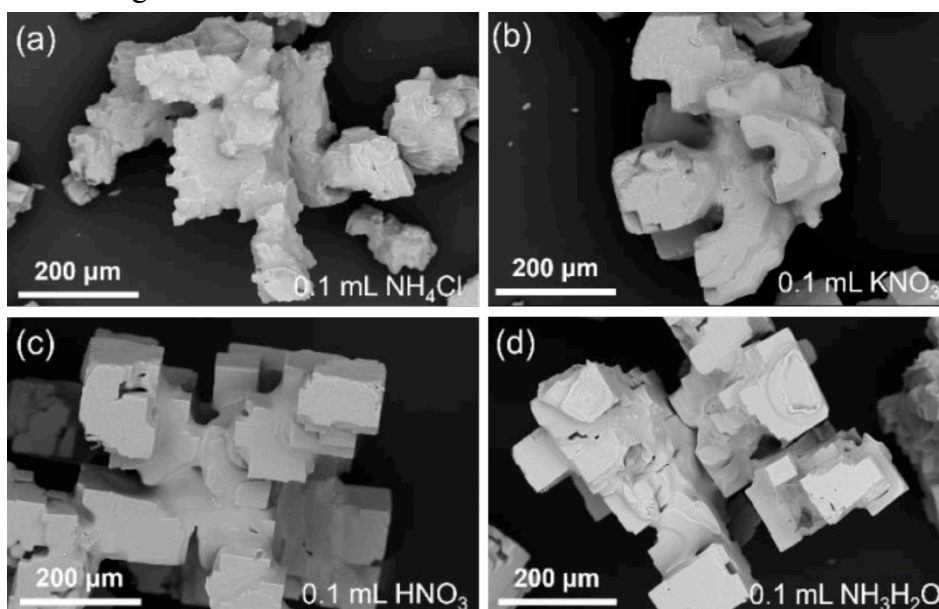


Fig. IV. 12. SEM morphology result of KCl crystals grwon by batch cooling experiments with 0.1 mL additive as NH_4Cl , KNO_3 , HNO_3 , and $\text{NH}_3\cdot\text{H}_2\text{O}$ stirring rate of 400 rpm and cooling rate at 3 $^\circ\text{C}/\text{h}$ from 30 $^\circ\text{C}$ for 60 min, respectively.

It's worth noting that to exclude the OH^- and H^+ ions impacts, additive ions NH_4Cl , KNO_3 , HNO_3 and $\text{NH}_3\cdot\text{H}_2\text{O}$ were also applied to batch cooling crystallization of KCl as shown in Fig. IV. 12 with dosage as 0.1% and 13 as 2%. It could be concluded that extra HNO_3 and $\text{NH}_3\cdot\text{H}_2\text{O}$ had limited influence on the shape of KCl crystals as hopper structure. However, with additive NH_4Cl in Fig. IV. 12a and 13a, both low and high dosage yield KCl crystal with well-grown branches from 8 corners, similar with results with extra HCl . With 0.1% and 2% extra KNO_3 in Fig. IV. 12b and 13b, both KCl crystals possessed cubic form with relatively perfect shape. The

shapes of these crystals were not in excellent coincidence with that with extra HCl and KOH, it could be ascribed to the minor impact of NH_4^+ and NO_3^- ions. Here, the supplementary results only aimed to help understand the extra composing K and Cl ions' influence on KCl crystals. The above results further demonstrated the idea of modulating crystallization based on intrinsic repeating unit of KCl crystals.

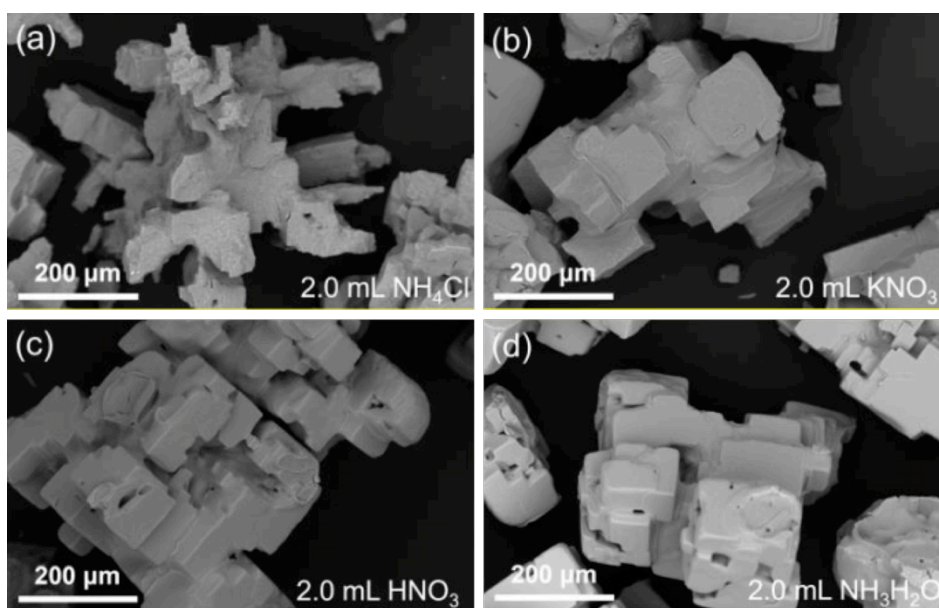


Fig. IV. 13. SEM morphology result of KCl crystals grown by bath cooling experiments with 2.0 mL additive as NH_4Cl , KNO_3 , HNO_3 , and $\text{NH}_3\cdot\text{H}_2\text{O}$ stirring rate of 400 rpm and cooling rate at 3 $^\circ\text{C}/\text{h}$ from 30 $^\circ\text{C}$ for 120 min, respectively.

4.2.3. Structural and surficial properties

4.2.3.1. Structure

Based on above work, various morphology of KCl crystal have been prepared including hollow cubic, smooth cubic, hopper and spherical KCl crystals as shown in inserted pictures in Fig. IV. 14, along with their corresponding XRD results that all of them showed high purity and crystallinity. It's clear that smooth cubic structure contains high percentage of (200) face while hollow cubic relatively more (220) face which could be a consequence of the inner beveling. For hopper structure, the abundant complicating exposing area displayed extra (222) faces. Limited faces of (200) and (400) were shown in spherical structure due to its isotropy. In conclusion, various shape with special exposing area would contribute to the different intensity of crystal faces, promising their further applications related to the properties of exposing faces.

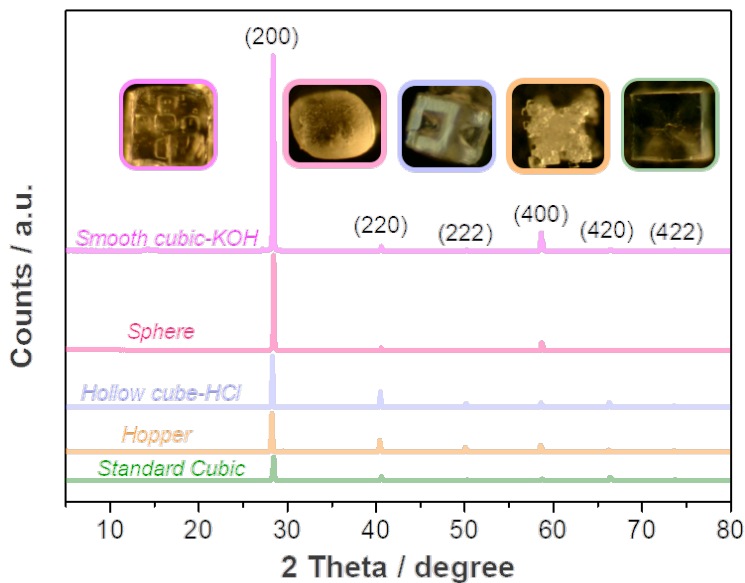


Fig. IV. 14. XRD results of smooth cubic with KOH, spherical, hollow cube with HCl, hopper and standard cubic KCl structure, and corresponding stereoscopic results.

4.2.3.2. Roughness

Aimed shapes prepared above guaranteed them with special structures for wider application but the surficial morphology of grown crystals remained unveiled. Here, SEM combined with three-dimensional graph was performed to help understand the surficial properties as shown in Fig. IV. 15. SEM and their corresponding three-dimensional results of smooth cubic with KOH additive in Fig. IV. 15a and 15b showed a relative flat surface on the cubic part, with a smooth corner instead of sharp one, indicating the preferred formation of foursquare face rather than prisms. The surface of spherical structure in Fig. IV. 15c and 15d exhibited a circular arc with relative high roughness which could ascribed to the formation mechanism of spherical structure from cubic structure as explained above. For hollow cubic structure in Fig. IV. 15e and 15f with addition of HCl, prisms with sharp corners remained with a foursquare hole on center of the six faces of one cubic structure. Similarly, hopper structure in Fig. IV. 15g and 15h showed holes in center of each face, with eight branches on direction of corners. On the contrary, the original basic cubic of KCl structure in Fig. IV. 15i and 15j displayed rather flat surfaces due to the well crystallization.

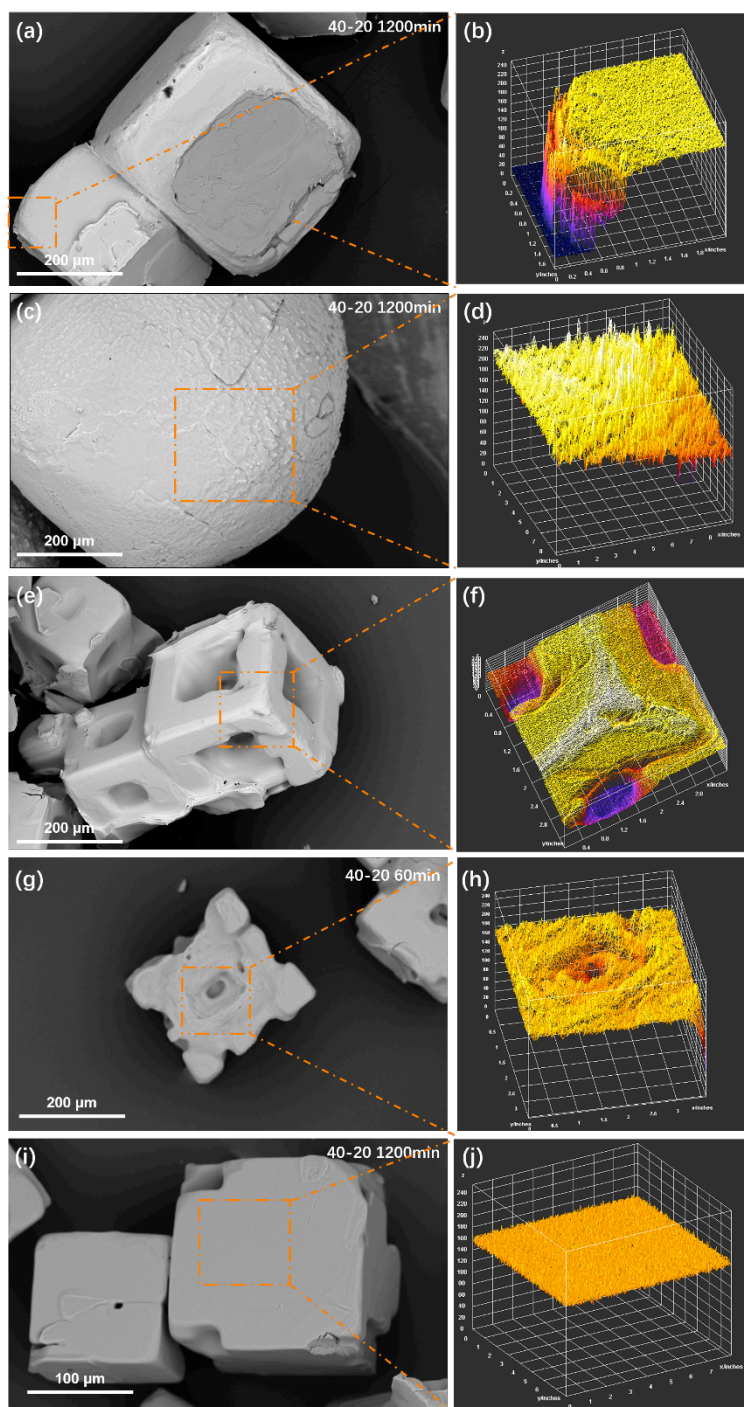


Fig. IV. 15. SEM results of smooth cubic with KOH, spherical, hollow cube with HCl, hopper and standard cubic KCl structure, and their surficial 3D plot results.

4.3. Conclusions

In summary, a green and controllable approach was proposed for preparation of various structure and morphology of KCl through supersaturation modulation. Hopper -, sphere- and hollow cube-like crystals were obtained in the work. The parameters

including stirring speed, additive seeds, pH condition, cooling range and rate in the supersaturation modulation technology were well researched and explained. At certain condition, the crystal would grow in a uniform state, otherwise, they would form as small pieces, abrasion of crystals, etc. Different products were analyzed in the structure, morphology and surficial property. Three-dimensional visualization was applied in detecting roughness and appearance of crystal. The main exposed faces for smooth cubic, hollow cubic, and hopper structure were (200), (220), and (400) facet, respectively, which could be a consequence of the inner beveling. Spherical structure surface showed a higher roughness than the others, which was originated from the formation mechanism of spherical structure to cubic structure. Herein, the work developed an environment-friendly method to prepare different crystal structure for application as template, flotation, and others.

References

- [1] X. Qu, B. Zhang, J. Zhao, B. Qiu, X. Chen, F. Zhou, X. Li, S. Gao, D. Wang, H. Yin, Salt-thermal methods for recycling and regenerating spent lithium-ion batteries: a review, *Green Chemistry* 25 (2023) 2992–3015. <https://doi.org/10.1039/D2GC04620B>.
- [2] P.S. Carvalho, G.G.F. Guimarães, L.F. Diniz, J. Ellena, C. Ribeiro, Highly water soluble agrichemicals by using engineered organic salts for reducing adverse environmental impacts, *Green Chemistry* 21 (2019) 6419–6429. <https://doi.org/10.1039/C9GC02439E>.
- [3] Y. Tang, F. Zhang, Z. Cao, W. Jing, Y. Chen, Crystallization of CaCO₃ in the presence of sulfate and additives: Experimental and molecular dynamics simulation studies, *J Colloid Interface Sci* 377 (2012) 430–437. <https://doi.org/10.1016/J.JCIS.2012.02.069>.
- [4] H. Peng, J. Gudgeon, J. Vaughan, Nucleation phenomena of supersaturated KCl solutions revealing by molecular dynamic simulation: Implication of dehydration shell process, *J Mol Liq* 283 (2019) 108–115. <https://doi.org/10.1016/J.MOLLIQ.2019.03.076>.
- [5] E. Li, H. Liang, Z. Du, D. Li, F. Cheng, Adsorption process of Octadecylamine Hydrochloride on KCl crystal surface in various salt saturated solutions: Kinetics, isotherm model and thermodynamics properties, *J Mol Liq* 221 (2016) 949–953. <https://doi.org/10.1016/J.MOLLIQ.2016.06.050>.
- [6] D. Zheng, M. Xu, J. Wang, Y. Ma, Y. Tian, Y. Shen, X. Wu, M. Yang, Nonisothermal crystallization kinetics of potassium chloride produced by stirred crystallization, *J Cryst Growth* 603 (2023) 127035. <https://doi.org/10.1016/j.jcrysgro.2022.127035>.

- [7] Poirier, J. P., Creep of crystals: High-temperature deformation processes in metals, ceramics and minerals, Cup (1985). <https://ui.adsabs.harvard.edu/abs/1985cup..book.....P/abstract> (accessed August 15, 2023).
- [8] S. Li, W.L. Song, X. Han, Q. Cui, Y. li Zhu, S. Jiao, Low-temperature graphitization of lignin via Co-assisted electrolysis in molten salt, *Green Energy & Environment* (2023). <https://doi.org/10.1016/J.GEE.2023.04.006>.
- [9] J. Phother-Simon, I. Hanif, T. Jonsson, J. Liske, High-Temperature corrosion of P91/T91, 304L, Sanicro 28 and Inconel 625 exposed at 600 °C under continuous KCl deposition, *Fuel* 357 (2024) 130012. <https://doi.org/10.1016/j.fuel.2023.130012>.
- [10] C. Li, J. Yao, Y. Huang, C. Xu, D. Lou, Z. Wu, W. Sun, S. Zhang, Y. Li, L. He, X. Zhang, Salt-templated growth of monodisperse hollow nanostructures, *J Mater Chem A Mater* 7 (2019) 1404–1409. <https://doi.org/10.1039/C8TA11318A>.
- [11] I.L. Egun, H. He, D. Hu, G.Z. Chen, Molten Salt Carbonization and Activation of Biomass to Functional Biocarbon, *Adv Sustain Syst* 6 (2022) 2200294. <https://doi.org/10.1002/ADSU.202200294>.
- [12] S. Solgi, F. Samavat, S. Mirzakuchaki, M. Sasani Ghamsari, Effect of different type of dopants on the enhancement of KCl single crystal optical properties, *Optik (Stuttg)* 241 (2021) 166554. <https://doi.org/10.1016/j.ijleo.2021.166554>.
- [13] B. Jing, C. Peng, Y. Wang, Q. Liu, S. Tong, Y. Zhang, M. Ge, Hygroscopic properties of potassium chloride and its internal mixtures with organic compounds relevant to biomass burning aerosol particles, *Sci Rep* 7 (2017) 43572. <https://doi.org/10.1038/srep43572>.
- [14] R. Majgier, C.L. Rääf, A. Mandowski, C. Bernhardsson, OSL PROPERTIES IN VARIOUS FORMS OF KCl AND NaCl SAMPLES AFTER EXPOSURE TO IONIZING RADIATION, *Radiat Prot Dosimetry* 184 (2019) 90–97. <https://doi.org/10.1093/rpd/ncy189>.
- [15] R. Majgier, M. Biernacka, A. Mandowski, Influence of thermal treatment on OSL regeneration in potassium chloride, *Radiat Meas* 90 (2016) 242–246. <https://doi.org/10.1016/j.radmeas.2016.01.019>.
- [16] K. Shunkeyev, A. Tilep, Sh. Sagimbayeva, A. Lushchik, Z. Ubaev, L. Myasnikova, N. Zhanturina, Zh. Aimaganbetova, The enhancement of exciton-like luminescence in KCl single crystals under local and uniaxial elastic lattice deformation, *Nucl Instrum Methods Phys Res B* 528 (2022) 20–26. <https://doi.org/10.1016/j.nimb.2022.08.002>.
- [17] L. V. Dikhtievskaya, V. V. Shevchuk, Inorganic modifiers controlling the physicochemical and mechanical properties of potassium fertilizer dispersions, *Russian Journal of Applied Chemistry* 87 (2014) 1223–1228. <https://doi.org/10.1134/S1070427214090055>.

- [18] M. Shiehpour, S. Solgi, M.J. Tafreshi, M.S. Ghamsari, ZnO-doped KCl single crystal with enhanced UV emission lines, *Applied Physics A* 125 (2019) 531. <https://doi.org/10.1007/s00339-019-2846-8>.
- [19] Y. Li, S. Xu, F. Meng, H. Liu, S. Sun, B. Liu, X. Zhang, X. Sun, C.K. Mahadevan, Insight into the photoluminescence and thermoluminescence properties of Tb ions doping KCl crystal grown by Cz method, *Journal of Materials Science: Materials in Electronics* 34 (2023) 2163. <https://doi.org/10.1007/s10854-023-11424-4>.
- [20] L. Huang, Z. Hu, H. Jin, J. Wu, K. Liu, Z. Xu, J. Wan, H. Zhou, J. Duan, B. Hu, J. Zhou, Salt-Assisted Synthesis of 2D Materials, *Adv Funct Mater* 30 (2020) 1908486. <https://doi.org/10.1002/ADFM.201908486>.
- [21] C.W. Kang, J.H. Ko, S.M. Lee, H.J. Kim, Y.J. Ko, S.U. Son, Noncovalent and covalent double assembly: unravelling a unified mechanism for the tubular shape evolution of microporous organic polymers, *J Mater Chem A Mater* 7 (2019) 7859–7866. <https://doi.org/10.1039/C9TA00464E>.
- [22] S. Jin, M. Chen, Z. Li, S. Wu, S. Du, S. Xu, S. Rohani, J. Gong, Design and mechanism of the formation of spherical KCl particles using cooling crystallization without additives, *Powder Technol* 329 (2018) 455–462. <https://doi.org/10.1016/j.powtec.2018.02.001>.
- [23] R. Cheula, M.D. Susman, D.H. West, S. Chinta, J.D. Rimer, M. Maestri, Local Ordering of Molten Salts at NiO Crystal Interfaces Promotes High-Index Faceting, *Angewandte Chemie International Edition* 60 (2021) 25391–25396. <https://doi.org/10.1002/ANIE.202105018>.
- [24] S. Gao, Y. Tang, Y. Gao, L. Liu, H. Zhao, X. Li, X. Wang, Highly Crystallized Co₂Mo₃O₈ Hexagonal Nanoplates Interconnected by Coal-Derived Carbon via the Molten-Salt-Assisted Method for Competitive Li-Ion Battery Anodes, *ACS Appl Mater Interfaces* 11 (2019) 7006–7013. https://doi.org/10.1021/ACSAMI.8B20366/ASSET/IMAGES/MEDIUM/AM-2018-20366_S_M003.GIF.
- [25] E.S. Sanil, K.H. Cho, S.K. Lee, U.H. Lee, S.G. Ryu, H.W. Lee, J.S. Chang, Y.K. Hwang, Size and morphological control of a metal–organic framework Cu-BTC by variation of solvent and modulator, *Journal of Porous Materials* 22 (2015) 171–178. <https://doi.org/10.1007/S10934-014-9883-7/FIGURES/8>.
- [26] D. Kyom Kim, J. Seul Byun, S. Moon, J. Choi, J. Ha Chang, J. Suk, Molten salts approach of metal-organic framework-derived nitrogen-doped porous carbon as sulfur host for lithium-sulfur batteries, *Chemical Engineering Journal* 441 (2022) 135945. <https://doi.org/10.1016/J.CEJ.2022.135945>.

- [27] S. Liu, J. Tian, L. Wang, H. Li, X. Sun, Organic solvent-induced controllable crystallization of the inorganic salt $\text{Na}_3[\text{Au}(\text{SO}_3)_2]$ into ultralong nanobelts and hierarchical microstructures of nanowires, *Nanoscale* 3 (2011) 1553–1557. <https://doi.org/10.1039/C0NR00690D>.
- [28] S. Bae, J.W. Jo, P. Lee, M.J. Ko, Controlling the Morphology of Organic-Inorganic Hybrid Perovskites through Dual Additive-Mediated Crystallization for Solar Cell Applications, *ACS Appl Mater Interfaces* 11 (2019) 17452–17458. https://doi.org/10.1021/ACSAMI.9B03929/ASSET/IMAGES/LARGE/AM-2019-03929A_0004.JPEG.
- [29] Y. Liu, J.H. He, J.Y. Yu, H.M. Zeng, Controlling numbers and sizes of beads in electrospun nanofibers, *Polym Int* 57 (2008) 632–636. <https://doi.org/10.1002/PI.2387>.
- [30] M.R. Singh, D. Ramkrishna, A comprehensive approach to predicting crystal morphology distributions with population balances, *Cryst Growth Des* 13 (2013) 1397–1411. https://doi.org/10.1021/CG301851G/ASSET/IMAGES/CG-2012-01851G_M044.GIF.
- [31] Y. Zhang, Y. Liu, S. Fu, F. Guo, Y. Qian, Morphology-controlled synthesis of Co_3O_4 crystals by soft chemical method, *Mater Chem Phys* 104 (2007) 166–171. <https://doi.org/10.1016/J.MATCHEMPHYS.2007.03.003>.
- [32] Z. Xie, M. Xin, L. Wei, X. Rao, M. Zeng, B. Liu, Q. Zhang, Morphology evolution and performance of zinc electrode in acid battery environment with ionic liquid, *J Energy Storage* 47 (2022) 103569. <https://doi.org/10.1016/J.EST.2021.103569>.
- [33] K. Sun, C. V. Nguyen, N.N. Nguyen, X. Ma, A. V. Nguyen, Crucial roles of ion-specific effects in the flotation of water-soluble KCl and NaCl crystals with fatty acid salts, *J Colloid Interface Sci* 636 (2023) 413–424. <https://doi.org/10.1016/J.JCIS.2023.01.038>.
- [34] S. Paul, C. Wang, K. Wang, C.C. Sun, Reduced Punch Sticking Propensity of Acesulfame by Salt Formation: Role of Crystal Mechanical Property and Surface Chemistry, *Mol Pharm* 16 (2019) 2700–2707. <https://doi.org/10.1021/ACS.MOLPHARMACEUT.9B0024>.
- [35] Z. Yang, L. Shi, H. Wang, J. Xiong, X. Xu, L. Sun, J. Jiang, Q. Zhuang, Y. Chen, Z. Ju, Crystallization-induced thickness tuning of carbon nanosheets for fast potassium storage, *J Colloid Interface Sci* 653 (2024) 30–38. <https://doi.org/10.1016/J.JCIS.2023.09.050>.
- [36] H. Cheng, Q. Hai, J. Song, X. Ma, C. Li, The role of Mg value and moisture content of decomposed products during the decomposition process of carnallite in aqueous solution: a novel monitoring method, *RSC Adv* 10 (2020) 20529–20535. <https://doi.org/10.1039/D0RA03567J>.

- [37] H. Cheng, H. Ma, Q. Hai, Z. Zhang, L. Xu, G. Ran, Model for the decomposition of carnallite in aqueous solution, *Int J Miner Process* 139 (2015) 36–42. <https://doi.org/10.1016/J.MINPRO.2015.04.007>.
- [38] J. Podder, S. Gao, R. Evitts, R. Besant, D. Matthews, Crystallization of carnallite from KCl-MgCl₂ brine solutions by solvent evaporation process and its structural and mechanical characterization, *Journal of Metals, Materials and Minerals* (2013).

Chapter V. Novel insights into sylvite flotation modulated by exposing facets

5.1. Introduction

KCl, one of key water-soluble minerals^[1], was mined and processed to provide potassium compounds for agricultural industry^[2] and other chemicals like medicine^[3], battery^[4], ceramics^[5], plastics^[6], etc. Since the 1940s, the majority of potash ore was extracted through flotation in potash industry^[7-9]. As the increased demand of potash elements and lower grade of potassium ore, potassium supply is in urgent requirement all over the world^[10,11]. Hence, further improving flotation recovery is critical for optimization of flotation system in industry.

Adjusting hydrophobicity of crystal surfaces and the selectivity of bubble and crystal interaction during flotation process were main way to improve recovery of potash ores^[12-14]. For decades, precursors focused on developing various surfactants (called as collectors) comprising of hydrophilic group and hydrophobic chain in difference of flotation selectivity and capability, such as, primary alkylamines (R-NH₂)^[15] in early stages, sodium alkylamines (R-SO₃Na)^[16], sodium alkylsulfates (R-OSO₃Na)^[17], and fatty acids (R-COOH)^[18]. Despite abundant types of collectors were applied in the industry, flotation recovery still requires further improvement.

Considering that most minerals are crystals whose one typical feature is the well-defined notion of standard repeating units with discernible crystallographic plane, crystal samples exhibit different physical and chemical properties with various exposing faces^[19-21]. For instance, one extreme but common example is two-dimensional crystal materials type showing obvious anisotropy like molybdenite^[22,23], mica^[24], talc^[25] and highly oriented pyrolytic graphite (HOPG)^[26] that can be easily exfoliated to layers along basal (001) plane but difficult to destroy from the other vertical (010) direction, where the latter plane with hanging unsaturated bonds tends to be more active to react with collectors and bubbles during flotation process^[27-29]. On behalf of natural KCl crystals which belongs to typical face-centered-cubic (FCC) type, the most common two structures with single-type exposing faces are i. six square (200) faces composing one cubic structure and ii. eight triangle (222) faces forming an octahedron structure^[30,31]. Moreover, thanks to KCl crystals' good solubility which highly relies on solution conditions^[32,33], samples with various exposing faces can be obtained during the crystallization process by

well-designed strategies. It is likely that the uncommon exposing facets may bring new possibility or show disadvantages, which should be well researched for reaching an ideal flotation recovery. Hitherto, few studies investigated the work about improving floatation of KCl by modulating exposing facets.

During the industrial production, the most used method to recover potassium is by cold decomposition followed with froth flotation using ODA (not only for recovery of KCl but also for restrain of tail mineral NaCl) as collector^[34,35]. Here, KCl crystals with only one type of exposing faces as (200) and (222) were obtained where the surfaces details were shown by atomic force microscope (AFM) to research their growing mechanisms. Flotation performances of two types of KCl samples as well as their corresponding interaction with ODA were well studied by fourier transform infrared spectroscopy (FTIR) and X-ray photoelectron spectroscopy (XPS). Besides, the induction time test and adhesion & adsorption force tests were conducted to further study the interaction behaviors during flotation process. The related mechanism of different flotation recovery with two types of KCl crystals were researched.

5.2. Results and discussion

5.2.1. Morphology characterization

By cooling and lead addition methods, two types of KCl crystals were successfully prepared and their morphology information was studied by SEM and stereoscopy, as shown in Fig. V. 1. It's clear that cubic morphology appeared during cooling method, while octahedron morphologies showed up with existence of small amount of lead ions. The uneven size distribution was due to the easily crystallization of KCl in solution but sieves helped to narrow samples to proper size ranges for other tests. In Fig. V. 1c and 1d, the cubic and octahedron samples shared nearly perfect shapes with only one type smooth surfaces, indicating their high crystallinity which was further researched by XRD test in the following results.

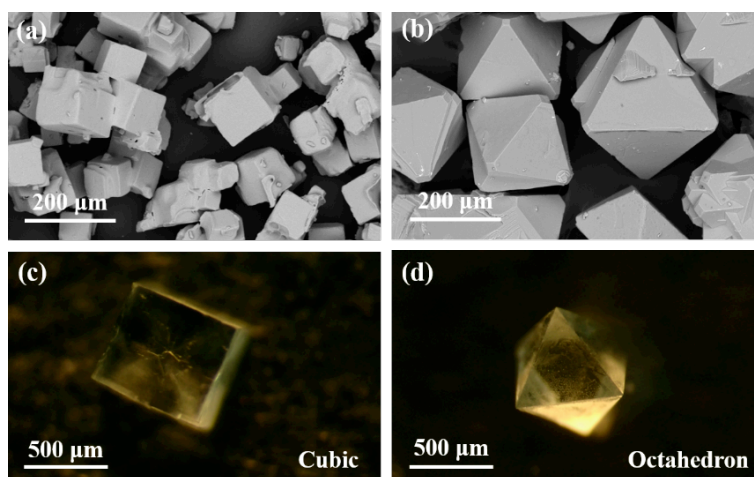


Fig. V. 1. SEM results of cubic (a) and octahedron (b) crystals, and their corresponding stereoscope results.

5.2.2. Crystal Structure

As one of the most important features of crystals, the crystalline structure of KCl samples with cubic and octahedron shapes were studied here. Firstly, the XRD test was performed to cubic and octahedron and corresponding results were displayed in Fig. V. 2. Peaks at around 24.5° , 28.5° , 40.6° , 50.2° , 58.8° , 66.5° and 73.8° were ascribed to (111), (200), (220), (222), (400), (420) and (422) faces of KCl crystals, which were in high agreement with the PDF#73-0306 data of KCl^[37,38]. The high and narrow peaks demonstrated that both two samples pertained high purity of KCl crystal while the cubic sample showed high intensity of (200) face and octahedron sample of (222) face, indicating their different main exposing faces. Besides, the addition of lead ions did not change the structure of KCl crystal but only the exposing face, giving the chance to study the influence of KCl exposing face on its recovery possibility as discussed in the coming part of this work.

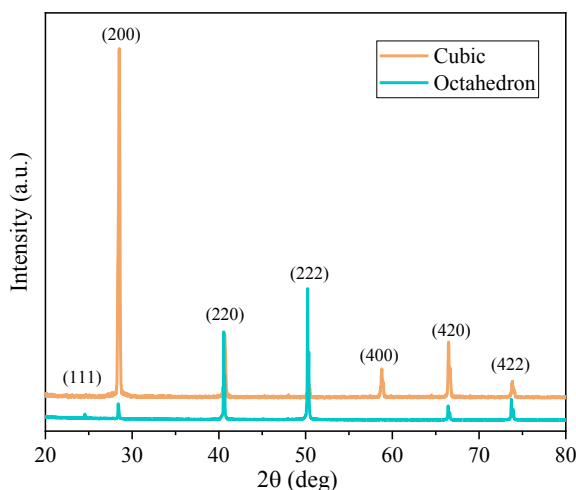


Fig. V. 2. XRD results of cubic and octahedron crystals.

5.2.3. Flotation affected by crystal facets

The flotation experiments of two types of crystals with (200) and (222) exposing faces with size range at 178-250 μm using ODA as collector were conducted, and the flotation kinetics results were shown as Fig. V. 3. Both flotation recovery in the process were highly coincident with classical first-order model, as listed in table V. 1. The flotation rate of KCl (200) was higher than that of KCl (222). The KCl (200) samples achieved a recovery at 83.35%, while recovery of KCl (222) was about 53.42%, demonstrating a better interaction between cubic KCl crystals with bubbles under collector as ODA.

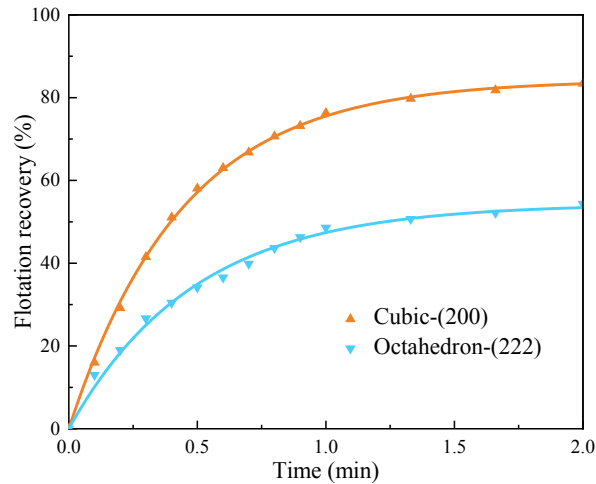


Fig. V. 3. Flotation kinetics results of KCl(200) and KCl(222) crystals using ODA.

Table V. 1. Kinetic parameters for flotation kinetics of classical first-order model.

Samples	Classical first-order model		
	ε_{∞} (%)	k_1 (min^{-1})	R^2
Cubic	84.24	2.27	0.999
Octahedron	54.31	2.06	0.994

5.2.4. Interaction between KCl crystal and collector

In most cases, the minerals would absorb collectors to reach a hydrophobic stage so as to attach to bubbles for being floated. The good flotation behaviors of two samples implied the possible interaction between KCl particles and ODA. Here, FTIR tests were used to study if ODA was absorbed on KCl crystals. From Fig. V. 4, it was clear that before flotation, both KCl (200) and KCl (222) samples showed peaks at 1638.00 and 1114.00 cm^{-1} , belonging to KCl^[39,40]. After reaction, there were new peaks at 2917.77, 2850.27, 1473.35 and 719.32 cm^{-1} on KCl (200) and 2919.70, 2852.20, 1473.35 and 875.53 cm^{-1} on KCl (222) samples, which all belong to ODA, demonstrating the successful adsorption of ODA on KCl samples^[41,42]. However, the interaction type remained unclear which needed further investigation by following XPS tests in Fig. V. 5.

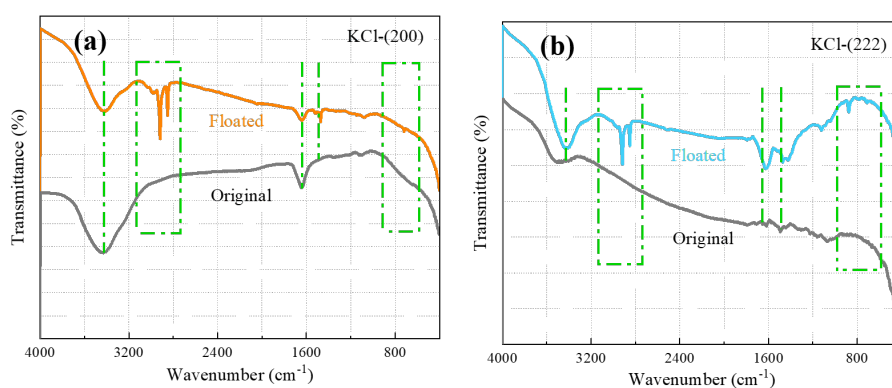


Fig. V. 4. FTIR results of KCl(200) and KCl(222) crystals before and after flotation, respectively.

To further figure out the interaction details between KCl crystals and collector ODA, binding energy information of different elements of KCl (222) before and after flotation was tested by XPS and the related results were displayed in Fig. V. 5. In the survey map, Pb, K and Cl element narrow map of original KCl (222) sample were shown in left four maps in Fig. V. 5a, 5c, 5e and 5g, respectively and their corresponding maps after flotation in right maps of Fig. V. 5b, 5d, 5f and 5h. Notably, the Pb 4f peaks at 138.64 eV and 143.65 eV in Fig. 5c belonged to KPb_2Cl_5 ^[43], it could be ascribed to the minor addition of Pb ions inserting in the crystal structure of KCl (222). By comparing the peaks between left and right, the binding energy difference could be clearly seen that no movement occurred in Pb 4f, K 2p and Cl 2p spectra, indicating that none of new chemical bonds appeared. As a consequence, the

force between KCl (222) and ODA do not belong to chemical adsorption but probably only physical reaction that needed other investigation.

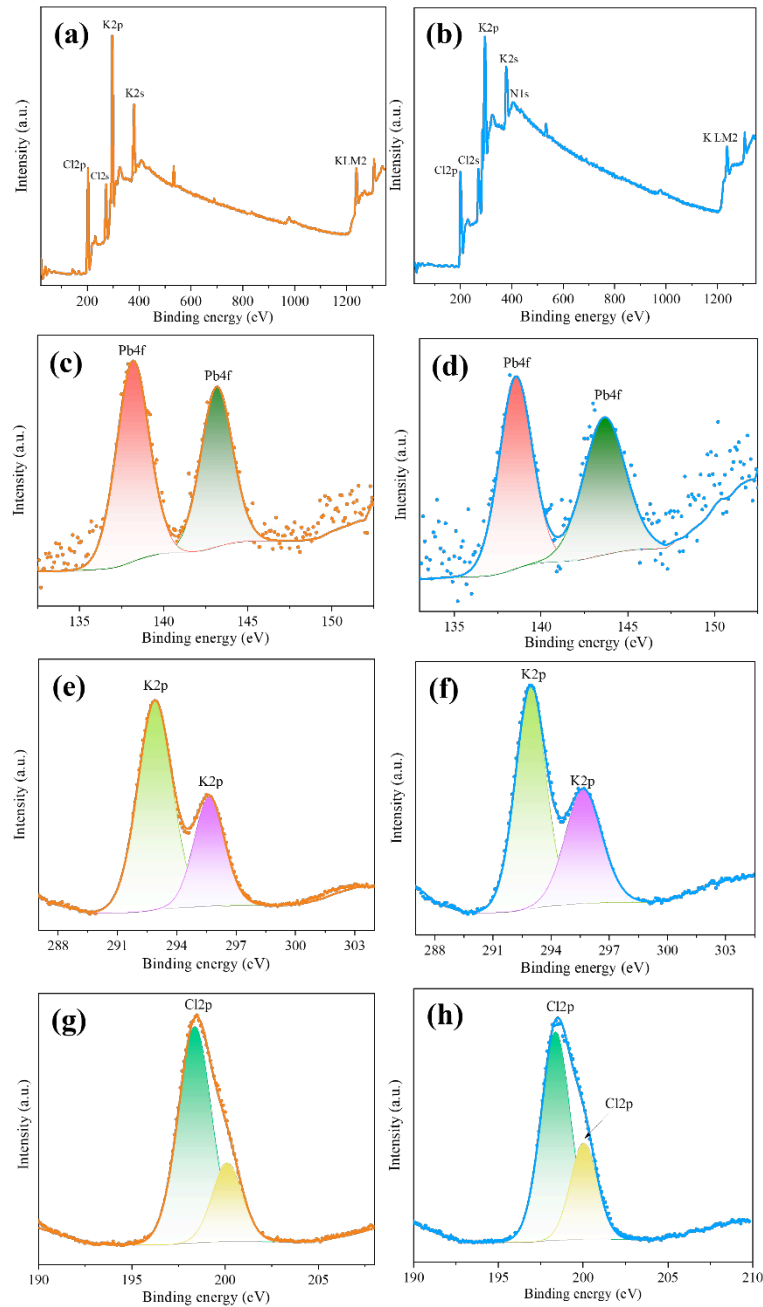


Fig. V. 5. XPS spectra of KCl(222) samples before: (a) survey, (c) Pb 4f, (e) K 2p, (g) Cl 2p and after flotation: (b) survey, (d) Pb 4f, (f) K 2p, (h) Cl 2p.

The above FTIR and XPS results suggested that the ODA's adsorption on KCl could be ascribed to non-chemical force. To reveal the mechanism, zeta potential of KCl (200), KCl (222) before and after reacting with ODA were tested and related

results were displayed in Fig.6. It's known the fact that ODA is a cationic collector with positive charge which was also demonstrated here. In Fig. V. 6, before reaction, KCl (222) and KCl (200) possessed -3.29 mV and -6.41 mV, respectively. According to previous work^[44], similar to LiCl with negative zeta potential, the hydration energy of K ion is higher than that of Cl ion which promotes the dissolve of K ions into solution instead of Cl ions on surface of KCl crystal structure, resulting in the more left Cl⁻ with negative charge of KCl crystals as demonstrated in Fig. V. 6. The different zeta potential of these two samples would be well explained in later discussion. Anyway, as a result, the more negative zeta potential of KCl (200) indicated the better static interaction with cation collector ODA (5.51 mV) than that of KCl (222) crystal during flotation, well explaining the different flotation behaviors. Afterwards, cubic and octahedron samples achieved an increased zeta potential to -0.38 and -0.32 mV, close to zero, suggesting the possible physical static force between KCl and ODA which was in coincidence with previous conclusion^[45].

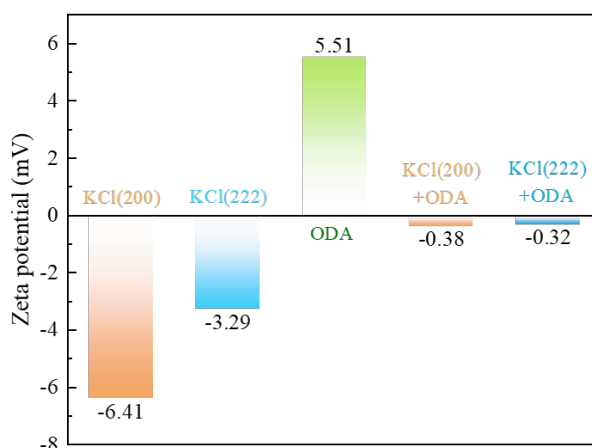


Fig. V. 6. Zeta potential results of KCl (200), KCl (222) crystals before and after reacting with ODA, and of ODA in saturate KCl solution.

As mentioned above, flotation happens by the selected adsorption by collectors on minerals surfaces to reach a hydrophobic condition in order to interact with bubbles. As a consequence, the surficial properties of minerals show a vital role in this reaction. AFM, as a powerful atomic level method to reveal the surficial morphology, was adopted to help understand the properties of KCl (200) and KCl (222) crystals whose slowly grown perfect samples pertained flat surfaces. Shown in Fig. V. 7a and 7b were the surficial morphology of cubic and octahedron from the microscope equipped with AFM where the former sample had a clean and flatten

surface but latter with several triangle islands. The KCl (200) sample with cubic structure was grown by mild evaporation which allowed a slow and steady growth to exhibit a nearly perfect cubic shape with flat surfaces, in coincidence with FCC crystal structure. However, the KCl (222) sample with octahedron shape was grown by a different way from cubic structure that on each (222) triangle face, the extra ions firstly formed a small triangle island and then bigger. Those islands finally successfully grow to connect with each other to form another layer, thus to realize a bigger octahedron crystal. More detailed surficial information was displayed in Fig. V. 7c, 7e by two-dimensional results and their corresponding three-dimensional results from AFM tests in Fig. V. 7d and 7f. It's worth noting that the AFM results were corresponding to their microscope results where a flat and clean spot was chosen to endow the engagement of the tip. It's clear that on the surface of KCl (200), there were many stages composing of layers with large amount of exposing "edges", indicating the growth of (200) faces were by layers and the possible plentiful hanging Cl⁻ on the edges that resulted in its lower zeta potential value. For KCl (222) sample, there was one triangle island in Fig. V. 7d and 7f, in consistent with the microscope result in Fig. 7b. The uneven distribution of smaller punctate hills on surface might be the undergrown triangle islands. One other fact that Cl ion possessed higher binding energy with Pb ion than that with K ion, further strengthened the ability of KCl (222) to confine Cl ions inside the structure rather than dissolve into bulk saline. Compared with layered surface with abundant exposing edges on KCl (200) surface, the island-formation growth method hindered the exposing of edges as well as hanging Cl⁻ and lead to the relatively more positive surficial charge than KCl (200), as demonstrated by previous zeta potential results. In addition, the surficial properties also played a vital role in minerals' hydrophilia which further influenced the interaction with bubbles during flotation process. Contact angle results of saturated KCl solution on KCl (200) and KCl (222) in Fig. V. 7g and 7h suggested that the former cubic sample had a less hydrophily which could be ascribed to its more exposing of Cl⁻ with lower hydration energy than K⁺. The less hydrophilic KCl (200) facilitated the adsorption of cubic KCl crystals with bubbles to obtain a better flotation recovery as described above. In consideration of the morphology and shape features of KCl (222) crystal, it's reasonable that one other disadvantage of its low floatability was that the unstable gravity center of octahedron structure hindered the attachment with bubbles during turbulent solution environment of flotation process.

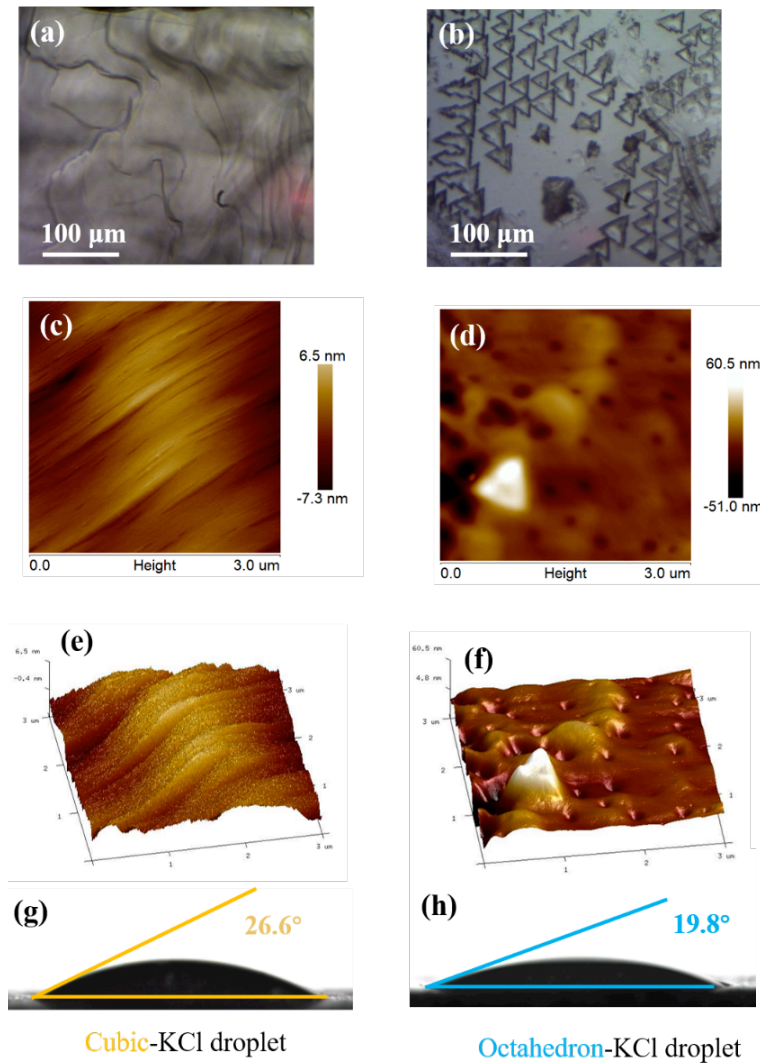


Fig. V. 7. (a, b) Micrographs, (c, d) two dimensional & (e, f) three-dimensional AFM and (g, h) contact angle results of KCl (200), KCl (222) crystals, respectively.

As one result from surficial properties, adhesion & adsorption forces between mineral particles and collectors are thought to be another important test to unveil the flotation mechanism. Known as one typical hydrophilic mineral, KCl processed a relatively bubble-repelling property. Here, the adhesion & adsorption forces between ODA-adsorbed KCl (222), KCl (200) samples with saturate KCl solution were studied to get a better understanding of the interaction behavior during flotation process, and the related results were displayed in Fig. V. 8 with a few typical records during the approaching & retracting process inserted in Fig. V. 8a. The real-time record of force revealed the adhesion force during the approach and retract procedure. It's clear that before contacting, the force was recorded to be a straight line without any change, until point A as shown in Fig. V. 8 (a₂), where a slight jump-into adhesion happened

with a force at $68.0 \mu\text{N}$. Afterwards, the liquid drop and sample KCl (200) platform moved together for a short time and then started the retract process. With the platform going down slowly, the adsorption occurred between the drop and sample, reaching a maximum adsorption force at $198.5 \mu\text{N}$ at point B. At last, the departure of drop from the sample occurred with the increase of distance at point C, the whole process ended with part of solution remaining on surface of sample which led to the remaining negative value instead of zero as shown in Fig. V. 8(a₄). Similarly, the adhesion and desorption force of sample KCl (222) in Fig. 8b were read as $100.4 \mu\text{N}$ and $280.5 \mu\text{N}$, respectively. The stronger interaction force between KCl (222) with KCl saturated solution implied its weaker interaction with bubbles due to the difference between liquid and gas properties. Hence, the adhesion & adsorption force between KCl (222) and bubbles would be lower than that between KCl (200) and bubbles, giving another explanation of the worse flotation recovery of KCl (222) crystals.

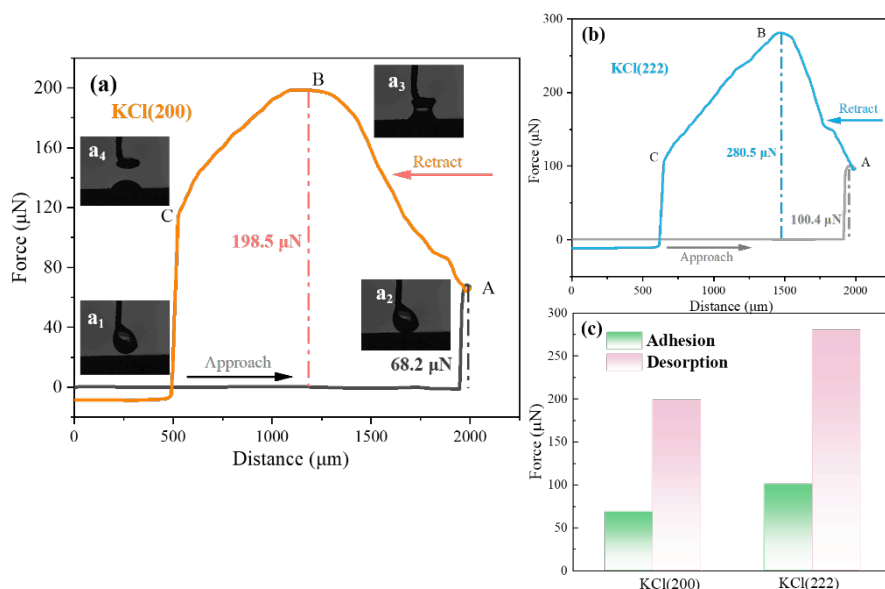


Fig. V. 8. Adhesion & adsorption force results of (a) KCl (200) and (b) KCl (222) crystals with saturated KCl drop, inserted in (a) were the photograph of (a₁) approaching, (a₂) contacting, (a₃) adhesion and (a₄) adsorption process, and (c) corresponding force information.

5.2.5. Illustration for flotation process

All the results above suggested that the KCl (200) samples pertained a better flotation recovery compared with KCl (222) samples, the related mechanism has been well studied and the main concepts were illustrated in Fig. V. 9. It is shown that KCl (200) sample with cubic structure has 6 square (200) surfaces where the K and Cl ions in solution get to be attracted to stages of multilayers with abundant of edges and

hanging unsaturated bonds. Nevertheless, KCl (222) crystal with octahedron structure contains 8 triangle (222) surfaces where new K and Cl ions form small triangle islands to help grow bigger octahedron structure. Its islands formation instead of layers piling up growing way indicated the integrality of KCl units with limited defects. The less hydrophily of Cl ions than K ions endows its higher possibility to stay in crystal structure while hydrated K ions preferring to resolve in solution (saturated KCl solution, in this case). The more hanging Cl ions on surfaces of KCl (200) than KCl (222) crystals well explained its weaker hydrophily as well as lower surface charge that further facilitate its floatability by using ODA.

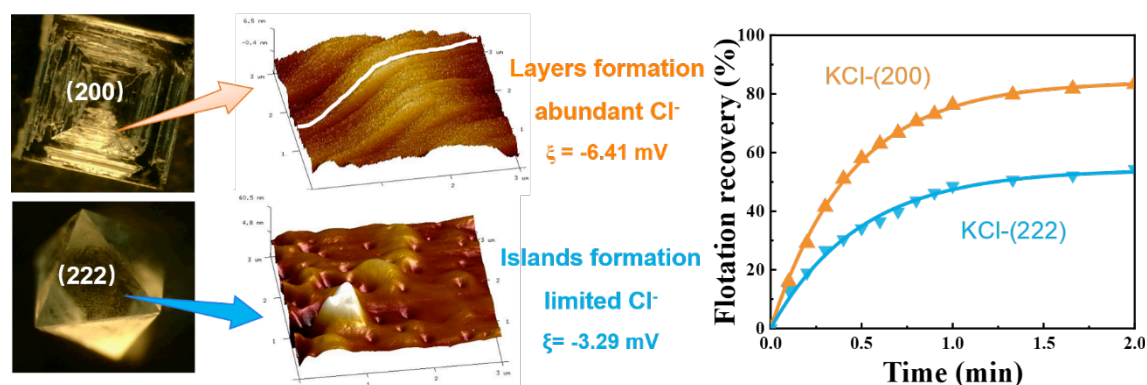


Fig. V. 9. Illustration of flotation behavior of KCl crystals with various exposing faces.

5.3. Conclusions

The KCl crystal with (200) and (222) exposing faces displayed various flotation recovery as 83.35% and 53.42%, respectively. The improved flotation ability of KCl (200) could be ascribed to the below mechanisms:

(1) By combining XRD and SEM results, it was concluded that KCl (200) samples was in cubic structure while KCl (222) samples with octahedron shape. FTIR result demonstrated the successfully adsorption of ODA on both KCl (200) and KCl (222) crystals after flotation, where XPS spectra helped to exclude the chemical interaction in between;

(2) Zeta potential tests demonstrated that KCl (200) crystals pertained a more negative zeta potential as -6.41 mV than that of KCl (222) as -3.29 mV, facilitating the stronger adsorption with cationic collector ODA with 5.51 mV surficial potential;

(3) The surfaces details obtained by AFM tests indicated that the growing method of KCl (200) crystals is by layers piling up to form stages with abundant edges and hanging Cl bonds, while KCl (222) was by formation of independent triangle islands with limited edges. The former sample with large amount of less

hydrated Cl bonds led to its lower zeta potential and less hydrophilic stage to show a better interaction with bubbles to reach a better flotation recovery.

(4) After adsorption of ODA, KCl (200) samples showed a weaker adhesion & adsorption force with KCl saturated solution than KCl (222), indicating its stronger interaction force with bubbles as well as easier floatability.

References

- [1] S. Titkov, Flotation of water-soluble mineral resources, *Int J Miner Process* 74 (2004) 107–113. <https://doi.org/10.1016/J.MINPRO.2003.09.008>.
- [2] S. Ge, S.Y. Foong, N.L. Ma, R.K. Liew, W.A. Wan Mahari, C. Xia, P.N.Y. Yek, W. Peng, W.L. Nam, X.Y. Lim, C.M. Liew, C.C. Chong, C. Sonne, S.S. Lam, Vacuum pyrolysis incorporating microwave heating and base mixture modification: An integrated approach to transform biowaste into eco-friendly bioenergy products, *Renewable and Sustainable Energy Reviews* 127 (2020) 109871. <https://doi.org/10.1016/J.RSER.2020.109871>.
- [3] L.A. Pardo, W. Stühmer, The roles of K⁺ channels in cancer, *Nature Reviews Cancer* 2013 14:1 14 (2013) 39–48. <https://doi.org/10.1038/nrc3635>.
- [4] H. Gao, L. Xue, S. Xin, J.B. Goodenough, A High-Energy-Density Potassium Battery with a Polymer-Gel Electrolyte and a Polyaniline Cathode, *Angewandte Chemie International Edition* 57 (2018) 5449–5453. <https://doi.org/10.1002/ANIE.201802248>.
- [5] K. Xu, J. Li, X. Lv, J. Wu, X. Zhang, D. Xiao, J. Zhu, Superior Piezoelectric Properties in Potassium–Sodium Niobate Lead-Free Ceramics, *Advanced Materials* 28 (2016) 8519–8523. <https://doi.org/10.1002/ADMA.201601859>.
- [6] Q. Cao, X. Wang, J.D. Miller, F. Cheng, Y. Jiao, Bubble attachment time and FTIR analysis of water structure in the flotation of sylvite, bischofite and carnallite, *Miner Eng* 24 (2011) 108–114. <https://doi.org/10.1016/J.MINENG.2010.10.006>.
- [7] H. Du, O. Ozdemir, X. Wang, F. Cheng, M.S. Celik, J.D. Miller, Flotation chemistry of soluble salt minerals: From ion hydration to colloid adsorption, *Minerals and Metallurgical Processing* 31 (2014) 1–20. <https://doi.org/10.1007/BF03402344/METRICAL>.
- [8] C. Zörb, M. Senbayram, E. Peiter, Potassium in agriculture – Status and perspectives, *J Plant Physiol* 171 (2014) 656–669. <https://doi.org/10.1016/j.jplph.2013.08.008>.
- [9] S.K. Jena, B. Mohanty, G. Padhy, J. Sahu, S.K. Kandi, Potassium recovery from muscovite using NaCl-roasting followed by H₂SO₄-leaching, *J Cent South Univ* 29 (2022) 1881–1894. <https://doi.org/10.1007/S11771-022-5052-3/METRICAL>.
- [10] E. Li, H. Liang, Z. Du, D. Li, F. Cheng, Adsorption process of Octadecylamine Hydrochloride on KCl crystal surface in various salt saturated solutions: Kinetics, isotherm model

- and thermodynamics properties, *J Mol Liq* 221 (2016) 949–953. <https://doi.org/10.1016/J.MOLLIQ.2016.06.050>.
- [11] X. Wu, Y. Chen, Z. Xing, C.W.K. Lam, S. Pang, W. Zhang, Z. Ju, Advanced Carbon-Based Anodes for Potassium-Ion Batteries, *Adv Energy Mater* 9 (2019). <https://doi.org/10.1002/aenm.201900343>.
- [12] Z. Huang, C. Cheng, H. Zhong, L. Li, Z. Guo, X. Yu, G. He, H. Han, L. Deng, W. Fu, Flotation of sylvite from potash ore by using the Gemini surfactant as a novel flotation collector, *Miner Eng* 132 (2019) 22–26. <https://doi.org/10.1016/J.MINENG.2018.11.055>.
- [13] Z. Huang, C. Cheng, Z. Liu, B. Feng, Y. Hu, W. Luo, G. He, X. Yu, W. Fu, Highly efficient potassium fertilizer production by using a gemini surfactant, *Green Chemistry* 21 (2019) 1406–1411. <https://doi.org/10.1039/C8GC03487G>.
- [14] J.S. Laskowski, From amine molecules adsorption to amine precipitate transport by bubbles: A potash ore flotation mechanism, *Miner Eng* 45 (2013) 170–179. <https://doi.org/10.1016/j.mineng.2013.02.010>.
- [15] K. Sun, C. V. Nguyen, N.N. Nguyen, X. Ma, A. V. Nguyen, Crucial roles of ion-specific effects in the flotation of water-soluble KCl and NaCl crystals with fatty acid salts, *J Colloid Interface Sci* 636 (2023) 413–424. <https://doi.org/10.1016/J.JCIS.2023.01.038>.
- [16] M. Hancer, M.S. Celik, J.D. Miller, The Significance of Interfacial Water Structure in Soluble Salt Flotation Systems, *J Colloid Interface Sci* 235 (2001) 150–161. <https://doi.org/10.1006/JCIS.2000.7350>.
- [17] O. Ozdemir, H. Du, S.I. Karakashev, A. V. Nguyen, M.S. Celik, J.D. Miller, Understanding the role of ion interactions in soluble salt flotation with alkylammonium and alkylsulfate collectors, *Adv Colloid Interface Sci* 163 (2011) 1–22. <https://doi.org/10.1016/J.CIS.2011.01.003>.
- [18] K. Hanumantha Rao, K.S.E. Forssberg, Mechanism of fatty acid adsorption in salt-type mineral flotation, *Miner Eng* 4 (1991) 879–890. [https://doi.org/10.1016/0892-6875\(91\)90071-3](https://doi.org/10.1016/0892-6875(91)90071-3).
- [19] Z. Liu, X. Zhong, Y. Liu, H. Rao, H. Wei, W. Hu, X. Nie, M. Liu, Adsorption and Mechanism of Glycine on the Anatase with Exposed (001) and (101) Facets, *Minerals* 12 (2022) 798. <https://doi.org/10.3390/MIN12070798>.
- [20] X. Gong, J. Yao, B. Yang, W. Yin, J. Guo, N. Song, Y. Wang, H. Sun, Activation–inhibition mechanism of diammonium hydrogen phosphate in flotation separation of brucite and calcite, *J Environ Chem Eng* 11 (2023) 110184. <https://doi.org/10.1016/J.JECE.2023.110184>.
- [21] J. Yao, W. Yin, E. Gong, Depressing effect of fine hydrophilic particles on magnesite reverse flotation, *Int J Miner Process* 149 (2016) 84–93. <https://doi.org/10.1016/J.MINPRO.2016.02.013>.

- [22] Y. Yuan, W. Zhan, F. Jia, S. Song, Multi-edged molybdenite achieved by thermal modification for enhancing Pb(II) adsorption in aqueous solutions, *Chemosphere* 251 (2020) 126369. <https://doi.org/10.1016/j.chemosphere.2020.126369>.
- [23] W. Zhan, Y. Yuan, C. Liu, P. Chen, Y. Liang, Y. Wang, J.L. Arauz-Lara, F. Jia, Preparation and application of 0D, 2D and 3D molybdenite: a review, *Minerals and Mineral Materials* 1 (2022) 5. <https://doi.org/10.20517/mmm.2022.04>.
- [24] M. Hirano, K. Shinjo, R. Kaneko, Y. Murata, Anisotropy of frictional forces in muscovite mica, *Phys Rev Lett* 67 (1991) 2642. <https://doi.org/10.1103/PhysRevLett.67.2642>.
- [25] W. Zhan, S. Yang, S. Bao, L. Ren, C. Liu, A novel insight of interaction mechanism of carboxymethyl cellulose with talc surface: A combined molecular dynamic simulation and DFT investigation, *Appl Clay Sci* 247 (2024) 107201. <https://doi.org/10.1016/J.CLAY.2023.107201>.
- [26] G. Moos, C. Gahl, R. Fasel, M. Wolf, T. Hertel, Anisotropy of Quasiparticle Lifetimes and the Role of Disorder in Graphite from Ultrafast Time-Resolved Photoemission Spectroscopy, *Phys Rev Lett* 87 (2001) 267402. <https://doi.org/10.1103/PhysRevLett.87.267402>.
- [27] Y. Chen, X. Chen, Y. Peng, The effect of sodium hydrosulfide on molybdenite flotation as a depressant of copper sulfides, *Miner Eng* 148 (2020) 106203. <https://doi.org/10.1016/J.MINENG.2020.106203>.
- [28] J. Yao, B. Yang, K. Chen, H. Sun, Z. Zhu, W. Yin, N. Song, Q. Sheng, Sodium tripolyphosphate as a selective depressant for separating magnesite from dolomite and its depression mechanism, *Powder Technol* 382 (2021) 244–253. <https://doi.org/10.1016/J.POWTEC.2020.12.040>.
- [29] G. Zhan, Z.C. Guo, Water leaching kinetics and recovery of potassium salt from sintering dust, *Transactions of Nonferrous Metals Society of China* 23 (2013) 3770–3779. [https://doi.org/10.1016/S1003-6326\(13\)62928-3](https://doi.org/10.1016/S1003-6326(13)62928-3).
- [30] E. Li, Z. Du, S. Yuan, F. Cheng, Low temperature molecular dynamic simulation of water structure at sylvite crystal surface in saturated solution, *Miner Eng* 83 (2015) 53–58. <https://doi.org/10.1016/J.MINENG.2015.08.012>.
- [31] T. d’Almeida, Y.M. Gupta, Real-Time X-Ray Diffraction Measurements of the Phase Transition in KCl Shocked along [100], *Phys Rev Lett* 85 (2000) 330. <https://doi.org/10.1103/PhysRevLett.85.330>.
- [32] A. Hossain, S. Roy, B.K. Dolui, Effects of thermodynamics on the solvation of amino acids in the pure and binary mixtures of solutions: A review, *J Mol Liq* 232 (2017) 332–350. <https://doi.org/10.1016/J.MOLLIQ.2017.02.080>.

- [33] Y. Yuan, W. Zhan, Y. Tian, A. López Valdivieso, H. Yi, S. Song, L.A. Cisternas, F. Jia, Novel strategy for improved sylvite flotation through controlled crystallization, *Miner Eng* 211 (2024) 108695. <https://doi.org/10.1016/J.MINENG.2024.108695>.
- [34] L. Wang, Y. Xu, H. Chen, X. Song, New insights into octadecylamine-monoacid selective adsorption on KCl/NaCl surface: Experimental and molecular dynamic simulation, *Appl Surf Sci* 554 (2021) 149613. <https://doi.org/10.1016/J.APSUSC.2021.149613>.
- [35] E. Li, Y. Zhang, Z. Du, D. Li, F. Cheng, Bubbles facilitate ODA adsorption and improve flotation recovery at low temperature during KCl flotation, *Chemical Engineering Research and Design* 117 (2017) 557–563. <https://doi.org/10.1016/J.CHERD.2016.11.016>.
- [36] L. Pastero, R. Cossio, D. Aquilano, {100} → {111} morphological change in KCl crystals grown from Pb²⁺-doped aqueous solutions, *CrystEngComm* 17 (2015) 7844–7855. <https://doi.org/10.1039/C5CE01425E>.
- [37] D.N. Krishnakumar, N.P. Rajesh, Growth and Optical Characterization of Europium and Cerium Doped KCl Single Crystals by Czochralski Method for Dosimetric Applications, *J Electron Mater* 48 (2019) 1629–1633. <https://doi.org/10.1007/S11664-018-06863-3/METRICS>.
- [38] H. Qiu, Y. Zhang, W. Huang, J. Peng, J. Chen, L. Gao, M. Omran, N. Li, G. Chen, Sintering Properties of Tetragonal Zirconia Nanopowder Preparation of the NaCl + KCl Binary System by the Sol-Gel-Flux Method, *ACS Sustain Chem Eng* 11 (2023) 1067–1077. <https://doi.org/10.1021/ACSSUSCHEMENG.2C05908>.
- [39] Y. Zhong, J. Chen, M. Su, J. Han, Q. Wu, Solid–liquid equilibrium, crystal type, solid solubility and thermal stability studies of potassium ammonium chloride solid solution, *Fluid Phase Equilib* 439 (2017) 24–30. <https://doi.org/10.1016/j.fluid.2017.02.015>.
- [40] M. Shiehpour, S. Solgi, M.J. Tafreshi, M.S. Ghamsari, ZnO-doped KCl single crystal with enhanced UV emission lines, *Applied Physics A* 125 (2019) 531. <https://doi.org/10.1007/s00339-019-2846-8>.
- [41] H. Wen, L. Liang, N. Xu, C. Liu, Multi-functional self-cleaning superhydrophobic cotton fabric as photothermal-reinforced crude oil separator, oil skimmer and underwater oil absorbent, *Sep Purif Technol* (2024) 126258. <https://doi.org/10.1016/j.seppur.2023.126258>.
- [42] K.-Y. Hwa, A. Ganguly, Effective monitoring of environmental hazardous drug moxifloxacin hydrochloride using silver selenide on octadecyl amine modified reduced graphene oxide composite, *J Environ Chem Eng* 12 (2024) 111694. <https://doi.org/10.1016/J.JECE.2023.111694>.
- [43] T. V. Vu, A.A. Lavrentyev, B.V. Gabrelian, D.D. Vo, K.D. Pham, N.M. Denysyuk, L.I. Isaenko, A.Y. Tarasova, O.Y. Khyzhun, DFT study and XPS measurements elucidating the electronic and optical properties of KPb₂Cl₅, *Opt Mater (Amst)* 102 (2020) 109793. <https://doi.org/10.1016/j.optmat.2020.109793>.

[44] J.D. Miller, S. Veeramasuneni, M.R. Yalamanchili, Recent contributions to the analysis of soluble salt flotation systems, *Int J Miner Process* 51 (1997) 111–123. [https://doi.org/10.1016/S0301-7516\(97\)00037-9](https://doi.org/10.1016/S0301-7516(97)00037-9).

[45] E. Li, H. Liang, Z. Du, D. Li, F. Cheng, Adsorption process of Octadecylamine Hydrochloride on KCl crystal surface in various salt saturated solutions: Kinetics, isotherm model and thermodynamics properties, *J Mol Liq* 221 (2016) 949–953. <https://doi.org/10.1016/J.MOLLIQ.2016.06.050>.

Chapter VI. Novel strategy for improved sylvite flotation through controlled crystallization

6.1. Introduction

Since As one of the most valued treasures from our planet, minerals^[1] always contain high value of resources such as steel^[2], iron^[3], copper^[4], *et al*^[5]. Apart from those insoluble materials, there are also other soluble or semi-soluble minerals including phosphogypsum^[6-8], calcium carbonate^[9], fluorite^[10] and another important type - inorganic salts like sylvite^[11]. The froth flotation^[12-14] has been widely used as a powerful method to recover most kinds of minerals. Tons of efforts have been devoted to improve the flotation recovery by various methods including exploring new types of collectors^[12,15,16], using different grinding medium^[17-19] adjusting mineral surficial properties^[20-22]. However, most of those methods focus on the trailing-end modulation instead of improving the mineral properties hindering the flotation process such as exposing faces, shapes and many other varieties that may bring out the better recovery of minerals themselves. To solve the flotation problem, it's vital to study the intrinsic properties of minerals so as to yield a direct control for ideal floatability.

One important feature of minerals is that most of them pertained to crystals with regularly arrangement of repeating units^[23-25]. In nature, they grow under certain conditions so as to exhibit predictable shapes according to their belonging crystal types^[26-28]. For instance, quartz was found with columnar shapes in clusters since its composing component SiO₂ belonged to tripartite or hexaxite crystal system while diamond was more found to be isolated ones with composing C element arranged by isoaxial crystal system rules^[29-31]. Among the broad types of natural minerals which require long period to form, soluble and semi-soluble minerals had the advantage to re-grow when contacting with liquid^[32-34], enlightening the idea of controllable design during crystallization process.

Sylvite^[35-37], as the main resource of potassium element, has been stressing researchers' attention as fertilizer, medicine and aerospace materials. Meanwhile, sylvite is also a kind of mineral constituent by KCl crystal with cubic crystal system and high solubility in water^[38,39]. Moreover, its solubility highly relies on solution temperature which promises the possibility to improve the flotation recovery by designing the crystallization process in solution^[40]. As mentioned above, the soluble

and semi-soluble minerals share the advantage to be re-constructed according to the later requirements^[41-43] like lower dosage of collector and foaming reagent, stronger interaction force with bubbles, greater difference with tailings, *et, al*, in order to yield a better flotation recovery.

Here, taking sylvite as an example, crystal growth of its composing crystal KCl was well designed to produce samples with different shapes and their related flotation behaviors were also described. By modulating the crystallization of KCl through solution temperature combined with evaporation and system turbulence, various shapes including cubic-, hopper- and needle-like KCl crystals were obtained without additional reagents. Afterwards, their different crystallization behavior was revealed by AFM. Flotation tests and related mechanisms were further researched in detail. This work paved a path to promote the flotation by modulating the crystallization process for soluble and semi-soluble minerals.

6.2. Results and discussion

6.2.1. Crystal structure and morphology

6.2.1.1. Crystal structure

According to the various strategies, three types of KCl crystals were collected and their corresponding structure was studied by XRD while their morphology information was researched by stereoscope as well as SEM. As FCC crystals, the crystallinity of KCl is a key parameter of its properties. Shown in Fig. VI. 1. were the XRD spectra of cubic-, hopper-like and needle-like structured KCl crystals. Their shared narrow and sharp peaks at around 28.43, 40.60, 50.27, 58.72, 66.45 and 73.76 degrees, in coincidence with the JCPD data of KCl^[44,45], indicating their high purity and well crystallinity. By comparing the peaks among three samples, all possessed the strong intensity of (200) facet. The highest (200) peak of hopper-like sample and lowest of needle-like sample could be ascribed to their special structure which should be further demonstrated by the morphological result.

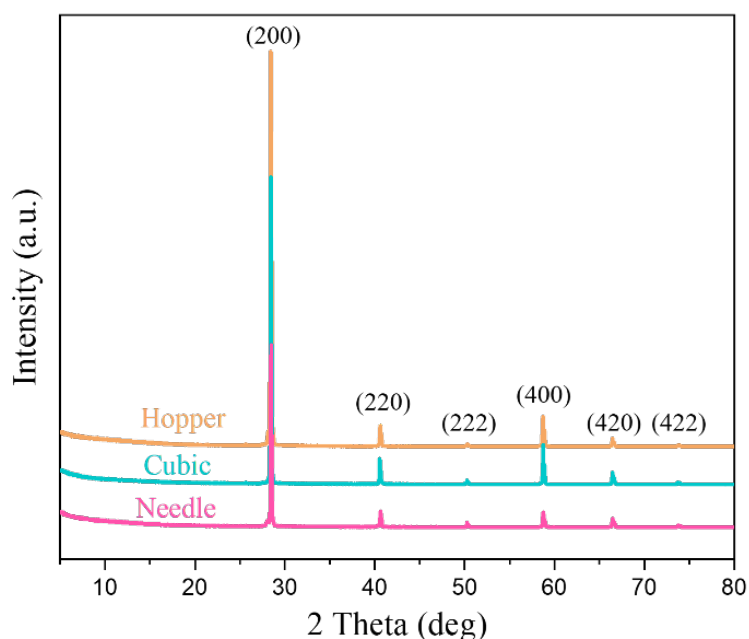


Fig. VI. 1. XRD patterns of cubic-, hopper- and needle-like KCl crystals.

6.2.1.2. Morphology

During flotation, the shape of minerals particles always stresses great attention of all researchers. Here, the morphology of three types of KCl samples were obtained by both stereoscope on the left and SEM on the right as shown in Fig. VI. 2. Intuitively, three samples exhibited various shapes with cubic-, hopper- and needle-like structure, respectively. It's worth noting that these crystals with different size distribution were due to the easily formation of KCl structure. Standard sieves were conducted to eliminate the size parameter before flotation tests. For first sample in Fig. VI. 2c and 2d, with constant cooling method, the higher concentration of K and Cl ions on corners lead to their preferential growth, resulting in the hopper-like structure. It's worth mentioning that hopper-like samples had a wild size distribution that one large particle was chosen in SEM test to display a detailed observation. Moreover, the needle-like structure in Fig. VI. 2e and 2f was thought to be originated by the fast crystallization along the one-dimensional direction.

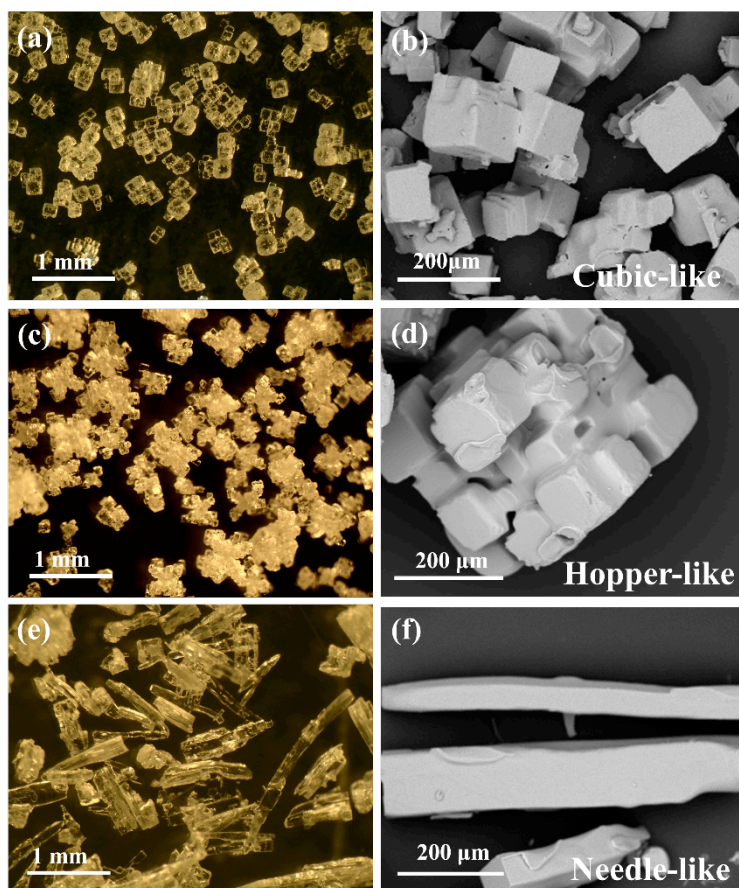


Fig. VI. 2. Stereoscopic (left) and SEM (right) images of (a, b) cubic-, (c, d) hopper- and (e, f) needle-like KCl crystals.

6.2.2. Crystal growth mechanism

The successful preparation of cubic-, hopper- and needle-like crystals were precisely designed by crystallization property of KCl. However, the detailed growth behavior remains unclear which might help to understand the inner mechanism so as to pave a path to later improvement of applications. Considering that KCl belongs to FCC type crystal whose surface is supposed to be flat square, AFM could be applied to image the topography of cubic KCl structure. What's more, the needle-like crystal formation was ascribed to the fast crystallization which could be similar with the fast spin-evaporation process during preparation of AFM samples. Thus, AFM was applied to study the surface detail in microscopic level for three types of KCl crystals: mild evaporation growth for large scale cubic-like KCl, fast spin evaporated growth of 10 μL saturated solution on mica for needle-like KCl, and still evaporation of 10 μL saturated solution on mica for hopper-like KCl.

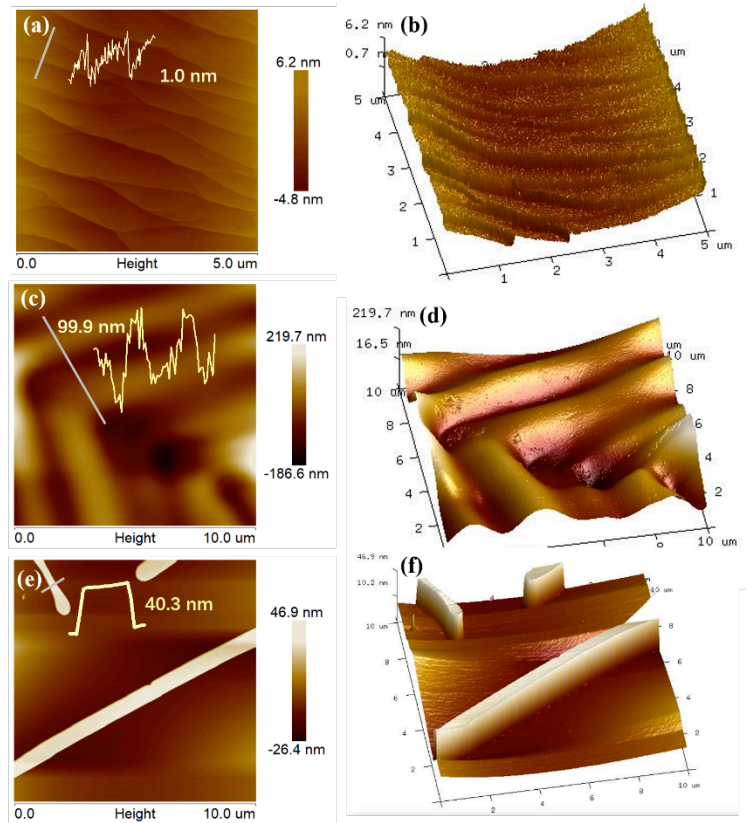


Fig. VI. 3. Two-dimensional (left) and three-dimensional (right) AFM images of (a, b) cubic-, (c, d) hopper- and (e, f) needle-like KCl crystals.

Shown in Fig. VI. 3 are their two-dimensional AFM result with the height information of lined area inserted, and corresponding three-dimensional result. Especially, due to the relatively large scale of cubic- and hopper- KCl crystal, the morphologies of chosen crystal for surficial test was obtained by optical microscope of AFM setup as displayed in Fig. VI. 4. The cubic crystal in Fig. VI. 4a showed a flat square surface, providing the excellent chance for scanning its surface in nanometer scale as shown in Fig. VI. 3a and 3b where the crystal grew by layers with height of ~ 1.0 nm which could be height of single layer of K-Cl. The seemed flat surface of cubic structure was actually full of stages as in the 3D result with abundant exposing edges.

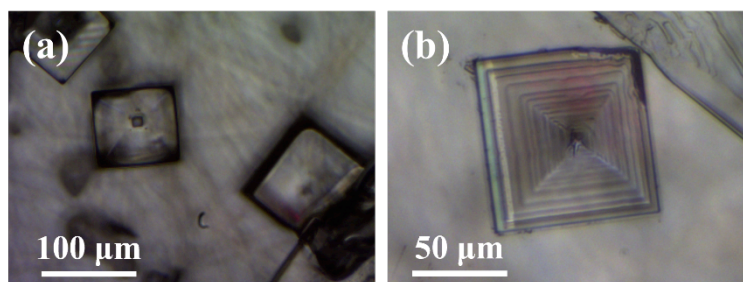


Fig. VI. 4. Stereoscopic images of cubic- and hopper-like KCl crystals.

Actually, the layered structure would be magnified by the fast still crystallization in form of arena-like structure like in Fig. VI. 4b. Instead of the smooth formation of cubic structure during mild evaporation, the layers parallel to four edges of the upper square appeared with fast growth. The corresponding AFM result in Fig. VI. 3c and 3d exhibited the stages-formation with height around 99.9 nm, much larger than that of cubic stage. With further growth of the arena-like structure in uniform solution environment with stirring and cooling, the stages would be amplified thus reach well-grown branches on eight corners, showing a hopper-like structure.

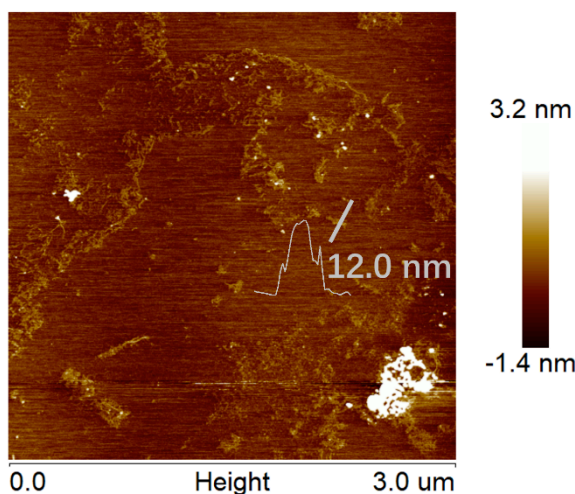


Fig. VI. 5. AFM image of KCl seeds with low concentration.

In the case of needle-like structure, the relatively small size of structure hindered the observation by microscope but its 2D and 3D AFM results in Fig. VI. 3e and 3f still helped to understand its growth details. Obviously, with the fast spin-evaporation method, the saturated KCl crystallized rapidly in form of thin and long structure, similar to needles samples during the cooling-evaporation combined strategy. The height of needle structure was about 40.3 nm which was ~ 40 folds of one single layer's height, indicating its property as KCl crystal. Although the fact that needle-like KCl possesses tiny size for microscope, it was feasible to observe its initial formation as crystal seeds during spin-evaporation process under low concentration of KCl. Here, KCl pure solution with concentration as 50 mg/L was prepared to study how the KCl would grow on surface of mica. The AFM result in Fig. VI. 5. demonstrated that at the beginning stage of crystallization, K and Cl ions would gather together for later growth. Interestingly, with spin-evaporation during sample preparation, these ions tended to form tiny thin chains with height around 12.0 nm, in

coincidence with the needle-like structure with saturated KCl solution. The mechanism of needle-like KCl crystal was concluded that with rapid crystallization, K and Cl ions firstly immigrated to form chains and then resulted in needle-like crystals.

6.2.3. Flotation test

With the unveiled mechanism of cubic-, hopper- and needle-like KCl crystal formation, their flotation behaviors were researched using ODA as collector, as shown in Fig. VI. 6. The floatability was in decreasing order of needle-like > hopper-like > cubic-like, where all fit well with classical first-order model as displayed in Table VI. 1. The highest flotation rate and recovery of needle-like KCl indicated its better interaction with ODA. Apart from needle-like structure, hopper-like structure pertained similar flotation recovery with cubic-like KCl but greater floating rate as 3.15 min^{-1} than 2.49 min^{-1} . It's reasonable to speculate that due to the special structure, hopper-like crystal with proper size could be quickly absorbed to bubbles with the four "feet" on top of branches, resulting in fast flotation rate at beginning. However, the final recovery was similar with cubic-structure indicated its limited improvement, which could be ascribed to its requirement of proper size of bubbles to be captured. For needle-like structure, its excellent flotation rate and recovery demonstrated the successful strategy of enhanced floatability of soluble crystal by manipulating its crystallization. The related mechanisms were studied as following parts.

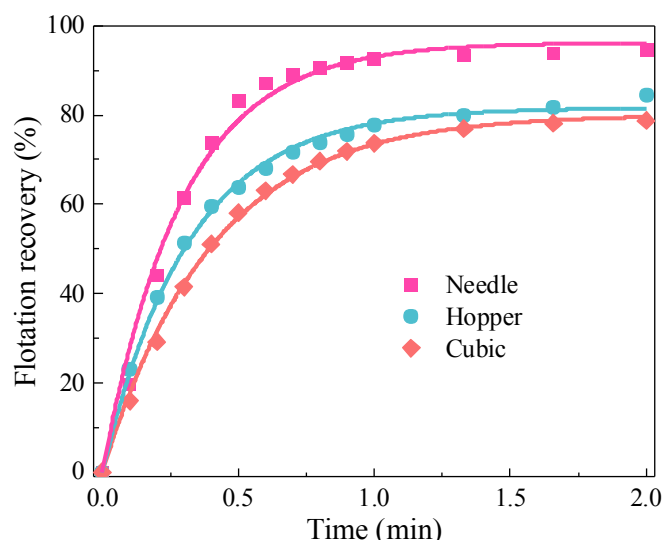


Fig. VI. 6. Flotation kinetics results of cubic-, hopper- and needle-like KCl crystals using ODA as collector.

Table VI. 1. Kinetic parameters for flotation kinetics of classical first-order model.

Classical first-order model			
Samples	ε_{∞} (%)	k_1 (min ⁻¹)	R^2
Cubic-like	80.08	2.49	0.998
Hopper-like	81.59	3.15	0.997
Needle-like	96.19	3.41	0.989

6.2.4. Flotation Mechanism

The good floatability of prepared cubic-, hopper- and needle-like KCl crystals suggested the possible interaction among particles, bubbles and collector ODA. To unveil flotation mechanism as well as the different behaviors of various samples, FTIR, XPS, BET, induction time and adsorption & desorption force tests were conducted as displayed as following content.

6.2.4.1. FTIR test

The adsorption of collector ODA on KCl crystals was first studied by FTIR. Shown in Fig. VI. 7. were the spectra of cubic-, hopper- and needle-like KCl crystals before (grey) and after (colored) interacted with ODA during flotation process. By comparing the grey and colored curves, it was clear the three samples all exhibited new peaks at around 2917.70 and 2850.5 cm⁻¹ that could be ascribed to the antisymmetric stretching vibration of methyl group (-CH₃) and the symmetric stretching strong absorption peak of methylene group (-CH₂) of ODA (Chun, 2009; Nawaz et al., 2012), demonstrating its successful adsorption on KCl crystals as collectors. The interaction type was then researched by XPS.

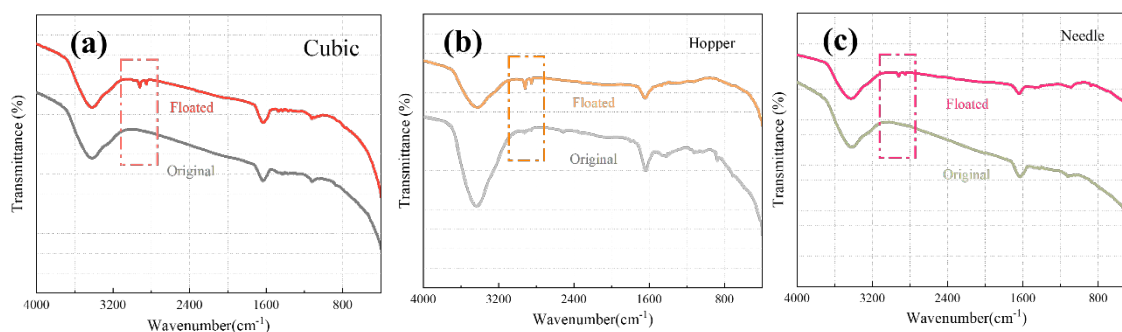


Fig. VI. 7. FTIR results of cubic-, hopper- and needle-like KCl crystals before and after flotation with ODA as collector, respectively.

6.2.4.2. XPS test

With the adsorption of ODA on KCl crystals, particles were successfully floated. The interaction between them was studied by XPS examine any new bonds where the binding energy information of K and Cl as shown in Fig. VI. 8 and 9. The related data was listed in Table VI 2 to facilitate comparison the binding energy of cubic-, hopper- and needle-like KCl before and after flotation. It's clear that three of samples showed similar binding energy of K and Cl peaks before flotation, indicating the high purity of KCl component. Besides, in each case of the cubic-, hopper- and needle-like KCl crystal, there was no changes before and after the flotation process, demonstrating that there was no new chemical production after interacting with ODA. Hence, the mechanism could be ascribed to the physical interaction like static force, as reported by previous research^[45].

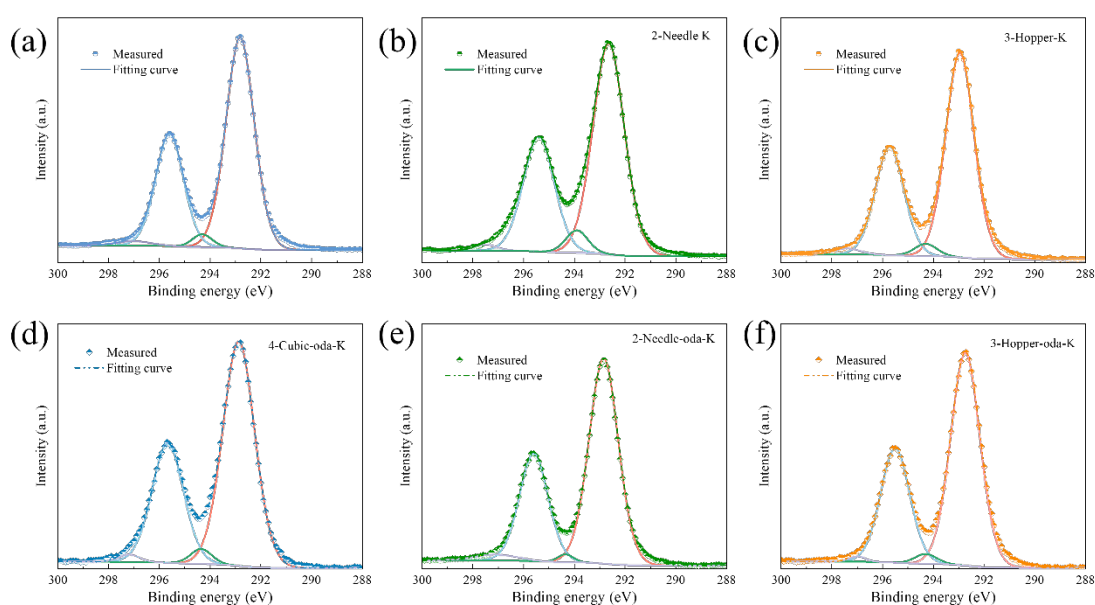


Fig. VI. 8. Potassium XPS survey of (a, d) cubic-, (b, e) needle- and (c, f) hopper-like KCl crystals before and after flotation.

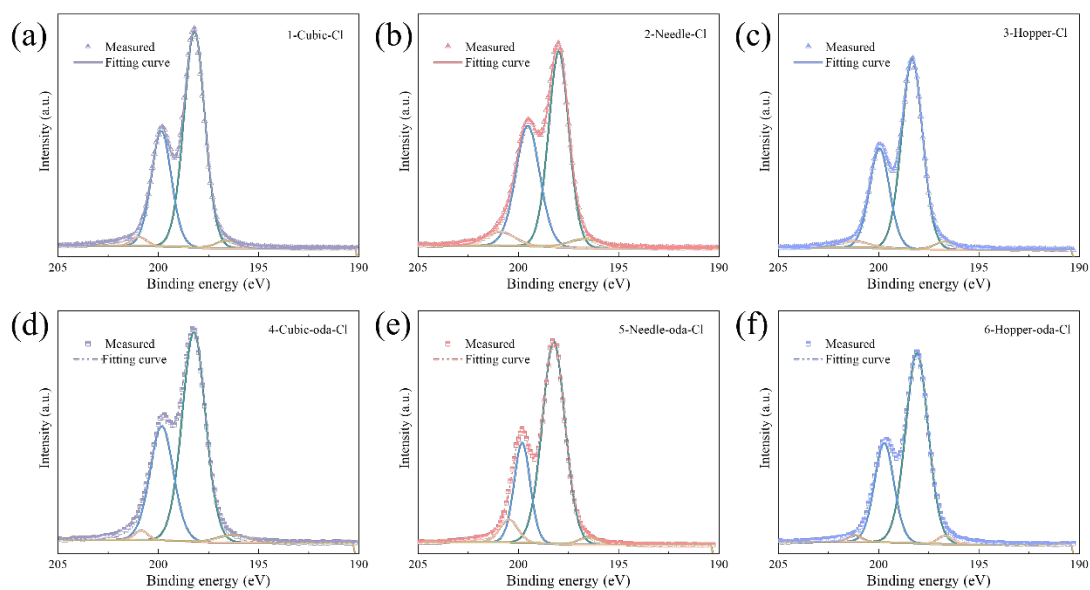


Fig. VI. 9. Chloride XPS survey of (a, d) cubic-, (b, e) needle- and (c, f) hopper-like KCl crystals before and after flotation.

Table VI. 1. Peaks of potassium and chloride XPS survey of cubic-, needle-, and hopper-like KCl crystals before and after flotation.

Cubic-KCl			Needle-KCl			Hopper-KCl		
Original	Floated	Shift	Original	Floated	Shift	Original	Floated	Shift
(eV)	(eV)	(eV)	(eV)	(eV)	(eV)	(eV)	(eV)	(eV)
292.80	292.87	-0.07	292.65	292.84	-0.19	292.95	292.74	0.21
295.58	295.67	-0.09	295.40	295.60	-0.20	295.72	295.50	0.22
K								
294.24	294.36	-0.12	293.90	294.35	-0.45	294.30	294.30	0.00
297.02	297.20	-0.18	297.50	297.10	0.40	297.40	297.00	0.40
198.20	198.23	-0.03	197.99	198.24	-0.25	198.33	198.09	0.24
199.85	199.83	0.02	199.53	199.81	-0.28	199.96	199.72	0.24
Cl								
200.96	200.85	0.11	200.92	200.48	0.44	201.30	201.20	0.10
196.60	196.33	0.27	196.70	196.50	0.20	196.70	196.70	0.00

6.2.4.3. BET test

The above XRD, FTIR and XPS results suggested that the prepared cubic-, hopper- and needle-like KCl samples possessed high purity, same exposing faces while stereoscope and SEM results exhibited their various shapes as well as surface area. Here, BET tests were applied to study the surface area of KCl crystals with three shapes. Fig. VI. 10. displayed the BET value of prepared crystals with size between

178-250 μm in N_2 atmosphere. The decreasing surface area values were in order of needle-like > hopper-like > cubic-like KCl crystal, in coincidence with their flotation recovery with ODA as collector. It's worth noting that different from normal collectors working as molecules, ODA in saturated salt solution with concentration higher than its CMC (4×10^{-5} mol/L) would function with flocs form. The size of those flocs relied on the concentration. In this case, the size of ODA flocs with concentration 5.56×10^{-5} mol/L in saturated KCl solution was tested by zeta potential apparatus. The tested size of flocs as ~ 3.2 μm , similar to previous research as 2.1 μm (Fangqin, 2012), much smaller than the interstices of hopper-like structure, implying that the higher surface area of KCl crystal, the more ODA flocs would be adsorbed. As a consequence, with same weight of crystals in flotation as 15 g, the needle-like structure with higher BET value could adsorb more ODA flocs so as to yield the best flotation recovery. One other important fact was that due to the fast grow of needle-like KCl, more cracks or defects could appear on surfaces of structure which resulted in its higher BET as well as higher flotation recovery.

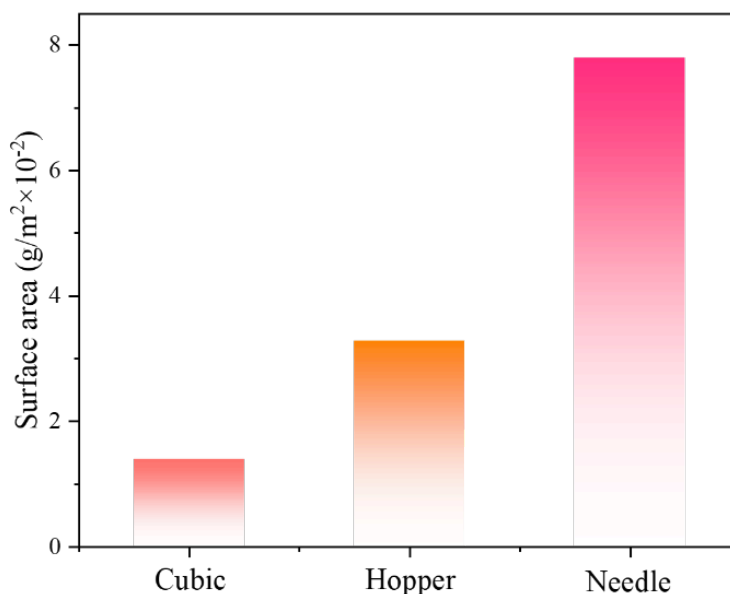


Fig. VI. 10. BET results of cubic-, hopper- and needle-like KCl crystals with size of 178-250 μm .

6.2.4.4. Induction time tests

Apart from the adsorption amount of ODA collector, induction time was one powerful test to predict the floatability of minerals. In this work, to study the flotation behavior of cubic-, hopper- and needle-like KCl crystals, conditions of induction time tests including ODA dosage and particle size range were with kept the same with

flotation process. Shown in Fig. VI. 11. were the induction time results of three samples where needle-like KCl sample had the shortest induction time as 30 ms. While Hopper-like structure showed a longer result as 100 ms, followed by the longest induction time of cubic-like KCl as 150 ms. The consequence in an increased induction time as needle-, hopper- and cubic-like structure was in consistent with their worse flotation recovery, indicating the better interaction between needle-like structure with bubble during flotation process. Besides, the inserted three pictures of KCl samples absorbing on bubble displayed their three-phase-contact (TPC) information that needle-like structure possessed long TPC on regard of its relatively lower gravity weight. In case of hopper- and cubic-like KCl, they had similar size but similar TPC result where the former had slightly less weight due to its special structure. Notably, the four parallel faces on one side of hopper structure could be anchored on bubbles with specific size to yield a more stable interaction than the one flat square face of cubic structure. As a consequence, needle-, hopper- and cubic-like structure KCl crystals showed a prolonged induction time thus behaved a declined floatability.

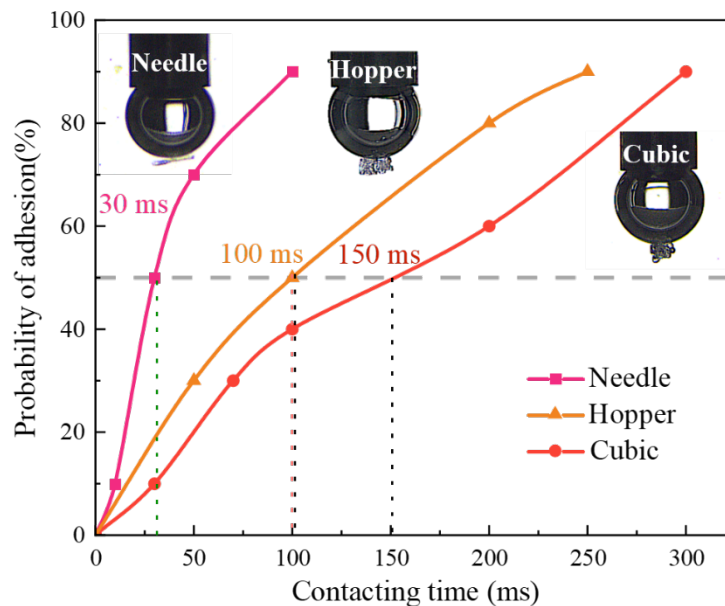


Fig. VI. 11. Induction time results of cubic-, hopper- and needle-like KCl crystals using ODA as collector.

6.2.4.5. Interaction

Although induction time reveals the reaction process between mineral and bubbles during flotation, the interaction details remain unclear. Here, the adhesion and

desorption forces between ODA adsorbed cubic-, hopper- and needle-like KCl crystals and saturated KCl solution were tested as displayed in Fig. VI. 12. Grey lines showed the approaching process of the KCl saturated drop to the mineral bed where three samples all appeared a slightly jump-into force, which was read as the adhesion force value as shown in Fig. VI. 12d. After approaching, sample bed and the drop contacted and moved together for a short time then started the retracting process with force recorded by colored lines. The desorption forces were read by the largest value where all results were exhibited in Fig. VI. 12d. Compared with cubic-like KCl, needle-like had the lower interaction force with saturated KCl solution which implied its stronger interaction with bubble, in coincidence with the different flotation of these two samples. Nevertheless, hopper-like structure had the highest adhesion & desorption with KCl saturated solution, which could be explained by its special structure that when approaching the drop, a certain part of solution emerged in the hollow part of hopper-structure and remained there, changing its original property so as to obtain a promoted interaction force. To some extent, this disadvantage of hopper-like structure hindered its floatability, resulting its near-equal recovery with cubic-like structure. As a result, the adhesion & desorption force tests well demonstrated the better flotation behavior of needle-like sample than cubic-like structure. Meanwhile, the special hopper-like structure had shorter induction time but a worst interaction with bubbles, exhibiting a similar flotation recovery with cubic-like samples.

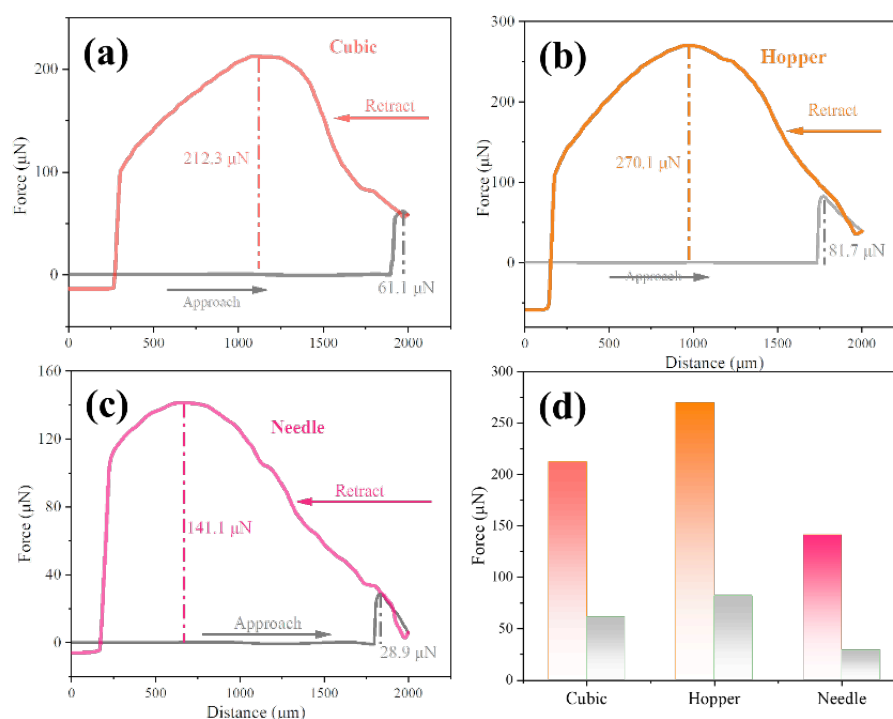


Fig. VI. 12. Adhesion & adsorption force results of (a) cubic- (b) hopper- and (c) needle-like KCl crystals with saturated KCl drop, and (d) corresponding force information.

6.3. Conclusions

In this work, a crystallization-controlled methodology was for the first time applied to enhance the flotation behavior of soluble mineral - KCl salt. Various strategies were precisely designed including fast crystallization with stirring, constant speed crystallization and fast still crystallization to grow KCl crystals with cubic-, hopper- and needle-like structure, respectively. Stereoscopy and SEM results showed their regular shape and XRD tested demonstrated their high crystallinity. The surficial information was obtained by AFM which also explained the growth mechanism. Then, the flotation tests by using ODA as collector indicated a declined recovery as needle-, hopper- and cubic-like sample, demonstrating the better performance of needle-like sample by modulating the crystallization. BET tests revealed the higher surface area of needle-like structure which could absorb more ODA flocs during flotation thus achieving a better recovery. Induction time as well as adhesion & desorption force tests further explained the faster and stronger interaction of needle-like sample with bubbles, resulting its best floatability. As a consequence, the enhanced flotation recovery of sylvite was achieved by modulation of its crystallization process, providing the methodology for other soluble minerals like hailite, picromerite and semi-soluble minerals like fluorite and phosphogypsum.

References

- [1] R.M. Potter, G.R. Rossman, Desert Varnish: The Importance of Clay Minerals, *Science* (1979) 196 (1977) 1446–1448. <https://doi.org/10.1126/SCIENCE.196.4297.1446>.
- [2] W.J.J. Huijgen, G.J. Witkamp, R.N.J. Comans, Mineral CO₂ sequestration by steel slag carbonation, *Environ Sci Technol* 39 (2005) 9676–9682. <https://doi.org/10.1021/ES050795F>.
- [3] L.A.J. Garvie, P.R. Buseck, Ratios of ferrous to ferric iron from nanometre-sized areas in minerals, *Nature* 1998 396:6712 396 (1998) 667–670. <https://doi.org/10.1038/25334>.
- [4] A.P. Chandra, A.R. Gerson, A review of the fundamental studies of the copper activation mechanisms for selective flotation of the sulfide minerals, sphalerite and

- pyrite, *Adv Colloid Interface Sci* 145 (2009) 97–110. <https://doi.org/10.1016/J.CIS.2008.09.001>.
- [5] W. Zhan, Y. Yuan, C. Liu, P. Chen, Y. Liang, Y. Wang, J.L. Arauz-Lara, F. Jia, Preparation and application of 0D, 2D and 3D molybdenite: a review, *Minerals and Mineral Materials* 1 (2022) 5. <https://doi.org/10.20517/mmm.2022.04>.
- [6] M. Aminul Haque, B. Chen, Y. Liu, S. Farasat Ali Shah, M.R. Ahmad, Improvement of physico-mechanical and microstructural properties of magnesium phosphate cement composites comprising with Phosphogypsum, *J Clean Prod* 261 (2020) 121268. <https://doi.org/10.1016/J.JCLEPRO.2020.121268>.
- [7] L.F.O. Silva, M.L.S. Oliveira, T.J. Crissien, M. Santosh, J. Bolivar, L. Shao, G.L. Dotto, J. Gasparotto, M. Schindler, A review on the environmental impact of phosphogypsum and potential health impacts through the release of nanoparticles, *Chemosphere* 286 (2022) 131513. <https://doi.org/10.1016/J.CHEMOSPHERE.2021.131513>.
- [8] J.W. Morse, R.S. Arvidson, A. Lüttge, Calcium carbonate formation and dissolution, *Chem Rev* 107 (2007) 342–381. <https://doi.org/10.1021/CR050358J>.
- [9] Z. Gao, C. Wang, W. Sun, Y. Gao, P.B. Kowalczyk, Froth flotation of fluorite: A review, *Adv Colloid Interface Sci* 290 (2021) 102382. <https://doi.org/10.1016/j.cis.2021.102382>.
- [10] Ö. Kilic, A.M. Kilic, Recovery of salt co-products during the salt production from brine, *Desalination* 186 (2005) 11–19. <https://doi.org/10.1016/J.DESAL.2005.05.014>.
- [11] M.S. Celik, M. Hancer, J.D. Miller, Flotation Chemistry of Boron Minerals, *J Colloid Interface Sci* 256 (2002) 121–131. <https://doi.org/10.1006/JCIS.2001.8138>.
- [12] S. Farrokhpay, The importance of rheology in mineral flotation: A review, *Miner Eng* 36–38 (2012) 272–278. <https://doi.org/10.1016/J.MINENG.2012.05.009>.
- [13] L. Xie, J. Wang, Q. Lu, W. Hu, D. Yang, C. Qiao, X. Peng, Q. Peng, T. Wang, W. Sun, Q. Liu, H. Zhang, H. Zeng, Surface interaction mechanisms in mineral flotation: Fundamentals, measurements, and perspectives, *Adv Colloid Interface Sci* 295 (2021) 102491. <https://doi.org/10.1016/J.CIS.2021.102491>.
- [14] E.N. Peleka, G.P. Gallios, K.A. Matis, A perspective on flotation: a review, *Journal of Chemical Technology & Biotechnology* 93 (2018) 615–623. <https://doi.org/10.1002/JCTB.5486>.
- [15] Z. Wu, X. Wang, H. Liu, H. Zhang, J.D. Miller, Some physicochemical aspects of water-soluble mineral flotation, *Adv Colloid Interface Sci* 235 (2016) 190–200. <https://doi.org/10.1016/J.CIS.2016.06.005>.

- [16] W. Zhang, W. Li, S. Li, Molten salt assisted self-activated carbon with controllable architecture for aqueous supercapacitor, *J Mater Sci Technol* 156 (2023) 107–117. <https://doi.org/10.1016/j.jmst.2022.12.079>.
- [17] Y. Peng, S. Grano, Effect of grinding media on the activation of pyrite flotation, *Miner Eng* 23 (2010) 600–605. <https://doi.org/10.1016/J.MINENG.2010.02.003>.
- [18] X. Zhang, Y. Qin, Y. Han, Y. Li, P. Gao, G. Li, S. Wang, A potential ceramic ball grinding medium for optimizing flotation separation of chalcopyrite and pyrite, *Powder Technol* 392 (2021) 167–178. <https://doi.org/10.1016/J.POWTEC.2021.07.006>.
- [19] J. Ju, Y. Feng, H. Li, Z. Xue, R. Ma, Y. Li, Research advances, challenges and perspectives for recovering valuable metals from deep-sea ferromanganese minerals: A comprehensive review, *Sep Purif Technol* 315 (2023) 123626. <https://doi.org/10.1016/J.SEPPUR.2023.123626>.
- [20] S. Lin, C. Wang, R. Liu, W. Sun, G. Jing, Surface characterization of molybdenite, bismuthinite, and pyrite to identify the influence of pH on the mineral floatability, *Appl Surf Sci* 577 (2022) 151756. <https://doi.org/10.1016/J.APSUSC.2021.151756>.
- [21] M. Tang, X. Tong, The relationship between anion distribution in process water and flotation properties of iron oxides, *Miner Eng* 154 (2020) 106378. <https://doi.org/10.1016/J.MINENG.2020.106378>.
- [22] J. Li, G. Nie, J. Li, Z. Zhu, Z. Wang, Colloids and Surfaces A : Physicochemical and Engineering Aspects Flotation separation of quartz and dolomite from collophane using sodium N-dodecyl- β -amino propionate and its adsorption mechanism, *Colloids Surf A Physicochem Eng Asp* 641 (2022) 128586. <https://doi.org/10.1016/j.colsurfa.2022.128586>.
- [23] L. Xu, J. Tian, H. Wu, S. Fang, Z. Lu, C. Ma, W. Sun, Y. Hu, Anisotropic surface chemistry properties and adsorption behavior of silicate mineral crystals, *Adv Colloid Interface Sci* 256 (2018) 340–351. <https://doi.org/10.1016/J.CIS.2018.02.004>.
- [24] W. Zhan, H. Yi, S. Song, Y. Zhao, F. Rao, Hydrophobic agglomeration behaviors of clay minerals as affected by siloxane structure, *Colloids and Surfaces A* 568 (2019) 36–42. <https://doi.org/10.1016/j.colsurfa.2019.01.061>.
- [25] D.B. Brooks, P.W. Andrews, Mineral Resources, Economic Growth, and World Population, *Science* (1979) 185 (1974) 13–19. <https://doi.org/10.1126/SCIENCE.185.4145.13>.

- [26] B. Chopard, H.J. Herrmann, T. Vicsek, Structure and growth mechanism of mineral dendrites, *Nature* 1991 353:6343 353 (1991) 409–412. <https://doi.org/10.1038/353409a0>.
- [27] H.L. Ehrlich, How microbes influence mineral growth and dissolution, *Chem Geol* 132 (1996) 5–9. [https://doi.org/10.1016/S0009-2541\(96\)00035-6](https://doi.org/10.1016/S0009-2541(96)00035-6).
- [28] P.D. Ihinger, S.I. Zink, Determination of relative growth rates of natural quartz crystals, *Nature* 2000 404:6780 404 (2000) 865–869. <https://doi.org/10.1038/35009091>.
- [29] F. Iwasaki, H. Iwasaki, Historical review of quartz crystal growth, *J Cryst Growth* 237–239 (2002) 820–827. [https://doi.org/10.1016/S0022-0248\(01\)02043-7](https://doi.org/10.1016/S0022-0248(01)02043-7).
- [30] Q. Zhang, D. Sánchez-Fuentes, A. Gómez, R. Desgarceaux, B. Charlot, J. Gàzquez, A. Carretero-Genevri, M. Gich, Tailoring the crystal growth of quartz on silicon for patterning epitaxial piezoelectric films, *Nanoscale Adv* 1 (2019) 3741–3752. <https://doi.org/10.1039/C9NA00388F>.
- [31] Y. Foucaud, J. Lainé, L.O. Filippov, O. Barrès, W.J. Kim, I. V. Filippova, M. Pastore, S. Lebègue, M. Badawi, Adsorption mechanisms of fatty acids on fluorite unraveled by infrared spectroscopy and first-principles calculations, *J Colloid Interface Sci* 583 (2021) 692–703. <https://doi.org/10.1016/J.JCIS.2020.09.062>.
- [32] D.H. Hoang, N. Kupka, U.A. Peuker, M. Rudolph, Flotation study of fine grained carbonaceous sedimentary apatite ore – Challenges in process mineralogy and impact of hydrodynamics, *Miner Eng* 121 (2018) 196–204. <https://doi.org/10.1016/J.MINENG.2018.03.021>.
- [33] L.O. Filippov, I. V. Filippova, O. Barres, T.P. Lyubimova, O.O. Fattalov, Intensification of the flotation separation of potash ore using ultrasound treatment, *Miner Eng* 171 (2021) 107092. <https://doi.org/10.1016/J.MINENG.2021.107092>.
- [34] M.B.M. Monte, J.F. Oliveira, Flotation of sylvite with dodecylamine and the effect of added long chain alcohols, *Miner Eng* 17 (2004) 425–430. <https://doi.org/10.1016/J.MINENG.2003.11.005>.
- [35] P. Thy, B.M. Jenkins, S. Grundvig, R. Shiraki, C.E. Lesher, High temperature elemental losses and mineralogical changes in common biomass ashes, *Fuel* 85 (2006) 783–795. <https://doi.org/10.1016/J.FUEL.2005.08.020>.
- [36] E. Osipova, V. Shevchuk, A. Stromski, V. Romanovski, Intensification of potash ore flotation by the introduction of industrial oils, *Journal of Chemical Technology & Biotechnology* 97 (2022) 312–318. <https://doi.org/10.1002/JCTB.6945>.

- [37]D. Weedon, S. Grano, T. Akroyd, K. Goncalves, R. Moura, Effects of high Mg²⁺ concentration on KCl flotation: Part I – Laboratory research, *Miner Eng* 20 (2007) 675–683. <https://doi.org/10.1016/J.MINENG.2007.01.006>.
- [38]E. Li, Z. Du, S. Yuan, F. Cheng, Low temperature molecular dynamic simulation of water structure at sylvite crystal surface in saturated solution, *Miner Eng* 83 (2015) 53–58. <https://doi.org/10.1016/J.MINENG.2015.08.012>.
- [39]M. Ejtemaei, M. Gharabaghi, M. Irannajad, A review of zinc oxide mineral beneficiation using flotation method, *Adv Colloid Interface Sci* 206 (2014) 68–78. <https://doi.org/10.1016/J.CIS.2013.02.003>.
- [40]Q. Feng, W. Yang, S. Wen, H. Wang, W. Zhao, G. Han, Flotation of copper oxide minerals: A review, *Int J Min Sci Technol* 32 (2022) 1351–1364. <https://doi.org/10.1016/J.IJMST.2022.09.011>.
- [41]C. Marion, R. Li, K.E. Waters, A review of reagents applied to rare-earth mineral flotation, *Adv Colloid Interface Sci* 279 (2020) 102142. <https://doi.org/10.1016/J.CIS.2020.102142>.
- [42]G. Ji, W. Wang, H. Chen, S. Yang, J. Sun, W. Fu, B. Yang, Z. Huang, Sustainable potassium chloride production from concentrated KCl brine via a membrane-promoted crystallization process, *Desalination* 521 (2022) 115389. <https://doi.org/10.1016/J.DESAL.2021.115389>.
- [43]X. Li, F. He, F. Behrendt, Z. Gao, J. Shi, C. Li, Inhibition of K₂SO₄ on evaporation of KCl in combustion of herbaceous biomass, *Fuel* 289 (2021) 119754. <https://doi.org/10.1016/J.FUEL.2020.119754>.
- [44]Q. Cao, H. Du, J.D. Miller, X. Wang, F. Cheng, Surface chemistry features in the flotation of KCl, *Miner Eng* 23 (2010) 365–373. <https://doi.org/10.1016/J.MINENG.2009.11.010>.
- [45]C. Fangqin, Study on Octadecylamine-HCl's Colloid Chemistry in KCl Flotation, *Journal of Shanxi University* (2012).

Chapter VII. Impact of Ethanol on flotation of sylvite flotation

7.1. Introduction

As the main resource of potassium element, sylvite has been one hot research subject due to the vital role that potassium played in crops growing, medicine and other fields[1–3]. Shortening of the cardiac action potential due to a brief injection of kcl following the onset of activity. The wildly practicable method to recover sylvite was by cold-decomposition followed by flotation method from carnallite[4], and thermal decomposition of carnallite[5]. Hitherto, tons of researches have been focused on the attempts to realize a batter flotation recovery[6]. However, most of them focused on the flotation behaviors with the idea of considering KCl as normal minerals as any other minerals but ignoring the fact that KCl is highly soluble in water, which may differ KCl from other non-soluble minerals.

One other problem that comes from high solubility of KCl in water is their easily caking phenomenon during filtering and storing process[7–9]. The difficulty to remove all liquid phase solution during filtering leads to the KCl particles covered by remnant saturated solution, which would entail caking effect and thus increase the particle size, generating extra impacts of gravity during later flotation process. One strategy that easily come up to mind was to use ethanol for washing out unnecessary solution. Besides, Yuan, et al. found that with the increase of the content of methanol and ethanol in solution, the solubility of picromerite in the mixed solvent was decreased, so the method of alcoholization could be applied to improve the crystallization rate of picromerite[10]. Previous studies had demonstrated the well distribution after ethanol applying during filtering process, however. the impact that came from ethanol for the crystal as well as later flotation was unclear yet.

Thanks to the strong polarity of ethanol, it could mix with water with any proportion, showing a relative low value of surface tension. Besides, KCl is highly soluble in water that could bring salting-out effect with ethanol in saturated KCl solution[11,12]. As a result, the ethanol might bring intricate effects on the flotation of KCl. In this work, this process was divided into two main aspects: one was the influence of ethanol on surficial properties of KCl crystals including structure and morphology. The other one was for the impact of ethanol on solution environment which could be vital for flotation process. It could be concluded that with addition of ethanol, KCl realized a better flotation behavior where the ethanol's salting out effect

introduced new (111) faces of KCl crystal with worse flotation behavior. As a consequence, with 0.2% addition of ethanol, KCl realized a best flotation recovery as 94.79%. This work demonstrated the successful strategy of ethanol addition to promote the KCl flotation by decreasing the solution surface tension.

7.2. Results and Discussion

7.2.1. Morphology and structure

Through the cooling method, the over-saturated KCl got to crystallize out in form of solid phase as cubic shape according to its intrinsic nature. Their morphologies were revealed by SEM as shown in Fig. VII. 1. It's seen that the samples exhibited shape of near cubic but with relatively rough surface. What's more, some crystals seemed to be attached to other ones which might be originated from the remaining saturated KCl solution during drying process. It's worth mentioning that they shared various sizes which would be excluded by sieving method before later flotation process.

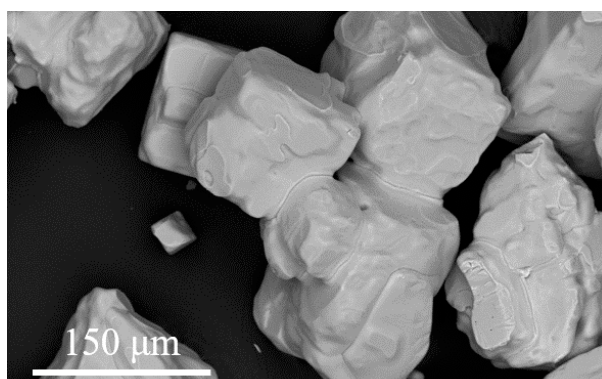


Fig. VII. 1. SEM result of cubic shaped KCl crystals through cooling method.

As a typical FCC type crystal, apart from morphological information, the structure of KCl sample was one other important feature. Here, the cubic-shaped KCl sample was tested by XRD to help understand its structure as displayed in Fig. VII. 2. By comparing the peaks with PDF#75-1674 card of pure KCl crystal[13,14], it was concluded that the prepared KCl cubic samples had high purity of FCC structured KCl.

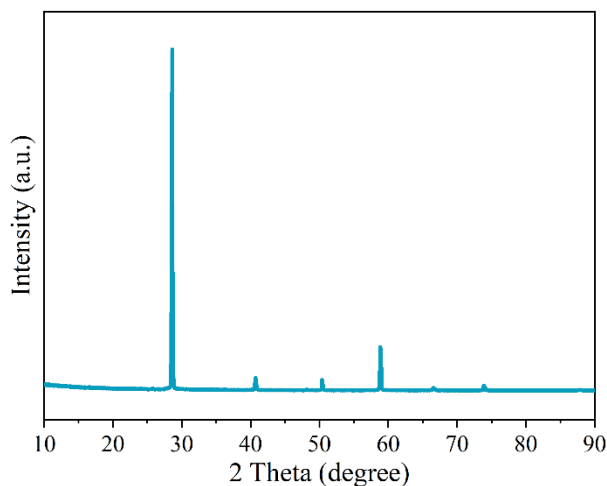


Fig. VII. 2. XRD result of cubic shaped KCl crystals through cooling method.

7.2.1.1. Morphologies of KCl modified by ethanol

To avoid the caking phenomenon of KCl samples as appeared in Fig. VII. 1, the common method was adding some ethanol to wash out the extra saturated KCl solution on surface of wet KCl samples. Shown in Fig. VII. 3 were the morphological results of KCl sample immersed in ethanol-KCl co saturated solution with various dosage of ethanol. In Fig. VII. 3a, it's seen that on the middle crystal, three small area showed a common oblique triangular plane, indicating their various exposing faces from the square faces of original cubic shaped KCl crystal. According to previous study, those triangle faces could be the (222) facet of one FCC structure KCl structure, indicating the changes of exposing faces by adding ethanol into the mother liquor. Similarly, it could be found also in other results of Fig. VII. 3b, 3c, 3d and 3e. Further changes could be demonstrated by XRD results.

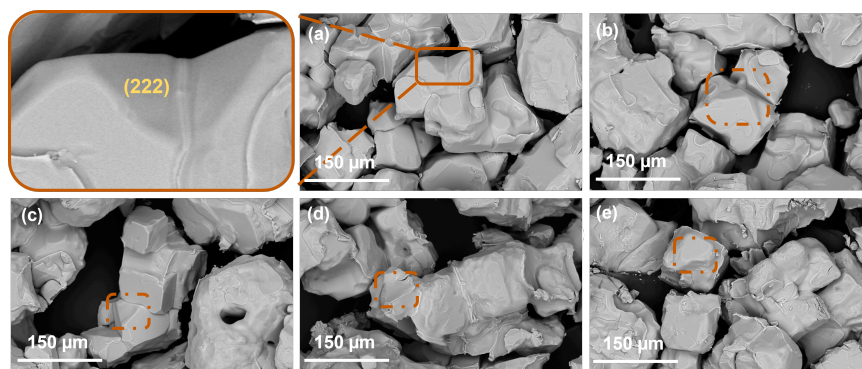


Fig. VII. 3. SEM results of cubic shaped KCl crystals immersed with co-saturated solution of ethanol and KCl with increasing ethanol content as 0.05%, 0.10%, 0.20%, 0.30% and 0.40%, respectively.

7.2.1.2. KCl crystal structure modified by ethanol

Based on above morphologies, one can draw the conclusion that the crystals shape has been modified which needs further demonstration for structural characterization. Here, XRD results of the KCl crystals immersed with co-saturated solution of ethanol-KCl with various ethanol content as 0.02%, 0.05% and 0.10% were displayed in Fig. VII. 4. Compared with original cubic KCl, strengthened peaks of (220) and (222) facets could be observed in KCl samples after immersing with KCl-ethanol co-saturated solution. Combined with SEM results, it was clear that the emerging triangle facets on corners of cubic KCl structure were the main reason for changes of XRD results. The mechanism of the new exposing faces of KCl could be related to the dissolve of relative less stable K^+ and Cl^- ions on corners with higher contacting area with solution system. As a result, the eight corners of one cubic KCl structure tended to be more easily affected by scant changes of the solution environment (the addition of ethanol, in this case). Due to the high polarity of ethanol, the solubility of KCl in the water-ethanol complex solution would be decreased as the competition of ethanol and KCl resolved in water, resulting the salting-out effect of KCl which primarily occurred on the unstable corners as appeared in experiments of Chapter V.

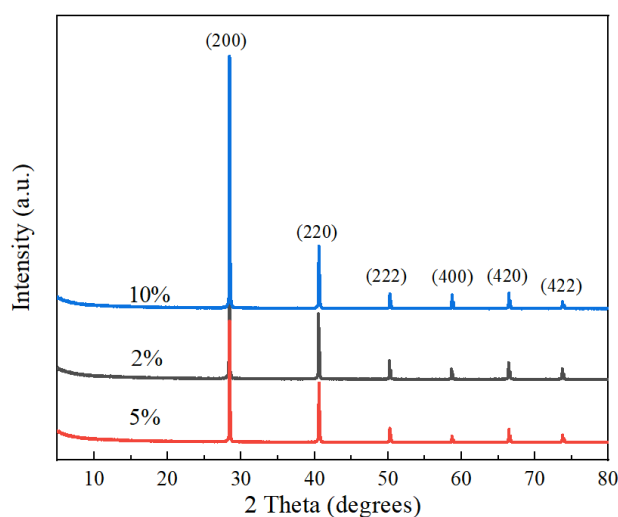


Fig. VII. 4. XRD results of cubic shaped KCl crystals immersed with co-saturated solution of ethanol and KCl with increasing ethanol content as 0.02%, 0.05% and 0.10%, respectively.

7.2.2. Flotation experiments

Shown in Fig. VII. 5 was the flotation recovery of KCl crystals (150-178 μm) with ODA as collector and various amount of ethanol addition in the mother liquor. With pure KCl saturated solution, the flotation recovery was only 83.04% while it increased to 92.36% with only slight addition of ethanol as 0.05%, demonstrating the successful strategy of improved flotation behavior. What's more, it's seen that with more ethanol up to 0.4%, flotation behavior was improved to 94.79% but then decreased to 91.49% with higher amount ethanol. Notably, the recovery was all above the original recovery without addition of ethanol. The flotation result indicated that the ethanol would improve the flotation of KCl samples but firstly increased, achieving a highest value as 0.2% but then decreased. The mechanism studied below was vital to help understand the behaviors.

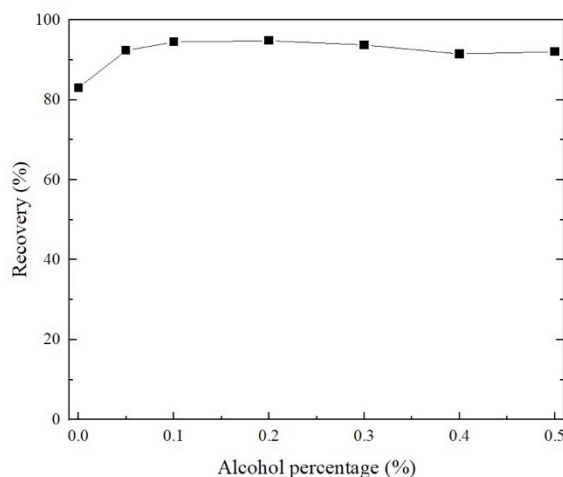


Fig. VII. 5. Flotation recovery of KCl samples with size range of 150-178 μm using ODA as collector and increasing amount of ethanol addition as 0%, 0.05%, 0.10%, 0.20%, 0.30% and 0.40%, respectively.

7.2.3. Mechanism

The changed flotation behaviors of KCl in existence of ethanol could be mainly ascribed to two aspects: one was the morphological and structural changes of KCl samples and the other was the different solution environment. Here, these two aspects were researched in detail to reach a throughout understanding of ethanol's impact on KCl flotation mechanism.

7.2.3.1. Morphologies of KCl with various amount of ethanol addition

With the addition of ethanol into KCl saturated solution, there might be some influences on surface of crystals. To unveil the changes, morphological information of KCl immersed in ethanol-KCl co-saturated solution with increasing percentage of 0%, 0.05%, 0.10%, 0.20%, 0.30% and 0.40% was demonstrated by SEM as displayed in Fig. VII. 3. The exposing (220) and (222) face was due to the resolve of 8 corners of one cubic structure of FCC crystal. The salting-out phenomenon occurred with addition of ethanol into saturate KCl solution where instant unsaturation appeared. As a consequence, the original cubic shaped KCl crystal would resolve due to the unsaturation. During this process, the most unstable atoms on corners would firstly dissolve into solution thus leaving triangle (222) faces.

7.2.3.2. Flotation mechanism

To study the flotation mechanism, interaction between KCl sample and ODA collector must be cleared first. FTIR has been used for testing the interaction as shown in Fig. VII. 6. By comparing the peaks before and after reacting with ODA[15], it was clear that new peaks of ODA appeared with the purple lines, indicating its successfully adsorption on KCl surface. However, the adsorption type could not be directly determined by FTIR which needed further research by XPS in Fig. VII. 7.

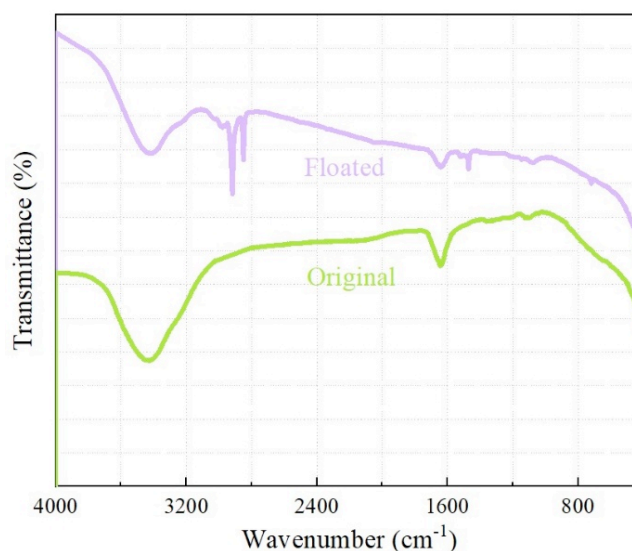


Fig. VII. 6. FTIR spectra of pure KCl before and after flotation using ODA as collector.

The XPS spectra in Fig. VII. 7. shown the survey, K 2p and Cl 2p spectra of KCl samples before and after reacting with ODA during flotation process[16]. By comparing peaks of K 2p and after Cl 2p, no changes occurred which indicated that no chemical reaction happened between KCl and ODA collector molecules. It could

be ascribed to the physical reaction in between. In conclusion, the ethanol's impact on flotation of KCl was mainly due to the influence of surface tension.

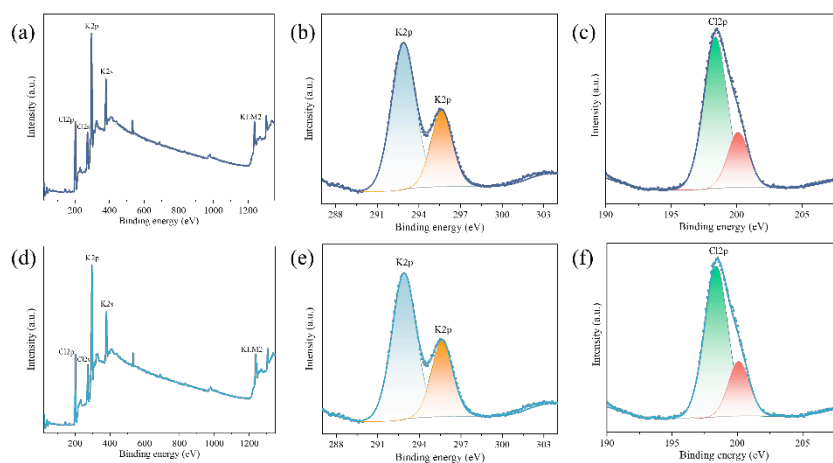


Fig. VII. 7. XPS spectra of KCl before and after flotation using ODA as collector: survey(a), (d); K 2p(b), (e) and Cl 2p(c), (f).

7.2.3.3. Surface tension

It is known for decades about the flotation mechanism that only when the natural or modified hydrophobic mineral particles were obtained, bubbles could attach them thus to form a stable system for floating up to liquid surface. In this case, the mother liquor offered the role as the possibility of formation as well as the endurance of bubbles. To study the ethanol influence of flotation mother liquor, the essential parameter was thought to be the surface tension which was closely related to the reaction of mineral particles and bubbles. Here, the same mother liquor with flotation containing various amount of ethanol addition as 0%, 0.05%, 0.10%, 0.20%, 0.30%, 0.40% and 0.50% were prepared and their surface tension data was obtained as shown in Fig. VII. 8. The tendency of mother liquor's surface tension realized a decreased line with increasing dosage of ethanol, indicating the easier formation ability of bubbles as well as the better flotation recovery. However, as seen in previous section, the recovery of KCl with increasing addition of ethanol did not uni-directionally rise but reached a highest value under 0.2% ethanol and then decreased. This could be explained by the co-effect of both surficial properties and solution environment, that is, the more exposing triangle (222) face area with less interaction ability with ODA hindered the flotation, while lower surface tension of mother liquor under addition of

ethanol, would affect the final flotation recovery and reach a best balance with 0.2% addition.

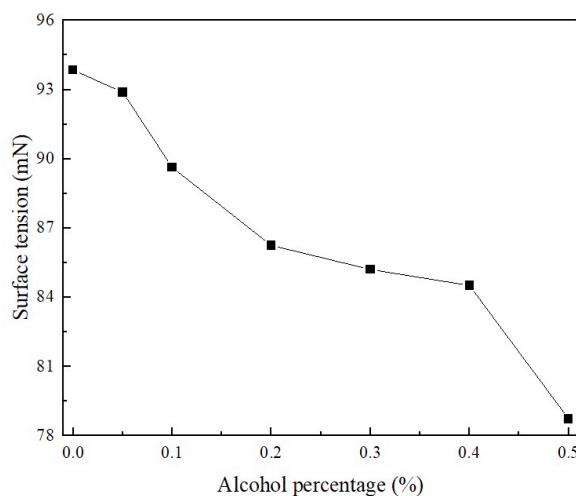


Fig. VII. 8. Surface tension of KCl solution with increasing amount of ethanol addition as 0%, 0.05%, 0.10%, 0.20%, 0.30%, 0.40% and 0.50%, respectively.

7.3. Conclusions

In conclusion, ethanol has been applied as a dispenser for avoiding caking phenomenon for soluble salts like KCl, where the impact of ethanol on flotation of the latter was studied in this work in detail. The main impacts could be mainly divided into two parts: influence of ethanol on KCl sample morphology and on solution environment. SEM and XRD results demonstrated the emerging (220) and (222) faces of KCl samples which had been previously proved to show worse flotation recovery than the original cubic structure with (100) facets. However, the addition of ethanol into saturated KCl solution would induce a decreased surface tension of the ethanol-KCl co-saturated solution, which benefited the flotation process. In total, the advantage of lowered surface tension overcome the disadvantage of new exposing (222) and (220) facets, thus yielding a promoted recovery with existence of ethanol in KCl flotation. Based on the experiments, 0.2% dosage of ethanol addition was proved to show highest recovery as 94.79% compared with pure KCl solution as pregnant solution as 83.04%. The above results indicated the successful strategy of using limited dosage of ethanol as dispenser for preventing caking of KCl with an improved flotation recovery, which could be further demonstrated to realize the “killing two birds with one stone” effect with other soluble and insoluble minerals flotation.

References

- [1] S. WEIDMANN, Shortening of the cardiac action potential due to a brief injection of KCl following the onset of activity, *J Physiol* 132 (1956) 157. <https://doi.org/10.1113/JPHYSIOL.1956.SP005510>.
- [2] Suparman, A. Bhermana, L. Nuraini, W.A. Nugroho, J. Mulyono, Growth and yield of shallot using KCl fertilizer at peatlands in Central Kalimantan, Indonesia, *E3S Web of Conferences* 306 (2021) 01006. <https://doi.org/10.1051/E3SCONF/202130601006>.
- [3] R. Li, R. Yang, X. Chen, S. Yang, C. Ma, P. Liu, J. Qiao, Intracranial KCl Injection - An Alternative Method for Multifetal Pregnancy Reduction in the Early Second Trimester, *Fetal Diagn Ther* 34 (2013) 26–30. <https://doi.org/10.1159/000350174>.
- [4] X. Wang, J.D. Miller, F. Cheng, H. Cheng, Potash flotation practice for carnallite resources in the Qinghai Province, PRC, *Miner Eng* 66–68 (2014) 33–39. <https://doi.org/10.1016/J.MINENG.2014.04.012>.
- [5] H.H. Emons, T. Fanghänel, Thermal decomposition of carnallite ($\text{KCl} \cdot \text{MgCl}_2 \cdot 6\text{H}_2\text{O}$)-comparison of experimental results and phase equilibria, *J Therm Anal Calorim* 35 (2005) 2161–2167. <https://doi.org/10.1007/BF01911881>.
- [6] E. Li, Y. Zhang, Z. Du, D. Li, F. Cheng, Bubbles facilitate ODA adsorption and improve flotation recovery at low temperature during KCl flotation, *Chemical Engineering Research and Design* 117 (2017) 557–563. <https://doi.org/10.1016/J.CHERD.2016.11.016>.
- [7] L.D. Hansen, F. Hoffmann, G. Strathdee, Effects of anticaking agents on the thermodynamics and kinetics of water sorption by potash fertilizers, *Powder Technol* 98 (1998) 79–82. [https://doi.org/10.1016/S0032-5910\(98\)00037-0](https://doi.org/10.1016/S0032-5910(98)00037-0).
- [8] Y. TAKAKURA, T. KAWABE, H. MORITA, Caking of KCl-NaCl Powder and its Prevention by Amino Acids, *NIPPON SHOKUHIN KOGYO GAKKAISHI* 40 (1993) 881–887. https://doi.org/10.3136/NSKKK1962.40.12_881.
- [9] Y. Wang, R.W. Evitts, R.W. Besant, Modelling crystal growth between potash particles near contact points during drying processes. Part I: Problem formulation, *Can J Chem Eng* 86 (2008) 192–198. <https://doi.org/10.1002/CJCE.20026>.
- [10] J. S. Yuan, Crystallization properties of schoenite in ethanol - water and methanol - water mixed solvents, *Chinese Journal of Process Engineering* 12 (2012) 631–635.
- [11] Y.D. Jiang, Salting-out effect on solvent extraction of ethanol and butanol, *JOURNAL-TSINGHUA UNIVERSITY* 40 (2000) 6–8.
- [12] J. Tóth, A. Kardos-Fodor, S. Halász-Péterfi, The formation of fine particles by salting-out precipitation, *Chemical Engineering and Processing: Process Intensification* 44 (2005) 193–200. <https://doi.org/10.1016/J.CEP.2004.02.013>.

- [13] S. Perumal, C.K. Mahadevan, Growth and characterization of multiphased mixed crystals of KCl, KBr and KI:1. Growth and X-ray diffraction studies, *Physica B Condens Matter* 369 (2005) 89–99. <https://doi.org/10.1016/J.PHYSB.2005.07.034>.
- [14] N. Folkesson, T. Jonsson, M. Halvarsson, L.G. Johansson, J.E. Svensson, The influence of small amounts of KCl(s) on the high temperature corrosion of a Fe-2.25Cr-1Mo steel at 400 and 500°C, *Materials and Corrosion* 62 (2011) 606–615. <https://doi.org/10.1002/MACO.201005942>.
- [15] A. Georgiev, I. Karamancheva, D. Dimov, I. Zhivkov, E. Spassova, FTIR study of the structures of vapor deposited PMDA–ODA film in presence of copper phthalocyanine, *J Mol Struct* 888 (2008) 214–223. <https://doi.org/10.1016/J.MOLSTRUC.2007.12.006>.
- [16] J. Stoch, M. Ladecka, An XPS study of the KCl surface oxidation in oxygen glow discharge, *Appl Surf Sci* 31 (1988) 426–436. [https://doi.org/10.1016/0169-4332\(88\)90004-9](https://doi.org/10.1016/0169-4332(88)90004-9).

Conclusions

Potash, as main resource of potassium element, presents primary role in agriculture area which greatly benefits both nature and human beings. To realize a prominent recovery of potassium element in form of KCl, flotation has been applied for decades with excellent recovery and selectivity. The most applied reagent for collecting KCl is ODA while the process remained space for further improved delicate research. Moreover, the soluble property of KCl endows it with special phenomenon that the resolve and re-crystallization may occur during flotation process. Taking KCl as one typical soluble mineral, the crystallization properties could be considered to show great impact on particle morphological as well as structural features. The crystallization-controlled flotation strategy was put up with in this work, for the first time, to shed some lights on soluble and semi-soluble mineral collecting area, which possessed great potential on understanding and designing the future flotation process for multiple minerals like hailite, carnallite and phosphogypsum, etc. Throughout this thesis, I came to the following conclusions:

1. Hopper-, sphere- and hollow cube-like crystals were obtained through various parameters including stirring speed, additive seeds, pH condition, cooling range and rate in the supersaturation modulation technology.

2. It was found that at certain condition, the crystal would grow in a uniform state, otherwise, they would form as small pieces, abrasion of crystals, etc. The solution environment showed great impact on the crystals' formation.

3. The main exposed faces for smooth cubic, hollow cubic, and hopper structure were (200), (220), and (400) facets, respectively, which could be a consequence of the inner beveling.

4. Spherical structure surface showed a higher roughness than the others, which was originated from the formation mechanism of spherical structure to cubic structure.

5. The KCl crystal with (200) and (222) exposing faces displayed various flotation recovery as 83.35% and 53.42%, respectively.

6. By combining XRD and SEM results, it was concluded that KCl (200) samples was in cubic structure while KCl (222) samples with octahedron shape. FTIR result demonstrated the successfully adsorption of ODA on both KCl (200) and KCl (222) crystals after flotation, where XPS spectra helped to exclude the chemical interaction in between.

7. Zeta potential tests demonstrated that KCl (200) crystals pertained a more negative zeta potential as -6.41 mV than KCl (222) as -3.29 mV, facilitating the stronger adsorption with cationic collector ODA with 5.51 mV surficial potential.

8. The surfaces details obtained by AFM tests indicated that the growing method of KCl (200) crystals is by layers-piling up to form stages with abundant edges and hanging Cl bonds, while KCl (222) was by formation of independent

triangle islands with limited edges. The former sample with large amount of less hydrated Cl bonds led to its lower zeta potential and less hydrophilic stage to show a better interaction with bubbles to reach a better flotation recovery.

9. The surfaces details obtained by AFM tests indicated that the growing method of KCl (200) crystals is by layers piling up to form stages with abundant edges and hanging Cl bonds, while KCl (222) was by formation of independent triangle islands with limited edges. The former sample with large amount of less hydrated Cl bonds led to its lower zeta potential and less hydrophilic stage to show a better interaction with bubbles to reach a better flotation recovery.

10. After adsorption of ODA, KCl (200) samples showed a weaker adhesion & adsorption force with KCl saturated solution than KCl (222), indicating its stronger interaction force with bubbles as well as easier floatability.

11. Various strategies were precisely designed including fast crystallization with stirring, constant speed crystallization and fast still crystallization to grow KCl crystals with cubic-, hopper- and needle-like structure, respectively.

12. Stereoscopy and SEM results showed their regular shape and XRD tested demonstrated their high crystallinity.

13. The flotation tests by using ODA as collector indicated a declined recovery as needle-, hopper- and cubic-like sample, demonstrating the better performance of needle-like sample by modulating the crystallization.

14. BET tests revealed the higher surface area of needle-like structure which could absorb more ODA flocs during flotation thus achieving a better recovery.

15. Induction time as well as adhesion & desorption force tests further explained the faster and stronger interaction of needle-like sample with bubbles, resulting its best floatability.

Personal achievement

1. **Y. Yuan**, W. Zhan, Wei Zhang, et al., “Controllably constructing morphology and structure of potassium chloride crystal by supersaturation modulation”, *Surfaces and Interfaces*, (2024) 52, 104973.
2. **Y. Yuan**, W. Zhan, A. Valdivieso-Lopez, et al., “Novel insights into sylvite flotation modulated by exposing facets”, *Powder Technology*, (2024) 443, 119969.
3. **Y. Yuan**, W. Zhan, T. Yang, et al., “Novel strategy for improve sylvite flotation through controlled crystallization”, *Mineral Engineering*, (2024) 211, 108695.
4. **Y. Yuan**, W. Zhan, F. Jia, et al., “The reduction mechanism of H₂AuCl₄ on the Surface of edge-rich molybdenum disulfide”, *Surfaces and interfaces*, (2022) 33, 102199.
5. **Y. Yuan**, W. Zhang, H. Yi, et al., “Mechanistic Insights into the Effect of Ethanol on Sylvite Flotation”, *Minerals Engineering (Under Review)*.
6. W. Zhan, **Y. Yuan**, Q. Weng, et al., “Enhanced Trace Gadolinium(III) Extraction via Tailored Chemisorption on Defect-Engineered Molybdenum Disulfide Electrodes”, *Chemical Engineering Journal*, (2025) 512, 162632.
7. S. Lei, **Y. Yuan**, H. Zhu, et al. “Enhancement of KCl flotation through crystallization regulation during carnallite decomposition”, *Surfaces and Interfaces*, (2024) 55, 105435.
8. W. Zhan, X. Zhang, **Y. Yuan**, et al., “Regulating Chemisorption and Electrosorption Activity for Efficient Uptake of Rare Earth Elements in Low Concentration on Oxygen-Doped Molybdenum Disulfide”, *ACS Nano*, (2024) 18, 7298-7310.
9. W. Zhan, **Y. Yuan**, X. Zhang, et al., “Efficient and selective Lead(II) removal within a wide concentration range through chemisorption and electrosorption coupling process via defective MoS₂ electrode”, *Separation and Purification Technology*, (2024) 329, 125183.
10. Y. Liang, W. Zhan, **Y. Yuan**, et al., “Manganese and oxygen dual-doping MoS₂ boosts reduction and adsorption activity toward efficient recovery of gold(I) from thiosulfate solutions”, *Journal of Alloys and Compounds*, (2022) 928, 167185.
11. W. Zhan, **Y. Yuan**, C. Liu, et al., “Preparation and application of 0D, 2D and 3D molybdenite: a review”. *Minerals and Mineral Materials*, (2022) 1, 5.